Contract No. W-7405-eng-26

MOLTEN-SALT REACTOR PROJECT

QUARTERLY PROGRESS REPORT
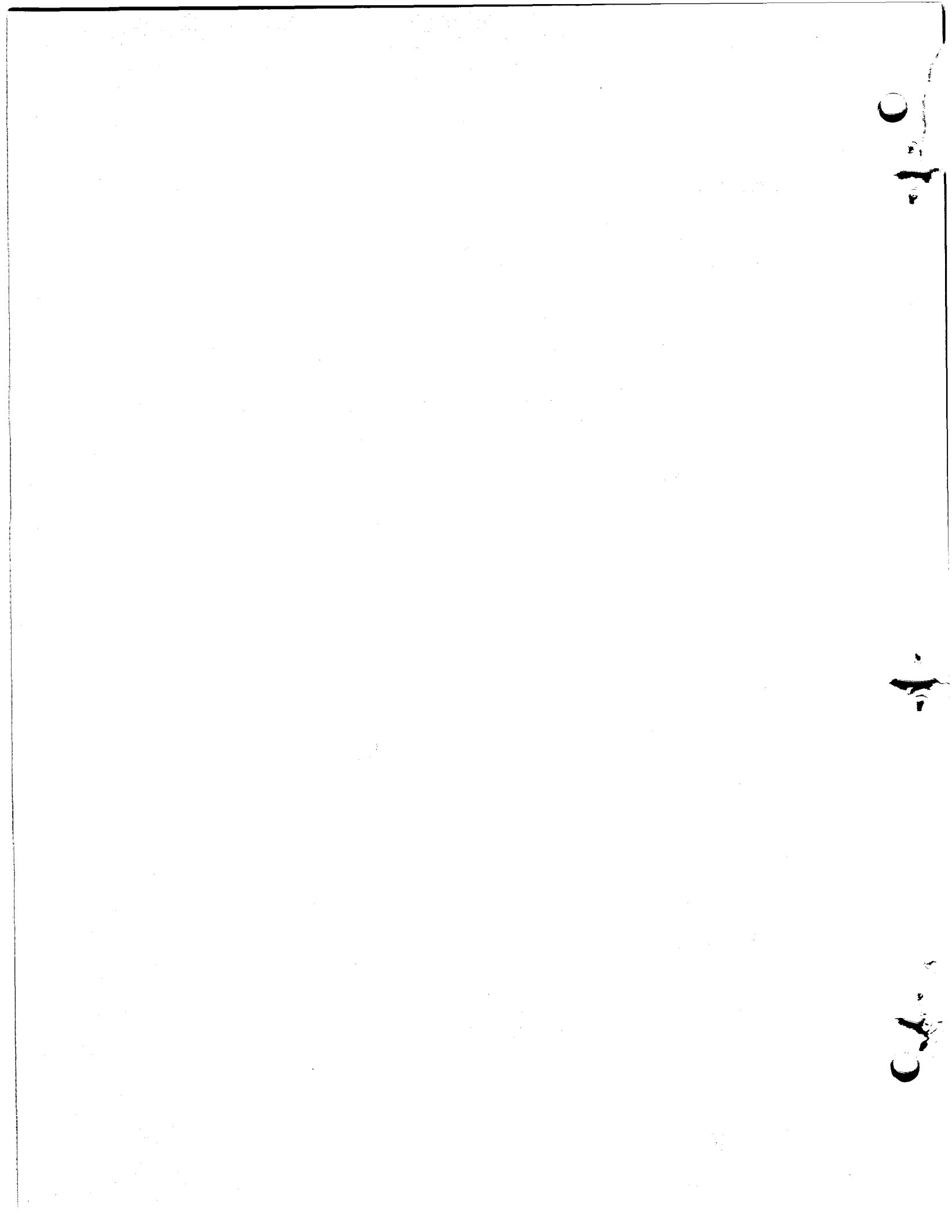
For Period Ending April 30, 1959

H. G. MacPherson, Project Coordinator

DATE ISSUED

JUN 26 1959

OAK RIDGE NATIONAL LABORATORY
Oak Ridge, Tennessee
operated by
UNION CARBIDE CORPORATION
for the
U.S. ATOMIC ENERGY COMMISSION

CONTENTS

SUMMARY

Part 1. Reactor Design Studies

1.1. Nuclear Calculations and Design Studies

The effects of fuel processing by the ion-exchange method at a
rate of once per year and at a rate of 12 times per year were compared
for the Interim Design Reactor fueled with U^{233}. Processing at the
higher rate gave insufficient improvement in performance to offer a
substantial economic advantage.

The nuclear performance of a one-region, graphite-moderated,
unreflected, thorium-conversion, molten-salt-fueled reactor was
studied to evaluate the effects of processing the fuel at the rate
of once per year and 12 times per year, the effects of decreasing
the thickness of the core vessel and adding a blanket, and the effects
of using a graphite core vessel and a blanket. The results of the
calculations indicated that the nuclear performance of the one-region
reactor fueled with U^{235} and processed by either the volatility or
ion-exchange methods at the rate of one fuel volume per year is com-
petitive with the best performance of the solid fuel systems, and
therefore the molten-salt reactor will yield lower over-all fuel costs
when the potential economies of continuous, chemical processing of
the fluid fuel are realized.

The initial nuclear characteristics of a one-region, heterogeneous,
graphite-moderated and -reflected, thorium-conversion, molten-salt-
fueled reactor were studied. It was found that with 13 mole % ThF_4 in
the fuel, a maximum regeneration ratio of 0.846 could be obtained
with an inventory of approximately 1150 kg of U^{235}. With 7 mole %
ThF_4 in the fuel, an estimated maximum regeneration ratio of 0.798 at
an inventory of approximately 900 kg of U^{235} was obtained.

Calculations were also made of the performance of two-region,
graphite-moderated, molten-salt-fueled, breeder reactors. Spherical

reactors, 5 ft in diameter, with fuel volume fractions of 0.10 and 0.15% were studied. Results were obtained for reactors with power levels of 125 and 250 Mw. It was found that the only reactor with a doubling time less than 20 years was the 250-Mw reactor having a fuel volume fraction of 0.10.

The effects of fast-neutron reactions in Be^9 on the reactivity of molten-salt-fueled reactors were studied. It was found that Be^9 is an appreciable poison in homogeneous, molten-salt-fueled reactors, but it has negligible effect in graphite-moderated, molten-salt-fueled reactors.

Work is continuing on the design of a 30-Mw, one-region, experimental, molten-salt reactor.

1.2. Component Development and Testing

Tests of salt-lubricated hydrodynamic journal bearings were continued in order to obtain operating data on which to base an optimum design. Assembly of a thrust-bearing tester was nearly completed. An existing centrifugal sump pump is being modified for service tests of a salt-lubricated journal bearing, and means for flexibly mounting the bearing to the pump casing are being investigated.

The modified Fulton-Sylphon bellows-mounted seal being subjected to an endurance test in a PK-P type of centrifugal pump has continued to seal satisfactorily for more than 12,000 hr of operation. Operation of an MF type of centrifugal pump with fuel 30 as the circulated fluid has continued to be satisfactory through more than 15,500 hr, with the past 13,500 hr of operation being under cavitation damage conditions. A small frozen-lead pump seal on a 3/16-in.-dia shaft has operated since the first 100 hr of 7500 hr of operation with no lead leakage. A similar seal on a 3 1/4-in.-dia shaft has operated 3600 hr, with an average leakage rate of 9 cm^3/hr. Operational data suggest that the seal should be redesigned to provide better coolant control and packing to decrease the annulus between the seal and the shaft.

Construction work continued on the remote maintenance demonstration facility. The work is on schedule and is to be completed by

June 30, 1959.

The operation of long-term forced-circulation corrosion-testing loops continued in 15 test stands. Tests of two Inconel loops that had operated for one year were terminated. Salt samples were removed periodically from two loops that contain sampling devices.

The in-pile loop operated previously in the MTR was disassembled. It was found that oil which had leaked past the pump shaft seal and filled the oil trap on the purge outlet line was polymerized by radiation, and the polymerized oil plugged the outlet line. The second in-pile loop, which was modified to minimize the probability of purged line plugging and activity release, was installed in the MTR on April 27.

1.3. Engineering Research

The enthalpy, heat capacity, viscosity, and surface tension have been experimentally obtained for several additional fluoride salt mixtures containing BeF_2 with varying amounts of UF_4 and/or ThF_4. Altering the salt composition toward higher percentages of the high-molecular-weight components resulted in substantial decreases in both the enthalpy and heat capacity. The viscosity showed some increase (of the order of 10%) as the percentage of UF_4 and ThF_4 in the mixtures was increased. Initial flow calibrations of a full-scale mockup of the pump system designed for the study of interfacial film formation and heat transfer with BeF_2-containing salts have been completed; assembly of the components is proceeding. The flow characteristics of the sintered-metal-filled annulus of a double-walled tube have been obtained for two porosity conditions.

1.4. Instruments and Controls

Work has continued on molten-salt-fuel level indicators. Two Inconel "I"-tube-type elements were prepared for testing, and an INOR-8 element and test vessel are being constructed.

Six INOR-8 pressure transmitters and indicating systems were ordered for testing. These units are of the pneumatic-indicator type.

Part 2. Materials Studies

2.1. Metallurgy

Corrosion studies were completed on four INOR-8 and four Inconel thermal-convection loops. Metallographic examination of the INOR-8 loops, three of which operated for 1000 hr and the other for one year, revealed no observable attack. The Inconel loops, which represented three one-year tests and one 1000-hr test, showed intergranular void attack to depths ranging from 4 to 15 mils. Twelve thermal-convection-loop tests were initiated during this period. The scheduled tests of two forced-circulation loops were completed, and one new forced-circulation-loop test was started.

The effects of penetration of graphite by molten-fluoride-salt fuels are being investigated in order to evaluate the problems associated with the use of unclad graphite as a moderator. In static pressure penetration tests at 150 psia and 1300°F, partially degassed graphite was penetrated throughout by fuel 30 ($NaF-ZrF_4-UF_4$) but was not penetrated by fuel 130 ($LiF-BeF_2-UF_4$), as indicated by macroscopic examination. Thermal cycling of the graphite that was penetrated by fuel 30 did not result in damage to the graphite. Additional static and dynamic tests are planned.

A series of tests was run to further investigate the precipitation of uranium from fuel 130 held in a graphite crucible at 1300°F. The results of these tests supported the previous conclusion that the uranium precipitation was the result of the fuel reacting with oxygen supplied by degassing of the graphite.

Several brazing alloys were tested for compatibility with fuel 130. Coast Metals alloy No. 52 (89% Ni–4% B–5% Si–2% Fe) and pure copper brazed to Inconel and INOR-8 showed good resistance to fuel 130 in 1000-hr tests at 1300°F in a thermal-convection loop. The following brazing alloys showed some attack or porosity as a result of similar exposure to fuel 130: General Electric alloy No. 81 (70% Ni–19% Cr–11% Si), Coast Metals alloy No. 53 (81% Ni–8% Cr–4% Si–4% B–3% Fe), and a gold-nickel alloy (82% Au–18% Ni).

A specimen of INOR-8 was examined for evidence of carburization that had been exposed to fuel 130 for 4000 hr in a thermal-convection loop hot leg at a temperature of 1300°F. The presence of a 10-in. graphite insert in the hot leg of this loop did not cause carburization of the INOR-8.

No new creep data for INOR-8 became available during the quarter. Creep tests are presently in progress at 1100 and 1200°F with the fluoride salts of interest as the test environments, and these tests are expected to run in excess of 10,000 hr.

The critical results obtained from rotating-beam fatigue tests at 1500°F indicate that INOR-8 has significantly better fatigue resistance than Inconel. Creep and relaxation tests indicate that an unstable condition exists in the temperature range from 1100 to 1400°F. There is some indication that a second phase appears which causes contraction of the metal even under load.

Based on the results of tensile tests conducted on specimens of INOR-8 aged for 10,000 hr in the temperature range of 1000 to 1400°F, it has been concluded that INOR-8 does not exhibit embrittling tendencies that can be attributed to high-temperature instability. No significant differences were found between the tensile properties of the aged specimens and those of specimens in the annealed condition.

An effort is now being made to fabricate triplex heat exchanger tubing containing a prefabricated porous nickel core. Porous nickel tubes have been ordered from Micro Metallic Corp. to determine the feasibility of cladding the material with Inconel and INOR-8. A sample piece of porous nickel has been incorporated into the annular space formed between two Inconel tubes for conducting a preliminary cladding experiment.

Procedures are being developed for fabricating INOR-8 material ranging in size from thin-walled tubing to heavy plate. The procedures thus developed are being qualified in accordance with methods prescribed by the ASME Boiler Code.

The effects of various deoxidation and purification processes on the mechanical properties of INOR-8 weld metal are being studied

in an effort to improve the high-temperature ductility of INOR-8 weld metal. Several heats of weld metal containing various additives were cast and fabricated into weld wire for mechanical property evaluation.

A method was developed for brazing graphite to Inconel. A commercially available brazing alloy composed of silver, titanium, and copper was found that wet vacuum-degassed graphite. Such graphite-to-Inconel joints were used in the fabrication of equipment for studying the penetration of graphite by molten salts in a dynamic, high-pressure system.

2.2. Chemistry and Radiation Damage
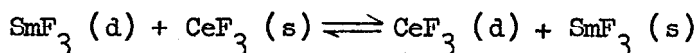
A revised phase diagram for the system $LiF-BeF_2-ThF_4$ was prepared that includes new data obtained from thermal-gradient quenching experiments. Quenched samples from experiments in which an equilibration period of 3 weeks was used revealed that the area of single-phase ternary solid solutions involving $3LiF \cdot ThF_4$ is greater than previously reported. A phase diagram showing the progress made thus far in the study of the $NaF-BeF_2-ThF_4$ was also prepared, and the identity and approximate locations of primary phases in the system $NaF-ThF_4-UF_4$ were determined.

The $SnF_2-NH_4HF_2$ system was investigated because of its potentialities as a strongly oxidizing, low-melting solvent for reprocessing fuels. Reliable data were obtained only in the range 0 to 40% SnF_2. A 15 mole % addition of SnF_2 gives a mixture with a melting point of about $100^{\circ}C$.

Measurements were made of the solubility of PuF_3 in $LiF-BeF_2-UF_4$ (70-10-20 mole %). The solubility values obtained were all higher than those obtained with $LiF-BeF_2$ mixtures having about the same LiF concentration but no UF_4.

The possibility of separating LiF from the mixture $LiF-BeF_2$ (63-37 mole %) by adding NaF and decreasing the temperature was investigated. In an initial experiment only 23% of the LiF remained in solution when the temperature of the mixture to which NaF was added at $700^{\circ}C$ was lowered to $490^{\circ}C$.

Tests were initiated for determining the rate of exchange in a proposed method for decreasing the total rare earth content of molten fluoride salts. The exchange reaction

$$SmF_3 \; (d) + CeF_3 \; (s) \rightleftharpoons CeF_3 \; (d) + SmF_3 \; (s)$$

is utilized by passing the salt through an isothermal bed of solid CeF_3 to lower the SmF_3 content, and then the temperature of the effluent salt is lowered to decrease the total rate earth content.

Two methods for separating uranium from fission products are being studied. In one method the reaction of UF_4 with BeO to produce UO_2 is utilized. In the other method, the reaction of UF_4 with water vapor produces UO_2. The sharpness of the separation with water vapor may be advantageous in processing schemes. It is thought that a process can be developed that will eliminate the need for fluorine and that will provide for the simultaneous removal of uranium and thorium. A further step would be required to remove the rare earths.

Measurements were made of the solubility of neon in $LiF-BeF_2$ and CO_2 in $NaF-BeF_2$.

In the study of the chemistry of the corrosion process, further samples of melts from operating INOR-8 and Inconel forced-circulation loops were analyzed for chromium. The chromium concentration in the $LiF-BeF_2-ThF_4-UF_4$ mixture in the INOR-8 loop reached a plateau of about 550 ppm after about 1200 hr of operation. The chromium concentration of the same salt mixture in the Inconel loop increased more rapidly than in the INOR-8 loop and after 1700 hr was still increasing. These tests are continuing.

Most investigations of corrosion behavior depend on accurate analyses for structural metal ions, and therefore anomalies in the present analytical methods are being studied.

Tests of the permeability of graphite by molten fluoride salts have continued. Three types of graphite that were specially treated to make them impervious were obtained from the National Carbon Company. The types designated ATL-82 and ATJ-82 were resistant to forced

impregnation with $LiF-MgF_2$ salt and were considerably resistant to penetration by a typical reactor fuel. Unexpectedly high concentrations of uranium in the center of the rods are being investigated.

The in-pile thermal-convection loop for testing fused-salt fuel in INOR-8 tubing in the LITR was operated in preliminary tests out-of-pile, and satisfactory circulation was obtained. Final assembly of the loop system is under way. Two fuel-filled INOR-8 capsules were installed in the MTR and are being irradiated at $1250^{O}F$.
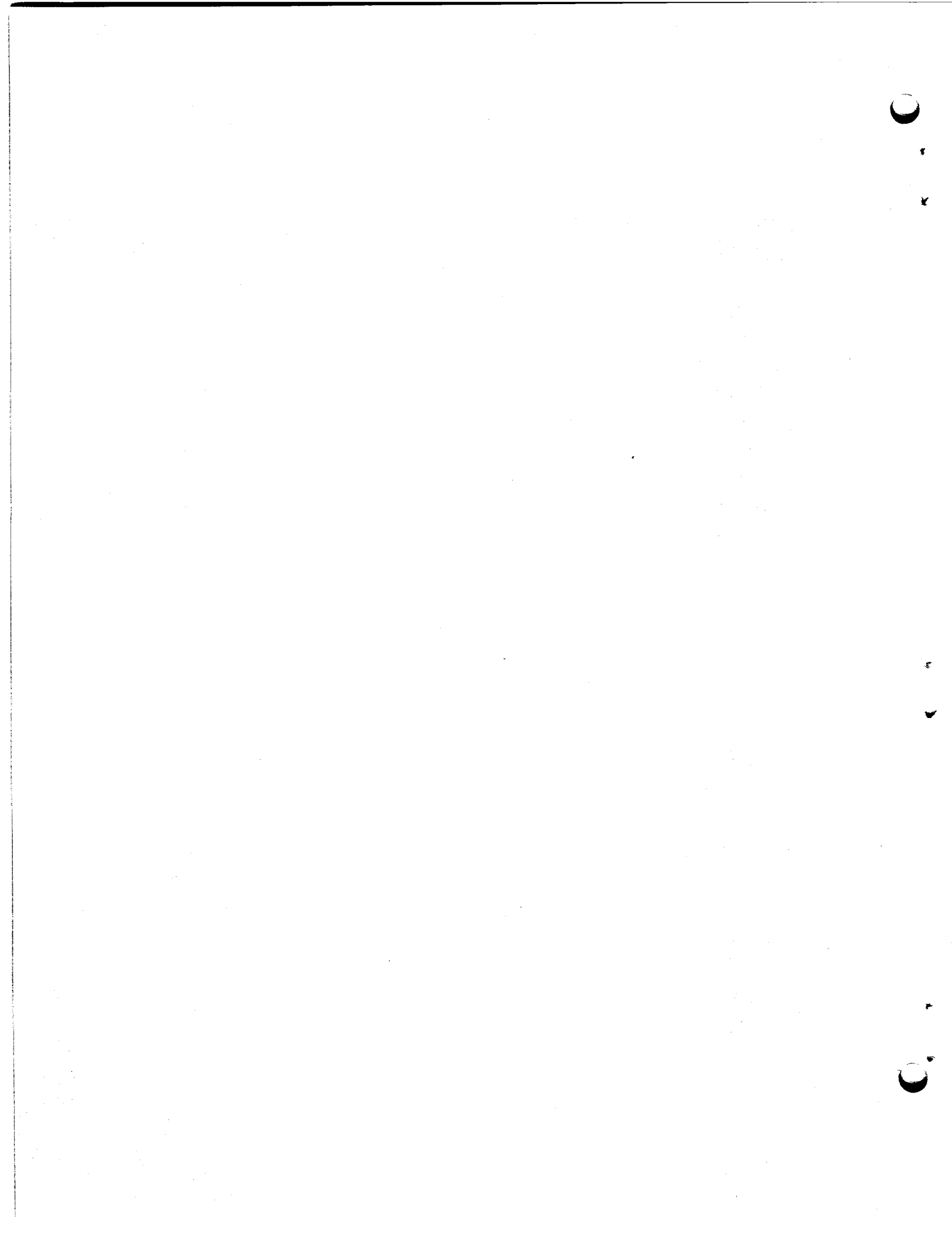
A device for testing a proposed fuel sampling and enriching mechanism was constructed and tested. It was found that the rate of solution of solid UF_4 in $LiF-BeF_2$ would be adequate for convenient enrichment procedures.

The use of molten ammonium bifluoride as a reactant for preparing both simple and complex fluorides and the preparation of pure chromous fluoride by the reaction of chromium metal with molten stannous fluoride were studied.

2.3. Fuel Processing

Studies of the processing of molten fluoride salt fuels by the fluoride-volatility process were continued. Further measurements of the solubility of neptunium (IV) in aqueous solutions saturated with $LiF-BeF_2-ThF_4-UF_4$ indicate that a solubility of the order of 0.0002 to 0.00005 mole % may be expected in actual processing.

PART 1.   REACTOR DESIGN STUDIES

1.1. NUCLEAR CALCULATIONS AND DESIGN STUDIES

Nuclear Calculations

Effect of Ion-Exchange Processing of Rare-Earth Fission Products on Performance of Interim Design Reactor Fueled with U^{233}

It was reported previously[1] that substantial savings in fuel burnup and inventory could be achieved in the Interim Design Reactor[2] fueled with U^{235} by passing the fuel salt rapidly through beds of CeF_3 to remove the rare earth fission products. The effect of ion exchange processing on the performance of the same reactor system fueled with U^{233} has now been studied. The results for two different processing rates — once per year and 12 times per year — are compared in Fig. 1.1.1. Processing at the rate of once per year (1.7 ft^3/day) could be performed either by the fluoride-volatility method[1] or by the ion-exchange method. Because of the high cost associated with the discarding of carrier salt in the volatility method, it is not feasible to use the volatility process for the higher rate.

It may be seen that processing at the higher rate gives only a small improvement in performance. It is doubtful therefore that the ion-exchange process offers any substantial economic advantage in the Interim Design Reactor system fueled with U^{233}.

Nuclear Performance of a One-Region, Graphite-Moderated, Unreflected, Thorium-Conversion, Molten-Salt-Fueled Reactor

The nuclear performance without processing to remove fission products of a reactor having a spherical core 14 ft in diameter and fuel channels 3.6 in. ID arranged in a square lattice on 8 in. centers, was described previously.[3] The performance of the same system with various processing rates and with other modifications has now been

---

[1] MSR Quar. Prog. Rep. Jan. 31, 1959, ORNL-2684, p 25.

[2] Molten Salt Reactor Program Status Report, ORNL-2634 (Nov. 12, 1958).

[3] MSR Quar. Prog. Rep. Jan. 31, 1959, ORNL-2684, p 31.

3
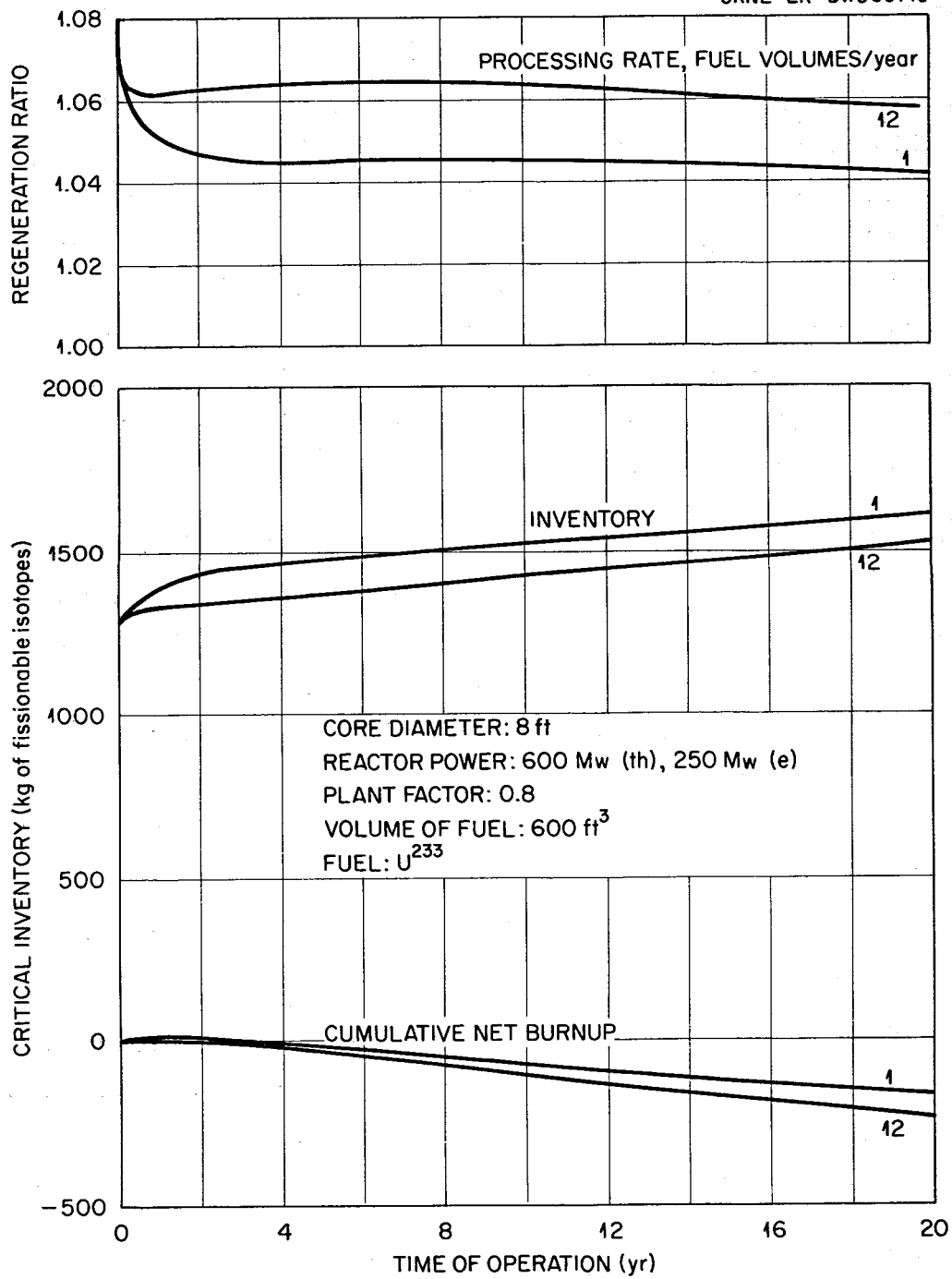
Fig. 1.1.1. Effect of Fuel Processing Rate on Nuclear Performance of Spherical, Homogeneous, Two-Region, Molten-Salt-Fueled, Breeder Reactor.

studied, and typical results are presented in Table 1.1.1 and in Fig. 1.1.2, where regeneration ratio, critical inventory, and net cumulative burnup are plotted as functions of time of operation. Without processing, the regeneration ratio falls from 0.8 to 0.5 in 20 years. The fuel additions required to override fission-product poisons are large; the critical inventory rises from 800 to 1800 kg of fuel, giving an average specific power of only 0.4 Mw/kg. The burnup is also large, averaging 0.45 g/Mwd.

Processing the fuel salt to remove fission products at the rate of one fuel volume per year (2.5 ft^3/day) stabilizes the regeneration ratio at above 0.8. The inventory averages about 750 kg. The burnup is reduced to 0.21 g/Mwd. Increasing the processing rate to 12 fuel volumes per year (30 ft^3/day) improves the performance only slightly.

Although it is uncertain that a core vessel and blanket could be incorporated into this reactor, it was of interest to evaluate the nuclear benefits of such an arrangement. Accordingly, the thickness of the INOR-8 reactor vessel wall was reduced to 1/2 in. for the calculations, and a 30-in. blanket containing 13 mole % ThF_4 in a mixture of LiF and BeF_2 was added. The blanket system was processed 12 times a year by the fluoride-volatility method to remove U^{233}, which was added to the fuel salt. The fuel was processed 12 times a year by the ion-exchange method to remove fission products. The results of the calculations are presented in Table 1.1.2, and the performance is indicated in Fig. 1.1.2 by the lines labeled U^{235} 12,B. The regeneration ratio averaged in excess of 0.96 and approached 1.0 in the steady state. The critical inventory was not decreased significantly, but was shifted toward U^{233} in composition (90%). The burnup was reduced to 0.056 g/Mwd, and the reactor was practically self-sustaining. However, it was estimated that the savings in mills per kilowatt-hour effected by reducing the burnup costs would be more than offset by the additional capital costs of reactor vessel, blanket materials, pumps, processing equipment, and concomitant operating costs.

Table 1.1.1. Effect of Fuel Processing Rate on Nuclear Performance of One-Region, Graphite-Moderated, Unreflected, Thorium-Conversion, Molten-Salt-Fueled Reactor

Core diameter: 14 ft
Reactor power: 600 Mw(th), 250 Mw(e)
Plant factor: 0.8
Fuel volume: 900 ft^3
Fuel channels: 3.6 in. ID
Lattice: triangular, 8-in. centers
Core vessel: 1-in.-thick INOR-8
Blanket: none

	Initial State		After 20 Years with Fuel Processed Once per Year		After 20 Years with Fuel Processed 12 Times per Year	
	Inventory (kg)	Absorption Ratio[a]	Inventory (kg)	Absorption Ratio[a]	Inventory (kg)	Absorption Ratio[a]
Fissionable isotopes						
U^{233}			563	0.764	559	0.794
U^{235}	829	1.000	187	0.219	167	0.205
Pu^{239}			3	0.017	0.3	0.001
Fertile isotopes						
Th^{232}	38,438	0.783	38,438	0.776	38,438	0.807
U^{234}			218	0.051	222	0.054
U^{238}	64	0.008	142	0.017	136	0.017
Fuel carrier						
Li^7	6,328	0.054	6,328	0.052	6,328	0.055
F^{19}	37,571	0.025	37,571	0.025	37,571	0.026
Moderator						
Be^9	1,840	0.001	1,840	0.001	1,840	0.001
C^{12}		0.051		0.049		0.052
Fission products			181	0.034	15.3	0.003
Parasitic isotopes						
U^{236} and others			197	0.037	184	0.036
Miscellaneous						
Pa^{233}			17	0.009	17.8	0.010
Core vessel and leakage		0.149		0.151		0.155
Neutron yield, η	2.071		2.207		2.217	
Total fuel inventory, kg	829		754		726	
Cumulative net burnup, kg	0		757		686	
Net fuel requirement, kg	829		1,511		1,412	
Regeneration ratio	0.791		0.836		0.8683	

[a]Neutrons absorbed per neutron absorbed by fissionable isotopes.

6
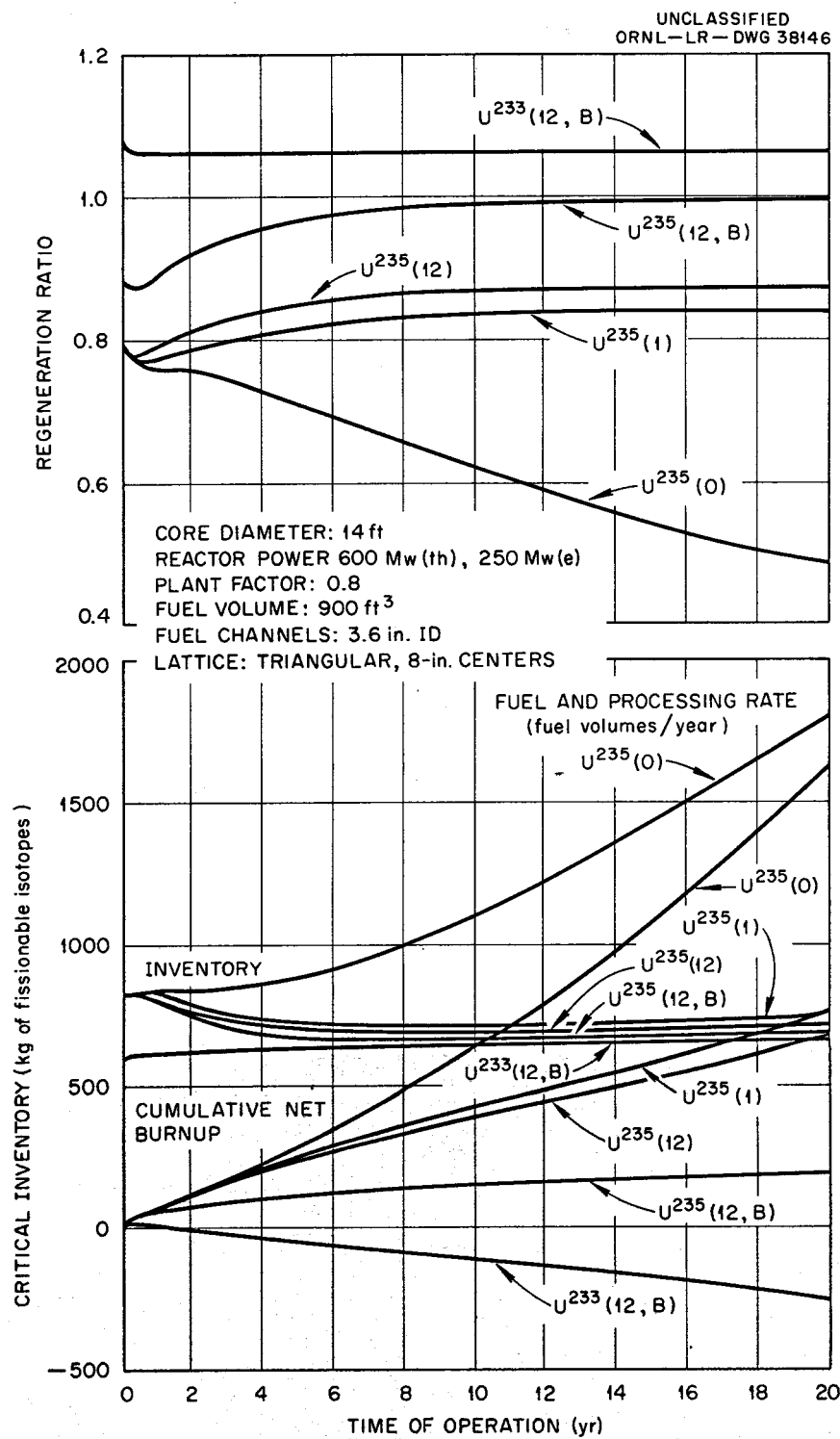
Fig. 1.1.2. Nuclear Performance of Spherical, Heterogeneous, Graphite-Moderated, One-Region, Unre-flected, Thorium-Conversion, Molten-Salt-Fueled Reactors.

Table 1.1.2. Effect of Core Vessel Material and Blanket on Nuclear Performance of One-Region, Graphite-Moderated, Thorium-Conversion, Molten-Salt-Fueled Reactor

Core diameter: 14 ft
Reactor power: 600 Mw(th), 250 Mw(e)
Plant factor: 0.8
Fuel volume: 900 ft^3
Fuel channels: 3.6 in. ID
Lattice: triangular, 8-in. centers
Blanket thickness: 30 in.
Fuel processing rate: 12 times per year

	Reactor with ½-in.-Thick INOR-8 Core Vessel				Reactor with Graphite Core Vessel			
	Initial State		After 20 Years		Initial State		After 20 Years	
	Inventory (kg)	Absorption Ratio[a]	Inventory (kg)	Absorption Ratio[a]	Inventory (kg)	Absorption Ratio[a]	Inventory (kg)	Absorption Ratio[a]
Fissionable isotopes								
U^{233} (fuel)			625	0.917	594	1.000	620	0.936
U^{233} (blanket)			1.7				3	
U^{235}	829	1.000	65	0.082			48	0.064
Pu^{239}			0.2	0.001				
Fertile isotopes								
Th^{232} (fuel)	38,438	0.783	38,438	0.831	38,438	0.933	38,438	0.852
Th^{232} (blanket)	76,765	0.095	76,765	0.101	76,765	0.156	76,765	0.149
U^{234}			239	0.060			277	0.072
U^{238}	64.3	0.008	104	0.013			1	
Fuel carrier								
Li^{7}	6,328	0.054	6,328	0.057	6,328	0.068	6,328	0.060
F^{19}	37,571	0.025	37,571	0.026	37,571	0.028	37,571	0.027
Moderator								
Be^{9}	1,840	0.001	1,840	0.001	1,840	0.001	1,840	0.001
C^{12}		0.051		0.054		0.063		0.056
Fission products			15	0.003			15.3	0.003
Parasitic isotopes								
U^{236} and others			122	0.026			20	0.003
Miscellaneous								
Pa^{233} (fuel)			18.1	0.010			18.6	0.011
Pa^{233} (blanket)			2.2				3	
Blanket carrier salt, core vessel and leakage		0.055		0.058		0.006		0.061
Neutron yield, η	2.071		2.240		2.256		2.241	
Total fuel inventory, kg	829		691		594		670	
Cumulative net burnup, kg	0		185		0		−245	
Net fuel requirement, kg	829		876		594		425	
Regeneration ratio	0.885		0.995		1.090		1.064	

[a]Neutrons absorbed per neutron absorbed by fissionable isotopes.

In a further extension of the calculations, the nuclear benefits to be obtained by the use of a graphite core vessel (in place of INOR-8) and fueling with U^{233} were studied. These changes are, of course, impractical in the present state of technology. However, the study was performed in order to define the limiting nuclear performance of this particular core and fuel system.

The results of the calculations are presented in Table 1.1.2, and the performance is indicated in Fig. 1.1.2 by the lines labeled U^{233} 12,B. The regeneration ratio is stabilized above 1.06, the average inventory is about 650 kg, and the cumulative net burnup is slightly negative, amounting to -250 kg of U^{233} in 20 years. However, 76 kg of this is required as increased inventory in the fuel salt to override fission products and nonfissionable isotopes.

It is concluded that the nuclear performance of the one-region reactor fueled with U^{235} and processed by either the volatility or ion-exchange methods at the rate of one fuel volume per year is competitive with the best performance of the solid fuel systems, and therefore the molten-salt reactor will yield lower over-all fuel costs when the potential economies of continuous, chemical processing of the fluid fuel are realized.

Initial Nuclear Performance of One-Region, Graphite-Moderated, Graphite-Reflected, Thorium-Conversion, Molten-Salt-Fueled Reactors

The initial nuclear characteristics of a heterogeneous, graphite-moderated and -reflected, one-region, molten-salt-fueled reactor were studied. The reactor considered in the study consists of a cylindrical core, 15 ft in dia and 15 ft high, surrounded by a 2.5-ft-thick graphite reflector contained in an INOR-8 pressure shell 1.5 in. thick. The core is penetrated by cylindrical fuel passages arranged in an 8-in. triangular lattice parallel to the core axis. The resulting unit cells are hexagonal and 15 ft long. This system has been investigated over a range of fuel volumetric fractions in the core and at two concentrations of thorium in the fuel salt. The initial nuclear characteristics of the system, with an external fuel volume of 673 ft^3, are

given in Tables 1.1.3 and 1.1.4 for the cases having 13 and 7 mole %
ThF_4 in the fuel, respectively; Fig. 1.1.3 shows the regeneration ratio
as a function of the system inventory.

The modified Oracle program Cornpone was used to calculate the
multiplication constant and group disadvantage factors for the fuel
and graphite. The results were then used for complete reactor calcu-
lations in spherical geometry on a core having the same volume as the
cylindrical core. Mean, homogeneized densities (atoms/cm^3) were used
for each element.

It may be seen from Fig. 1.1.3 that, in the case having 13 mole %
ThF_4 in the fuel, a maximum regeneration ratio of 0.846 is obtained
at an inventory of approximately 1150 kg of U^{235}. With 7 mole % ThF_4
in the fuel, an estimated maximum regeneration ratio of 0.798 at an
inventory of approximately 900 kg of U^{235} was obtained.

Nuclear Performance of Two-Region, Graphite-Moderated, Molten-Salt-Fueled, Breeder Reactor

The nuclear performance of spherical, graphite-moderated reactors,
5 ft in diameter with fuel volume fractions of 0.10 and 0.15, was
studied. The fuel channels were 2.6 in. in diameter and were arranged
in an 8-in. triangular lattice. These reactors were surrounded by
2-in.-thick graphite core vessels and 30-in.-thick blankets.

The fuel consisted of 71 mole % LiF, 16 mole % BeF_2, and 13 mole %
ThF_4 plus UF_4. The blanket salt had the same composition as the fuel,
but no UF_4.

The performance of these reactors over a period of 20 years was
calculated for power levels of 125 and 250 Mw. The processing rate
in all cases was 12 fuel volumes per year. The system volumes used
for these calculations are shown in Table 1.1.5; only the heat exchanger
volume was increased for higher power levels.

The results of the calculations are presented in Tables 1.1.6 and
1.1.7 and are plotted in Figs. 1.1.4, 1.1.5, and 1.1.6. It may be seen
that the only reactor with a doubling time less than 20 years is the
250-Mw reactor having a fuel volume fraction of 0.10. For both cores,

10

Table 1.1.3. Initial Nuclear Performance of a One-Region, Graphite-Moderated, Thorium-Conversion, Molten-Salt-Fueled Reactors with 13 mole % ThF_4 in the Fuel

| | Fuel Volumetric Fraction in the Core | | | | | | | | | | | |
| | 0.12 | | 0.16 | | 0.20 | | 0.22 | | 0.24 | | 0.28 | |
	Inventory (kg)	Absorption Ratio[a]	Inventory (kg)	Absorption Ratio	Inventory (kg)	Absorption Ratio	Inventory (kg)	Absorption Ratio	Inventory (kg)	Absorption Ratio	Inventory (kg)	Absorption Ratio
Fissionable isotope												
U^{235}	798.3	1	925.3	1	1,086	1	1,168	1	1,299	1	1,526	1
Fertile isotopes												
Th^{232}	42,338	0.804	46,883	0.820	51,408	0.837	53,671	0.836	55,954	0.831	60,480	0.823
U^{238}	59.9	0.005	69.4	0.006	81.4	0.008	87.6	0.009	97.4	0.011	114.5	0.012
Fuel carrier												
Li^7	6,974	0.064	7,723	0.061	8,469	0.055	8,841	0.055	9,217	0.049	9,963	0.046
F^{19}	41,350	0.023	45,789	0.026	50,208	0.026	52,418	0.028	54.648	0.027	59,068	0.030
Moderator												
Be^9	2,021	0.001	2,238	0.001	2,454	0.001	2,562	0.001	2,674	0.001	2,887	0.001
C^{12}	334,900	0.079	328,900	0.056	323,000	0.040	320,000	0.036	317,000	0.030	311,000	0.025
Core vessel capture plus leakage		0.105		0.104		0.089		0.089		0.093		0.091
Neutron yield, η	2.081		2.074		2.056		2.054		2.042		2.028	
Regeneration ratio	0.809		0.826		0.845		0.845		0.842		0.835	

[a]Neutrons absorbed per neutron absorbed in fissionable isotope.

Table 1.1.4. Initial Nuclear Performance of a One-Region, Graphite-Moderated, Thorium-Conversion, Molten-Salt-Fueled Reactors with 7 mole % ThF_4 in the Fuel

| | Fuel Volumetric Fraction in the Core | | | | | | | | | |
| | 0.12 | | 0.16 | | 0.20 | | 0.22 | | 0.24 | |
	Inventory (kg)	Absorption Ratio[a]	Inventory (kg)	Absorption Ratio	Inventory (kg)	Absorption Ratio	Inventory (kg)	Absorption Ratio	Inventory (kg)	Absorption Ratio
Fissionable isotope										
U^{235}	472	1	506		592	1	633	1	677	
Fertile isotope										
Th^{232}	22,926	0.710	25,387		27,837	0.769	29,060	0.771	30,300	
U^{238}	35.3	0.003	37.3		44.8	0.005	46.9	0.006	50.3	
Fuel carrier										
Li^{7}	6,641	0.105	7,355		8,065	0.097	8,420	0.099	8,777	
F^{19}	39,440	0.028	43,670		47,890	0.032	50,000	0.034	52,120	
Moderator										
Be^{9}	3,284	0.001	3,637		3,988	0.001	4,163	0.001	4,349	
C^{12}	334,900	0.135	328,900		323,000	0.072	320,000	0.066	317,000	
Core vessel capture plus leakage		0.123				0.100		0.101		
Neutron yield, η	2.105				2.076		2.078			
Regeneration ratio	0.713		0.760		0.774		0.777		0.787	

[a]Neutrons absorbed per neutron absorbed in the fuel.
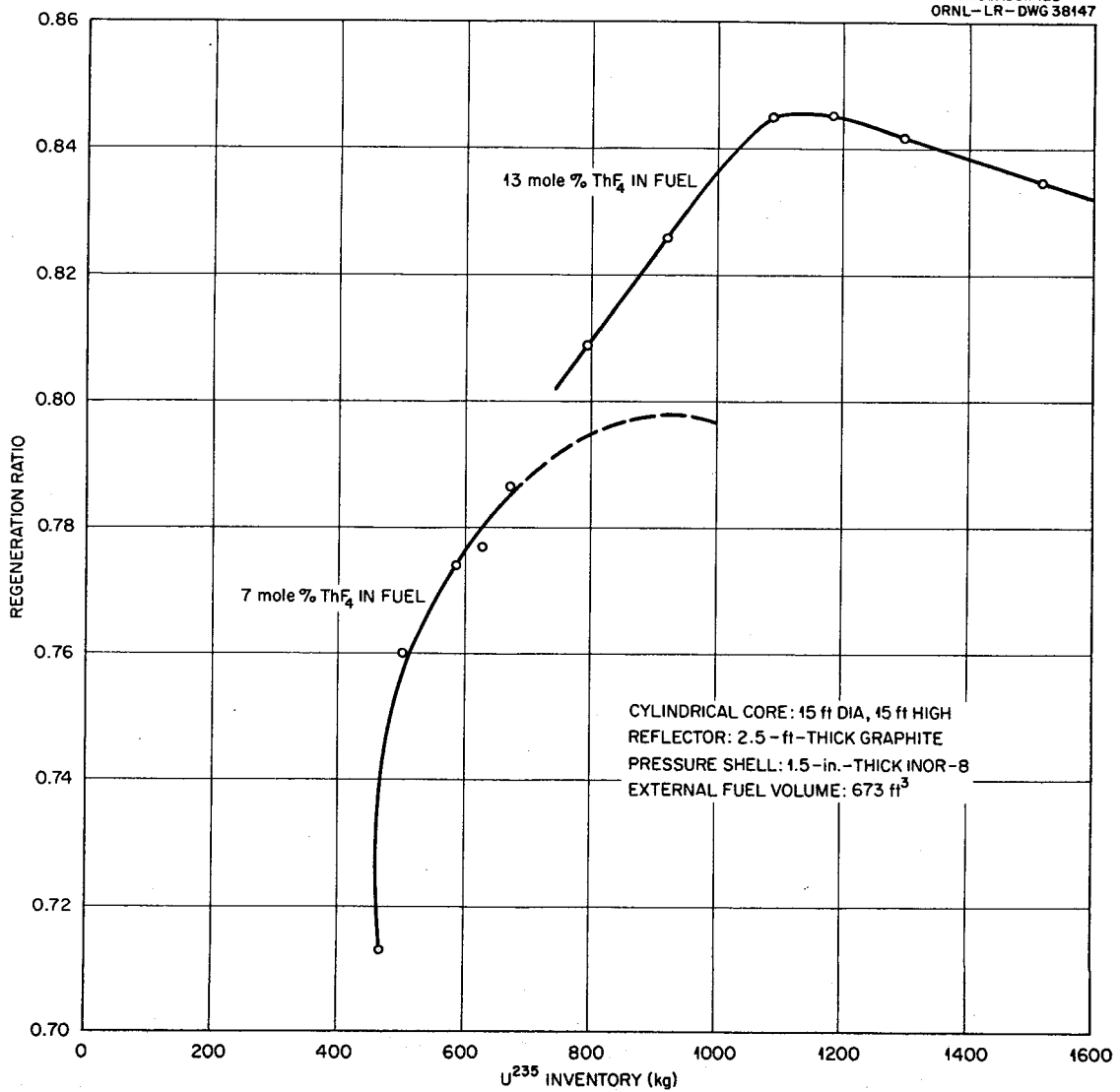
Fig. 1.1.3. Initial Nuclear Performance of One-Region, Graphite-Moderated, Thorium-Conversion, Molten-Salt-Fueled Reactors.

13

Table 1.1.5. Characteristics of Two-Region, Graphite-Moderated,
Molten-Salt-Fueled, Breeder Reactors

Fuel volume fraction in core	0.10		0.15	
Power, Mw	125	250	125	250
Fuel volume, ft^3				
Core	6.67	6.67	10	10
Heat exchanger	15	30	15	30
Other	15	15	15	15
Total	36.7	51.7	40	55
Average inventory, kg of fissionable isotopes	73	110	76	135
Average regeneration ratio	1.090	1.075	1.073	1.068
Annual production,[a] kg	2.15	4.45	1.7	3.2

[a]Annual production = annual average excess of U^{233} based on a reactor
lifetime of 20 years.

the regeneration ratio drops off at the higher power level. This was
to be expected because of the buildup of U^{234} and U^{236}; also, since
the processing rate was the same for all power levels, the concentration
of the fission fragments was increased at the higher power level.

Effects of Fast Neutron Reactions in Be^9 on Reactivity of Molten-Salt Reactors

The net effect of the reactions $Be^9(n,2n)2He^4$, and $Be^9(n,\alpha)He^6(\beta)Li^6$
on the reactivity of molten-salt reactors was studied. In a spherical,
two-region, homogeneous core 8 ft in diameter having a carrier salt
composed of 58 mole % LiF, 35 mole % BeF_2, and 7 mole % ThF_4, and U^{233}
fuel, the contribution of the reactions in Be^9 to the neutron multi-
plication was estimated to be -0.087. In a spherical, two-region,
heterogeneous, graphite-moderated, molten-salt reactor having a core
5 ft in diameter, a carrier salt composed of 71 mole % LiF, 16 mole %
BeF_2, and 13 mole % ThF_4, and fueled with U^{233}, the reactivity effect

Table 1.1.6. Nuclear Performance of Two-Region, Graphite-Moderated, Molten-Salt-Fueled, Breeder Reactors with Fuel Volume Fraction of 0.10

Core diameter: 5 ft
Lattice: triangular, 8-in. center
Fuel processing rate: 12 times per year

	For 125-Mw(th) Plant				For 250-Mw(th) Plant			
	Initial State		After 20 Years		Initial State		After 20 Years	
	Inventory (kg)	Absorption Ratio[a]	Inventory (kg)	Absorption Ratio[a]	Inventory (kg)	Absorption Ratio[a]	Inventory (kg)	Absorption Ratio[a]
Fissionable isotopes								
U^{233} (fuel)	59.1	1.000	67.9	0.910	83	1.000	99	0.898
U^{233} (blanket)			2.37				5	
U^{235}			7.8	0.088			13	0.098
Pu^{239}			0.038	0.002			0.10	0.004
Fertile isotopes								
Th^{232} (fuel)	1,567	0.402	1,567	0.335	2,207	0.402	2,207	0.322
Th^{232} (blanket)	21,527	0.720	21,527	0.660	21,520	0.720	21,520	0.648
U^{234}			39.8	0.092			64	0.100
U^{238}			1.34	0.002			4	0.005
Fuel carrier								
Li^{7}	258	0.027	258	0.020	363	0.027	363	0.019
F^{19}	1,532	0.013	1,532	0.012	2,158	0.013	2,158	0.012
Moderator								
Be^{9}	75	0.001	75	0.001	106	0.001	106	0.001
C^{12}		0.042		0.032		0.042		0.031
Fission products			3.18	0.006			6	0.008
Parasitic isotopes								
U^{236} and others			6.21	0.014			13	0.021
Miscellaneous								
Pa^{233} (fuel)			1.51	0.008			3	0.011
Pa^{233} (blanket)			3.05				6	
Blanket carrier salt, core vessel, and leakage		0.060		0.055		0.060		0.054
Neutron yield, η	2.265		2.238		2.265		2.232	
Total fuel inventory, kg	59.1		78.1		83.0		117	
Cumulative net burnup, kg	0		−72.2		0		−123	
Net fuel requirement, kg	59.1		5.9		83.0		−6	
Regeneration ratio	1.122		1.080		1.122		1.064	

[a]Neutrons absorbed per neutron absorbed by fissionable isotopes.

Table 1.1.7. Nuclear Performance of Two-Region, Graphite-Moderated, Molten-Salt-Fueled, Breeder Reactors with Fuel Volume Fraction of 0.15

Core diameter: 5 ft
Lattice: triangular, 8-in. center
Fuel processing rate: 12 times per year

| | For 125-Mw(th) Plant | | | | For 250-Mw(th) Plant | | | |
| | Initial State | | After 20 Years | | Initial State | | After 20 Years | |
	Inventory (kg)	Absorption Ratio[a]	Inventory (kg)	Absorption Ratio[a]	Inventory (kg)	Absorption Ratio[a]	Inventory (kg)	Absorption Ratio[a]
Fissionable isotopes								
U^{233} (fuel)	59	1.000	72	0.907	103	1.000	127	0.901
U^{233} (blanket)			2				4	
U^{235}			9	0.090			17	0.095
Pu^{239}			0.1	0.003			0.2	0.004
Fertile isotopes								
Th^{232} (fuel)	1,710	0.472	1,710	0.384	2,987	0.472	2,987	0.378
Th^{232} (blanket)	23,487	0.642	23,487	0.589	23,527	0.642	23,527	0.585
U^{234}			44	0.095			81	0.099
U^{238}			2	0.003			4	0.004
Fuel carrier								
Li^7	282	0.027	282	0.019	492	0.027	492	0.019
F^{19}	1,671	0.019	1,671	0.017	2,920	0.019	2,920	0.017
Moderator								
Be^9	82	0.001	82	0.001	143	0.001	143	0.001
C^{12}		0.028		0.020		0.028		0.020
Fission products			3	0.006			6	0.007
Parasitic isotopes								
U^{236} and others			6	0.017			13	0.020
Miscellaneous								
Pa^{233} (fuel)			2	0.010			3	0.011
Pa^{233} (blanket)			3				5	
Blanket carrier salt, core vessel, and leakage		0.052		0.048		0.052		0.047
Neutron yield, η	2.241		2.211		2.241		2.209	
Total fuel inventory, kg	59		82		103		148	
Cumulative net burnup, kg	0		−59		0		−108	
Net fuel requirement, kg	59		23		103		40	
Regeneration ratio	1.114		1.061		1.114		1.055	

[a]Neutrons absorbed per neutron absorbed by fissionable isotopes.

CORE DIAMETER: 5 ft
LATTICE: TRIANGULAR, 8-in. CENTERS
FUEL: U^{233}
FERTILE MATERIAL: Th^{232}

0.10 FUEL VOLUME FRACTION, 125Mw

0.10 FUEL VOLUME FRACTION, 250Mw

0.15 FUEL VOLUME FRACTION, 125Mw

0.15 FUEL VOLUME FRACTION, 250Mw

REGENERATION RATIO

REACTOR OPERATING TIME (yr)
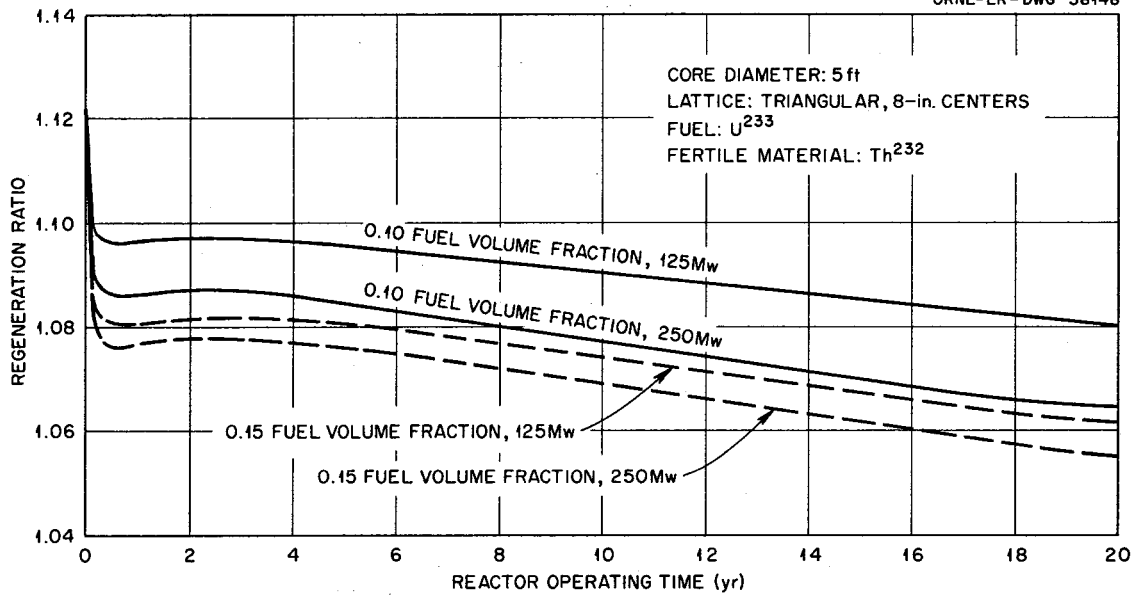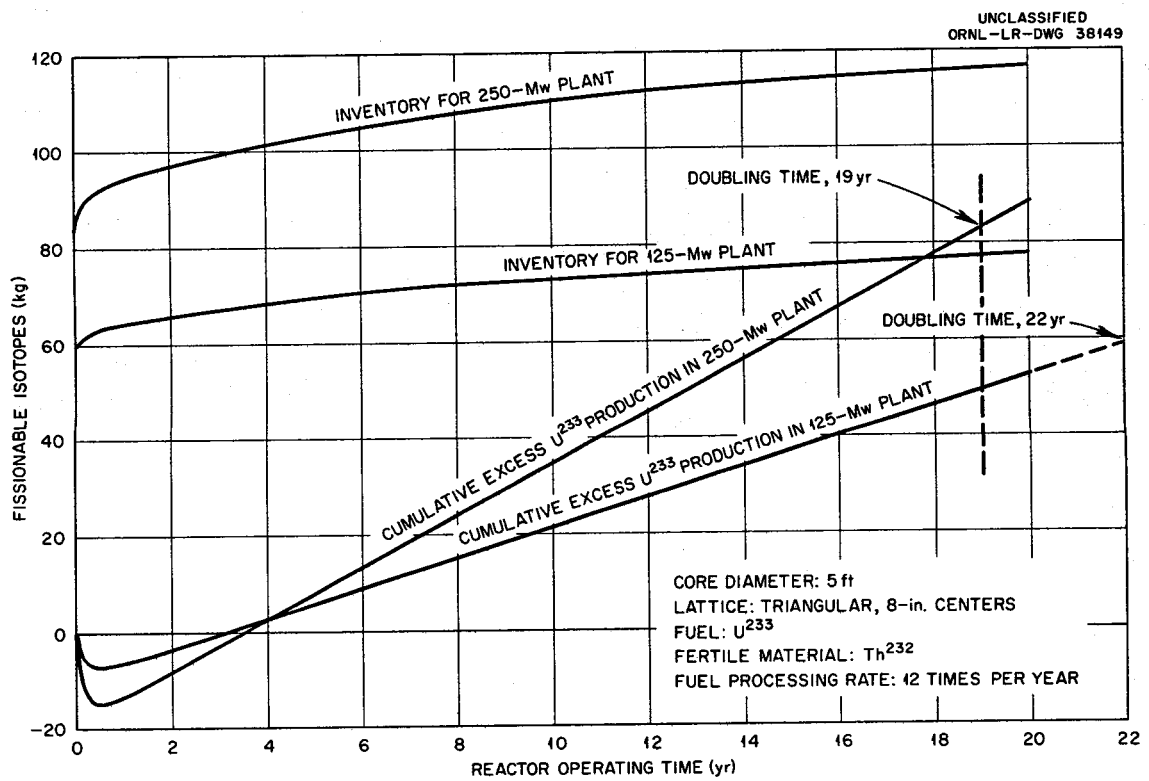
Fig. 1.1.4. Regeneration Ratio vs Reactor Operating Time for Two-Region, Graphite-Moderated, Molten-Salt-Fueled, Breeder Reactors.

Fig. 1.1.5. Inventory and Excess U^{233} Production vs Reactor Operating Time for Two-Region, Graphite-Moderated, Molten-Salt-Fueled, Breeder Reactors with a Fuel Volume Fraction of 0.10.

CORE DIAMETER: 5 ft
LATTICE: TRIANGULAR, 8-in. CENTERS
FUEL: U^{233}
FERTILE MATERIAL: Th^{232}
FUEL PROCESSING RATE: 12 TIMES PER YEAR

INVENTORY FOR 250-Mw PLANT

INVENTORY FOR 125-Mw PLANT

CUMULATIVE EXCESS U^{233} PRODUCTION IN 250-Mw PLANT

CUMULATIVE EXCESS U^{233} PRODUCTION IN 125-Mw PLANT

FISSIONABLE ISOTOPES (kg)

REACTOR OPERATING TIME (yr)
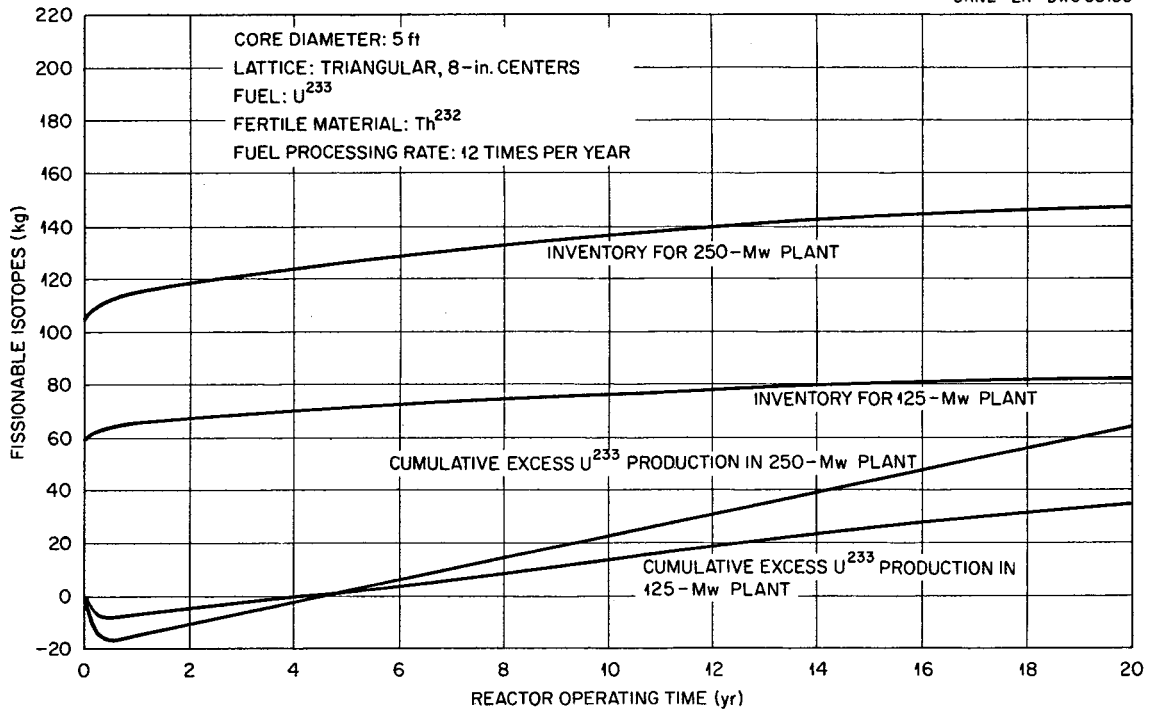
Fig. 1.1.6. Inventory and Excess U^{233} Production vs Reactor Operating Time for Two-Region, Graphite-Moderated, Molten-Salt-Fueled, Breeder Reactors with a Fuel Volume Fraction of 0.15.

19

was only -0.00077. It was concluded that Be^9 is an appreciable poison in homogeneous, molten-salt-fueled reactors, but has negligible effect in graphite-moderated molten-salt-fueled reactors.

Oracle Code MSPR-Cornpone 020

A revision has been made of the element absorption edit of Oracle code MSPR-Cornpone 020, which now permits an immediate edit on paper tape. Previously it was necessary to wait for curve-plotter pictures. It is now possible to compute the breeding ratio and prepare the input for Sorghum as soon as the case is run.

The cross-section tape has been checked and corrected where necessary, and an edit has been obtained for the cross sections. The elements now included in the cross section library are listed below:

Code Number	Element	Code Number	Element
00	U^{233}	13	Nickel
01	U^{235}	14	Chromium
02	U^{238}*	15	Molybdenum
03	Thorium*	16	Aluminum
04	Pu^{239}	17	Lithium (0.01 % Li^6)
05	Fluorine	18	Carbon
06	Oxygen	19	Alloy-8
07	Boron	1A	U^{234}
08	Sodium	1B	U^{236}
09	Beryllium	1C	Np^{237}
0A	Bismuth	1D	Pa^{233}
0B	Cerium	1E	Li^7
0C	Two Fission Products	1F	Thorium (2)
0D	U^{238} (0)	20	Thorium (0)
0E	U^{238} (20)	21	Thorium (1)
0F	U^{238} (Metal)	22	Thorium (4)
10	U^{238} (10)	23	Thorium (10)
11	Deuterium	24	Thorium (25)
12	Iron	25	Thorium (0.25)

26	Hydrogen	2B	Thorium (26G)
27	Thorium (0.75)	2C	Thorium (29G)
28	Thorium (0.50)	30	Thorium (13)
29	Thorium (7)	31	Pu^{240}
2A	Thorium (13G)		

There are 32 lethargy groups, with the last at $1180°F$. Element $U^{238}*$ has zero absorption cross sections in all groups. It must be combined with one of the other U^{238} options listed, which have zeros for all cross sections except absorption, to compose a complete set of cross sections for U^{238}. The options permit the selection of a set of absorption cross sections properly adjusted with respect to resonance saturation and Doppler broadening. The numbers in parentheses indicate the concentration in mole % of $U^{238}F_4$ in mixtures of LiF and BeF_2 such as those used in the molten-salt reactors. Thorium is treated similarly, and absorption cross section options for both mixtures with lithium and beryllium fluorides and graphite (denoted by G in parentheses) are available.

Design of 30-Mw Experimental Reactor

Work is continuing on the 30-Mw, one-region, experimental, molten-salt reactor described in the previous report.[4] The basic reactor concept has remained unchanged. More details of the equipment have been developed, and various auxiliary system layouts are being studied. A reactor site has been selected for design purposes, and perspective drawings of a test reactor building have been prepared.

The bayonet-type fuel-to-coolant heat exchanger is being redesigned in an effort to simplify the fabrication problems. Design data for use in layout studies have been prepared for a U-tube, U-shell, coolant-salt-to-steam superheater.

---

[4]MSR Quar. Prog. Rep. Jan. 31, 1959, ORNL-2684, p 3.

Fuel Drain System

The fuel drain system consists of four 2-1/2-ft-dia vessels approximately 20 ft long. These tanks will be suspended in a vertical position and manifolded to the reactor with pressure-siphon drain lines. Two drain vessels will be required to contain the fuel system inventory, and each pair of tanks will have a separate system to isolate it from the reactor. The two extra drain tanks will provide capacity for a spare salt volume, which may be used for fuel system cleaning or decontamination operations.

The vessels will be preheated and afterheat will be removed with a recirculating gas system. This gas system, as in the case of the reactor gas system, will include a blower, heater, and cooler packages enclosed in a loop.

The drain system criticality problem is being investigated. A multiplication constant of less than 0.5 was obtained for one drain vessel presumed to contain the entire fuel system UF_4 inventory in an LiF-BeF_2 salt mixture. As a further check, the U^{235} was assumed to settle out in the vessel as an oxide compound, and multiplication constants are being obtained for four different geometries of fuel concentrate, with one edge reflected by the salt mixture. A maximum multiplication constant has not yet been obtained, but, with the fuel concentrated in a cube, the multiplication constant was 0.83. It is believed that this value would increase slightly with further settling of the fuel. The bottom section of the drain vessel will therefore be made with a smaller diameter to reduce the potential hazard.

Gamma Heating in the Core Vessel of the 30-Mw Experimental Reactor

The heat generation in the core vessel of the experimental reactor has been calculated using the Oracle program Ghimsr.[5,6] The total heat

---

[5] L. G. Alexander and J. W. Miller, Heat Generation in the One-Region, Experimental Molten-Salt Reactor, ORNL-2746 (to be published).

[6] D. B. Grimes, Ghimsr, Gamma Heating in Molten-Salt Reactors, ORNL CF 59-5-40 (to be published).

generation was 2.30 w/cm^3 at the inner surface of the core vessel. The individual contributions to the total heating are given below:

Source	Heating (w/cm^3)
Prompt gamma rays	0.61
Delayed gamma rays	0.52
Inelastic scattering gamma rays	0.34
Beryllium capture gamma rays	0.02
Fluorine capture gamma rays	0.07
Uranium capture gamma rays	0.15
Core vessel capture gamma rays	0.59
Total	2.30

1.2. COMPONENT DEVELOPMENT AND TESTING

Salt-Lubricated Bearings for Fuel Pumps

Hydrodynamic Journal Bearings

The sixth test of a journal bearing operating in molten-salt fuel 130 (LiF-BeF$_2$-UF$_4$, 62-37-1 mole %), as described previously,[1] was terminated on schedule. During this test the temperature of the salt was increased in 50°F increments from 1200 to 1500°F. Performance was satisfactory throughout the entire test, which was conducted at a constant journal speed of 1200 rpm and a constant radial load of 200 lb. The total operating time for this test was 192 hr.

A seventh test was then performed with the bearing and journal used in the fifth and sixth tests. This test also consisted of steady-state operation at a journal speed of 1200 rpm and a radial load of 200 lb, but start-stop operations were carried out three times at each test temperature. The temperature was varied as in the sixth test from 1200 to 1400°F in 50°F increments. On attempting a second restart at the 1400°F temperature level, an increase in the power required was noted, and the test was halted. The total operating time for this test was 216 hr. Inspection revealed a galled spot on the loaded side of the bearing.

The eighth test was conducted to study the effect of increasing the bearing radial clearance (measured at room temperature) to 0.007 in. All bearings previously tested had a radial clearance of 0.005 in. Molten-salt fuel 130 at 1200°F was used for this test, and the bearing radial load was varied from 50 to 500 lb at each of two journal speeds, 600 and 1200 rpm. After 356 hr of operation, including 39 start-stop sequences, a sudden increase in power halted the test. At the time the power increase occurred the journal was operating at 600 rpm, and the load was being increased from 300 to 400 lb; the load had reached 382 lb. From the standpoint of minimum film-thickness, these conditions were the

---

[1] MSR Quar. Prog. Rep. Jan. 31, 1959, ORNL-2684, p 39.

most stringent yet imposed in these molten-salt-lubricated bearing tests.

A carburized INOR-8 journal was used with an uncarburized INOR-8 bearing for the ninth test. The tester was started and stopped 260 times during a period of operation of 272 hr at 1200°F. The journal speed was 1200 rpm and the bearing was loaded to 200 lb. Both the bearing and the journal were in good condition, with undamaged surfaces, at the end of the test. The bearing is shown in Fig. 1.2.1 and the journal in Fig. 1.2.2.

Hydrodynamic Thrust Bearings

Assembly of the thrust-bearing tester described previously[1] is nearly completed. The thrust-load actuator is being given preliminary tests prior to being fitted to the rotary portion of the tester.

Test of Pump Equipped with One Salt-Lubricated Journal Bearing

Detailed design work is nearly complete on the modifications to be made to a PK type of centrifugal sump pump in order to replace the lower oil-lubricated bearing with a molten-salt-lubricated hydrodynamic journal bearing. The external motor of the PK pump is being replaced with an integral, totally enclosed motor. The configuration of the modified pump is intended to simulate, in large measure, that of the pump proposed for use in an experimental molten-salt reactor. Proposals have been received for the fabrication of the motor and the pump shaft, and purchase orders are being placed. An existing facility is being prepared for tests of this pump.

Bearing Mountings

Means are being investigated for flexibly mounting INOR-8 bearings to INOR-8 pump casings so that thermal distortion between the bearing and the pump shaft journal can be accommodated. A diaphragm type of mounting and a mounting that is somewhat similar to the Westinghouse "Thermoflex" mount are being studied.

O   1   2   3

INCHES
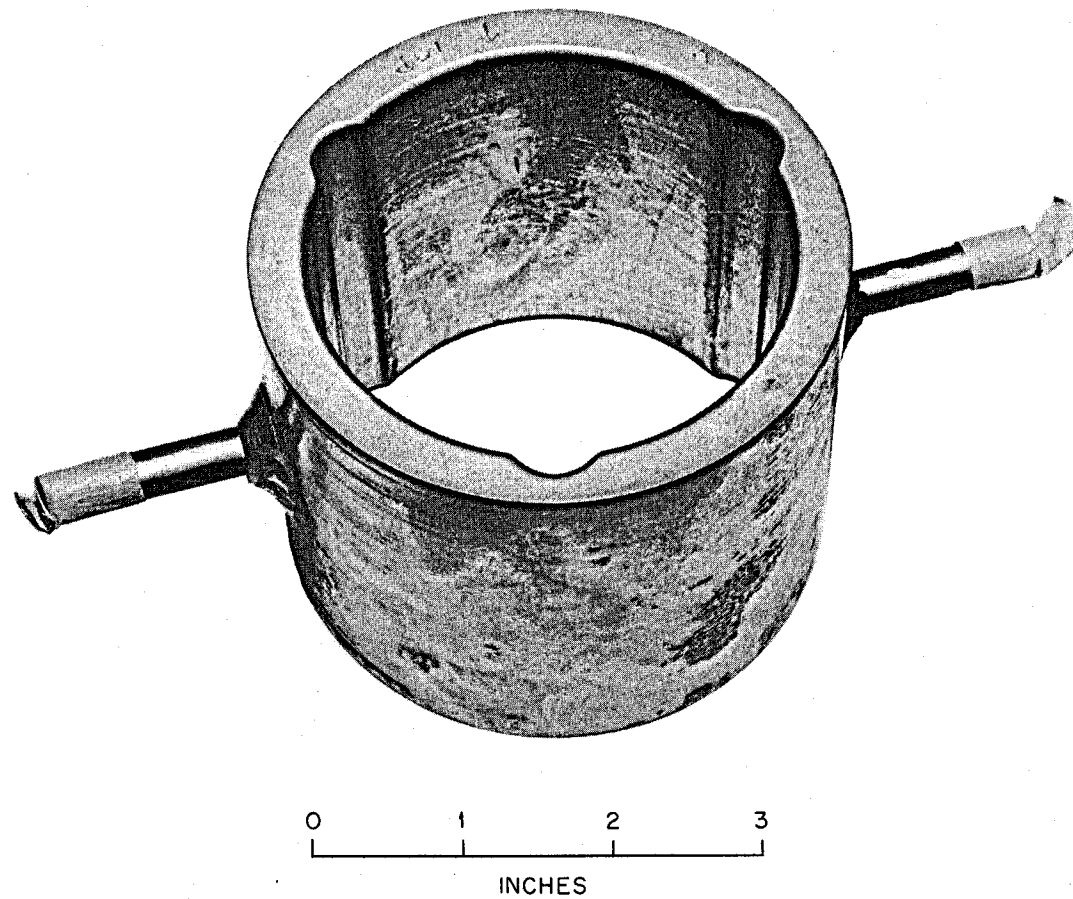
Fig. 1.2.1. INOR-8 Bearing After Operation for 272 hr at 1200°F with Molten-Salt Lubrication.


O   1   2   3

INCHES
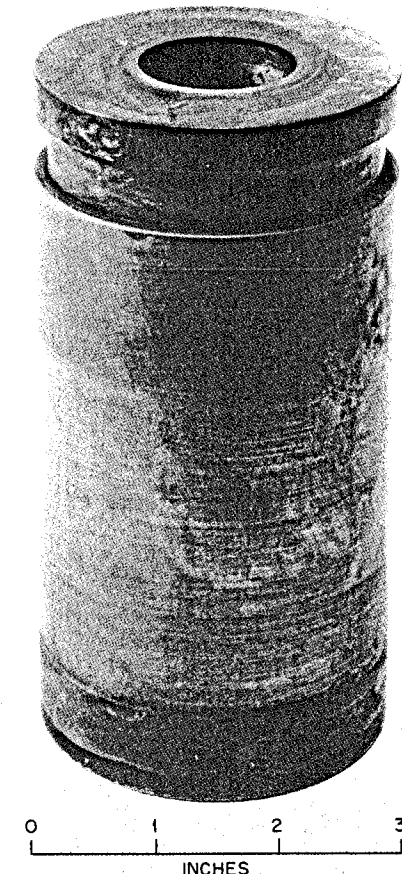
Fig. 1.2.2. Carburized INOR-8 Journal After Operation for 272 hr at 1200°F with Molten-Salt Lubrication.

Mechanical Seals for Pumps

The modified Fulton-Sylphon bellows-mounted seal[2] being subjected to an endurance test in a PK-P type of centrifugal pump has accumulated an additional 1848 hr of operation since the previous report period, for a total of 12,478 hr. The pump has been operating at a temperature of 1200°F, a shaft speed of 2500 rpm, and a NaK flow rate of 1200 gpm. The maximum test-seal leakage rate was 3.5 cm^3/day; however, on an averaged basis, the leakage is still negligible. Two pump stoppages occurred — one for reworking·the drive motor commutator and replacing the motor brushes, and one as a precautionary measure during a power outage.

Pump Endurance Testing

An MF type of centrifugal pump has continued in operation,[3] and has logged more than 15,500 hr (approximately 1 3/4 yr) of continuous operation. No maintenance has been performed on the pump during this period. During the last 13,465 hr, a cavitation endurance test has been under way with the pump operating at the steady-state conditions of 2700 rpm, 645 gpm, and 2.5-psig pump tank cover gas pressure at 1200°F. During the quarter the pump was stopped five times. Two stops were momentary and were caused by power outages. One stop was of 65 min duration for replacing brushes in the motor-generator set. One stop was of 30 min duration for calibrating the pressure-measuring devices. One stop was for 60 min for freeing the system throttle valve that had become stuck.

Frozen-Lead Pump Seal

The small frozen-lead pump seal being tested on a 3/16-in.-dia shaft, as described previously,[4] has operated continuously since it was

---

[2]MSR Quar. Prog. Rep. Jan. 31, 1959, ORNL-2684, p 42.

[3]MSR Quar. Prog. Rep. Jan. 31, 1959, ORNL-2684, p 42.

[4]W. B. McDonald, E. Storto, and J. L. Crowley, MSR Quar. Prog. Rep. Oct. 31, 1958, ORNL-2626, p 23.

started on June 13, 1958. The accumulated operating time is more than
7500 hr. Except for slight leakage of lead during the first 100 hr of
operation, there has been no further leakage.

The large lead pump seal with a 3 1/4-in.-dia rotating shaft has
been operating for 3600 hr. Leakage of solid lead from the seal is
sporadic. The average leakage rate for the time operated is 9 cm^3/hr.
Operational data suggest that the seal should be redesigned to provide
better coolant control and to incorporate a short, resilient packing to
decrease the annulus between the seal and the shaft. A detailed
description of the equipment was presented previously.[5] At the present
time, the operating conditions are the following

Shaft speed	975–1000 rpm
Argon pressure over molten lead in tank	0–3 psig
Seal cooling water flow rate	0.8 gpm
Temperature rise in cooling water	~25°F
Temperature where seal is formed	180–190°F

Techniques for Remote Maintenance of the Reactor System
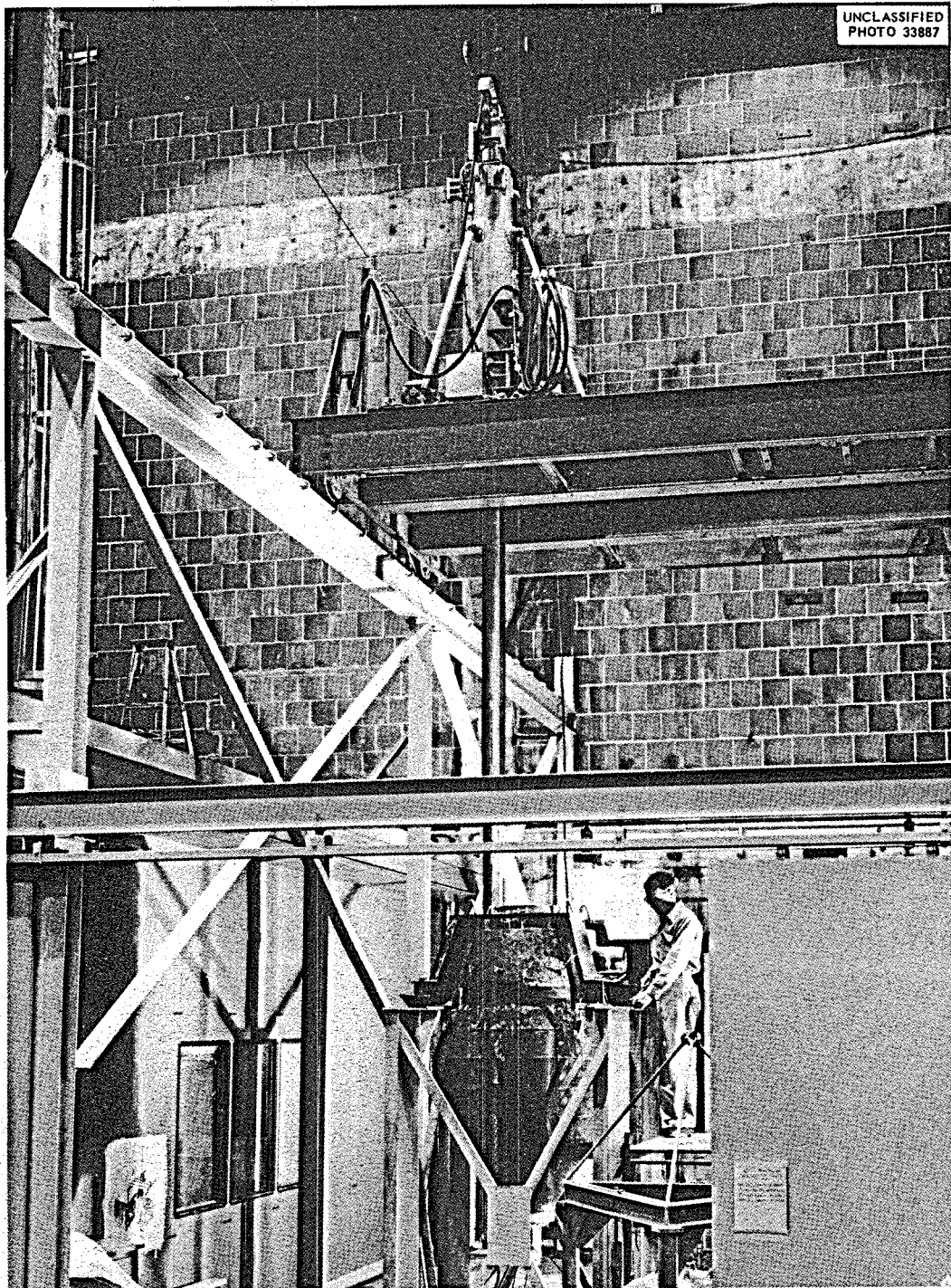
Progress has been made in the design and construction, Fig. 1.2.3,
of a remote maintenance demonstration facility. The scheduled completion
date is June 30, 1959, and all phases of the work are on schedule.

The General Mills mechanical arm manipulator, 3 1/2- and 6-in.
Inconel piping subassemblies, dummy heat exchangers, salt dump tank,
dummy reactor, two closed-circuit television systems (Fig. 1.2.4), and
the spool for joining the pump and motor have been received. One of the
20 sets of freeze-flange pipe joints (Fig. 1.2.5) is on hand, and the
modifications required to adapt an existing PK type of pump for use in
this facility have been completed.
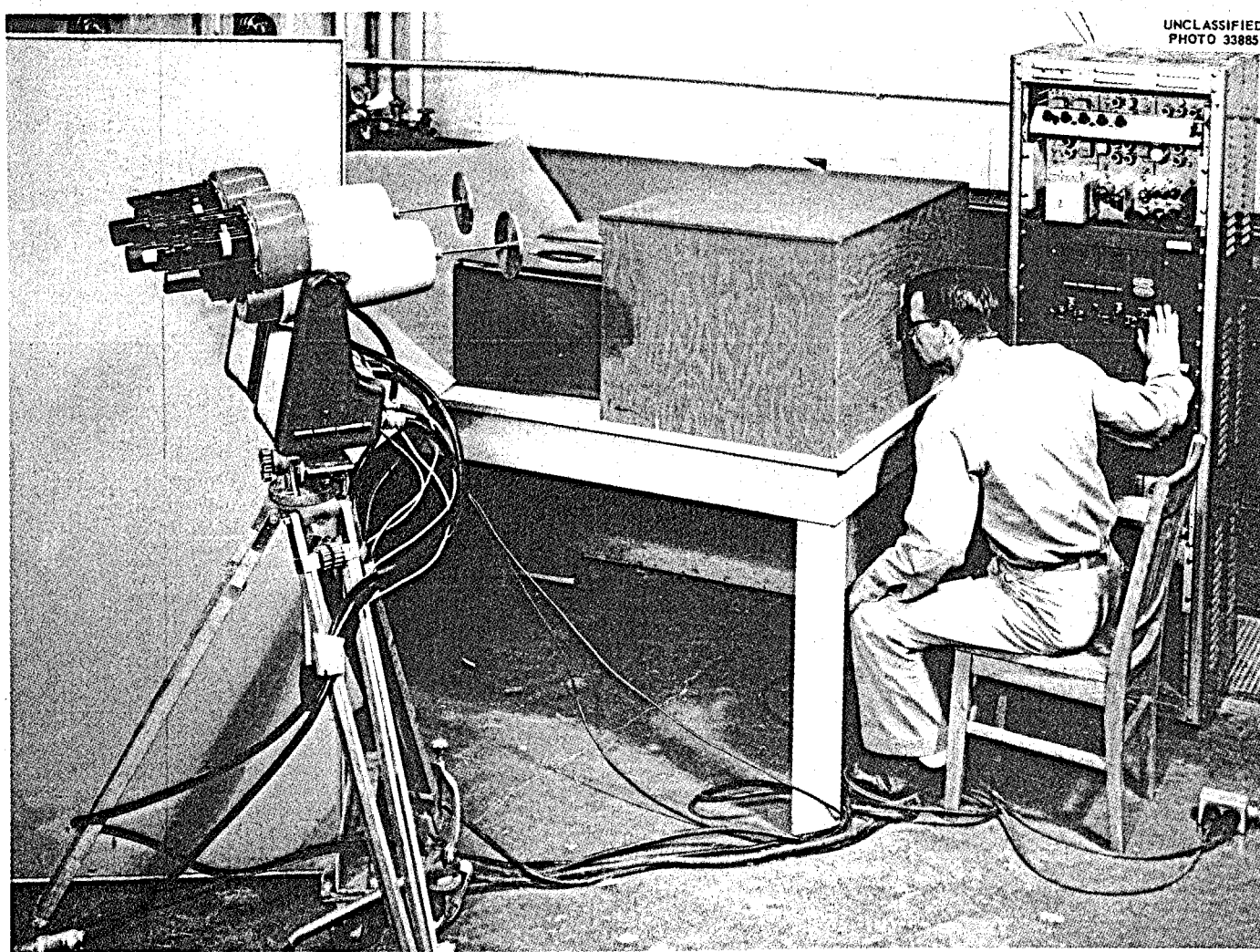
Eleven pipe preheater and insulation units that were designed to

---

[5]MSR Quar. Prog. Rep. Jan. 31, 1959, ORNL-2684, p 43.
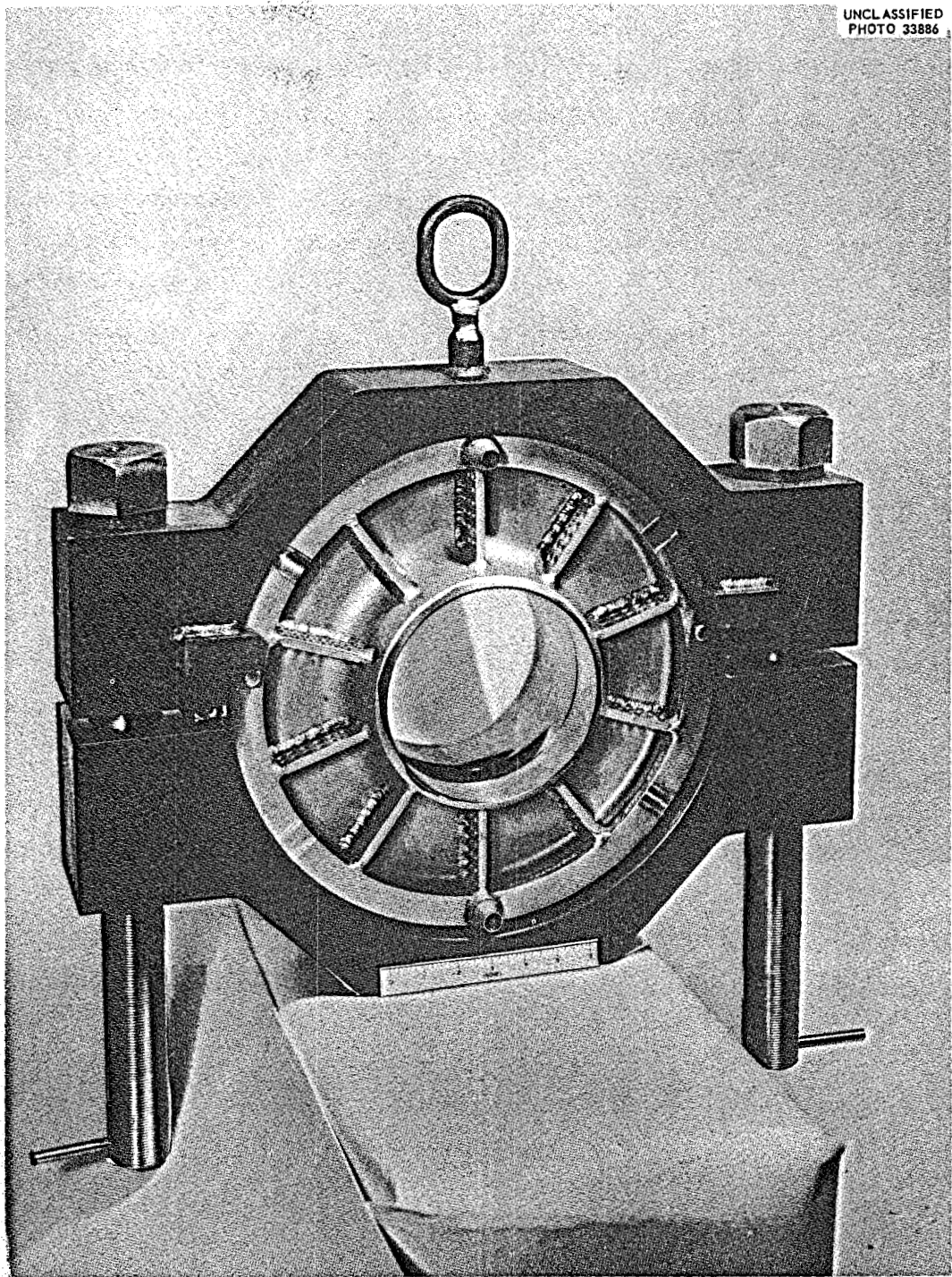
Fig. 1.2.3. Remote Maintenance Demonstration Facility Under Construction.

Fig. 1.2.4. Closed-Circuit Stereo Television Equipment for Remote Maintenance Demonstration Facility.

Fig. 1.2.5. A Freeze-Flange Joint for a 6-in. Pipe in the Remote Maintenance Demonstration Facility.

contain electric heaters and insulation in one package are being fabricated. These units are to be removable and replaceable in short sections with the use of the General Mills manipulator. Specially designed spring-type pipe supports are being procured. Three gas and compressed-air control cabinets are being fabricated.

Installation of the General Mills manipulator, heat exchangers, dummy reactor, salt-circulating pump, salt piping, service piping, pump-lube-oil piping, and electric heater control cabinets is in progress.

Design, Construction, and Operation of Materials Testing Loops

Forced-Circulation Loops

The operation of long-term forced-circulation corrosion-testing loops was continued. Fourteen test loops are presently in operation, two Inconel loops were terminated as scheduled during the quarter, and one new Inconel loop was started. A loop fabricated of INOR-8 is presently being installed.

The two Inconel loops, designated 9344-2 and 9377-3 in Table 1.2.1, were terminated after one year of operation. The facilities from which these loops were removed have now been revised according to the latest design[6] for long-term operation. Of the 15 available loop facilities, 11 are of the improved design, and the remaining four loops are in various stages of improvements.

Several momentary power failures caused interruption of power to the loops during the quarter, but flow resumed in all the loops after power was restored, and there were no freeze-ups. The power failures that have occurred since the beginning of this molten-salt-reactor corrosion-testing program and the results of such failures are described in Table 1.2.2.

The loops designated MSRP-12 and 9377-5 in Table 1.2.1 contain molten-salt-sampling devices. It was necessary to add 600 g of salt

---

[6]J. L. Crowley, MSR Quar. Prog. Rep. June 30, 1958, ORNL-2551, p 36.

Table 1.2.1. Forced-Circulation Loop Operations Summary as of March 31, 1959

Loop Designation	Loop Material and Size	Composition Number of Circulated Fluid[a]	Approximate Flow Rate (gpm)	Approximate Reynolds Number	Maximum Wall Temperature (°F)	Temperature Difference Across Loop (°F)	Hours of Operation at Conditions Given	Special Features	Comments
9354-3	INOR-8 Hot leg, $\frac{3}{8}$ in. sched 40 Cold leg, $\frac{1}{2}$ in. OD, 0.045 in. wall	84	2.8	4500 5400	1200	100	10,565	Contains a Hastelloy B pump	Normal operation
9344-2	Inconel, $\frac{1}{2}$ in. OD, 0.045 in. wall	12	2.5	8200	1200	200	8,800		Terminated Jan. 28, 1959 after one year of operation
9377-3	Inconel, $\frac{1}{2}$ in. OD, 0.045 in. wall	131	2	3400	1300	200	8,770		Terminated March 18, 1959 after one year of operation
9354-1	INOR-8, $\frac{1}{2}$ in. OD, 0.045 in. wall	126	2.5	2000	1300	200	8,661		Normal operation
9354-5	INOR-8, $\frac{3}{8}$ in. OD, 0.035 in. wall	130	1	2200	1300	200	7,748	Contains box of graphite rods in hot fluid stream, with surface ratio of 2:3[b]	Normal operation
9354-4	INOR-8 Hot leg, $\frac{3}{8}$ in. sched 40 Cold leg, $\frac{1}{2}$ in. OD, 0.045 in. wall	130	2.5	3000 3500	1300	200	5,852	Contains two machined sample inserts in resistance-heated section[c]	One sample insert removed Feb. 17, 1959 after 5000 hr of operation; loop restarted with same fluid; normal operation otherwise
MSRP-7	INOR-8, $\frac{1}{2}$ in. OD, 0.045 in. wall	133	1.8	3100	1300	190	5,573	This loop and all others below have redesigned safety features[d]	Normal operation
9377-4	Inconel, $\frac{1}{2}$ in. OD, 0.045 in. wall	130	1.8	2600	1300	200	5,565		Normal operation
MSRP-6	INOR-8, $\frac{1}{2}$ in. OD, 0.045 in. wall	134	1.8	2300	1300	200	5,183		Normal operation
MSRP-8	INOR-8, $\frac{1}{2}$ in. OD, 0.045 in. wall	124	2	4000	1300	200	4,957		Normal operation
MSRP-9	INOR-8, $\frac{1}{2}$ in. OD, 0.045 in. wall	134	1.8	2300	1300	190	4,789		Normal operation
MSRP-10	INOR-8, $\frac{1}{2}$ in. OD, 0.045 in. wall	135	2	3400	1300	200	4,623		Normal operation
MSRP-11	INOR-8, $\frac{1}{2}$ in. OD, 0.045 in. wall	123	2	3200	1300	190	4,227		Normal operation
MSRP-12	INOR-8, $\frac{1}{2}$ in. OD, 0.045 in. wall	134	1.8	2300	1300	200	3,659	Contains a molten-salt sampling device[e]	Normal operation
9377-5	Inconel, $\frac{1}{2}$ in. OD, 0.045 in. wall	134	1.8	2300	1300	190	3,031	Contains a molten-salt sampling device[e]	Normal operation
9377-6	Inconel, $\frac{1}{2}$ in. OD, 0.045 in. wall	133	1.8	3100	1300	190	793		Began operation Feb. 26, 1959

[a]Composition 12: NaF-KF-LiF (11.5-42-46.5 mole %) Composition 130: LiF-BeF$_2$-UF$_4$ (62-37-1 mole %)
Composition 84: NaF-LiF-BeF$_2$ (27-35-38 mole %) Composition 131: LiF-BeF$_2$-UF$_4$ (60-36-4 mole %)
Composition 123: NaF-BeF$_2$-UF$_4$ (53-46-1 mole %) Composition 133: LiF-BeF$_2$-ThF$_4$ (71-16-13 mole %)
Composition 124: NaF-BeF$_2$-ThF$_4$ (58-35-7 mole %) Composition 134: LiF-BeF$_2$-ThF$_4$-UF$_4$ (62-36.5-1-0.5 mole %)
Composition 126: LiF-BeF$_2$-UF$_4$ (53-46-1 mole %) Composition 135: NaF-BeF$_2$-ThF$_4$-UF$_4$ (53-45.5-1-0.5 mole %)
[b]J. L. Crowley, *MSR Quar. Prog. Rep. Jan. 31, 1958*, ORNL-2474, p 31.
[c]*Ibid.*, p 32.
[d]J. L. Crowley, *MSR Quar. Prog. Rep. June 30, 1958*, ORNL-2551, p 36, Fig. 1.2.16.
[e]J. L. Crowley, *A Sampling Device for Molten Salt Systems*, ORNL-2688 (to be issued).
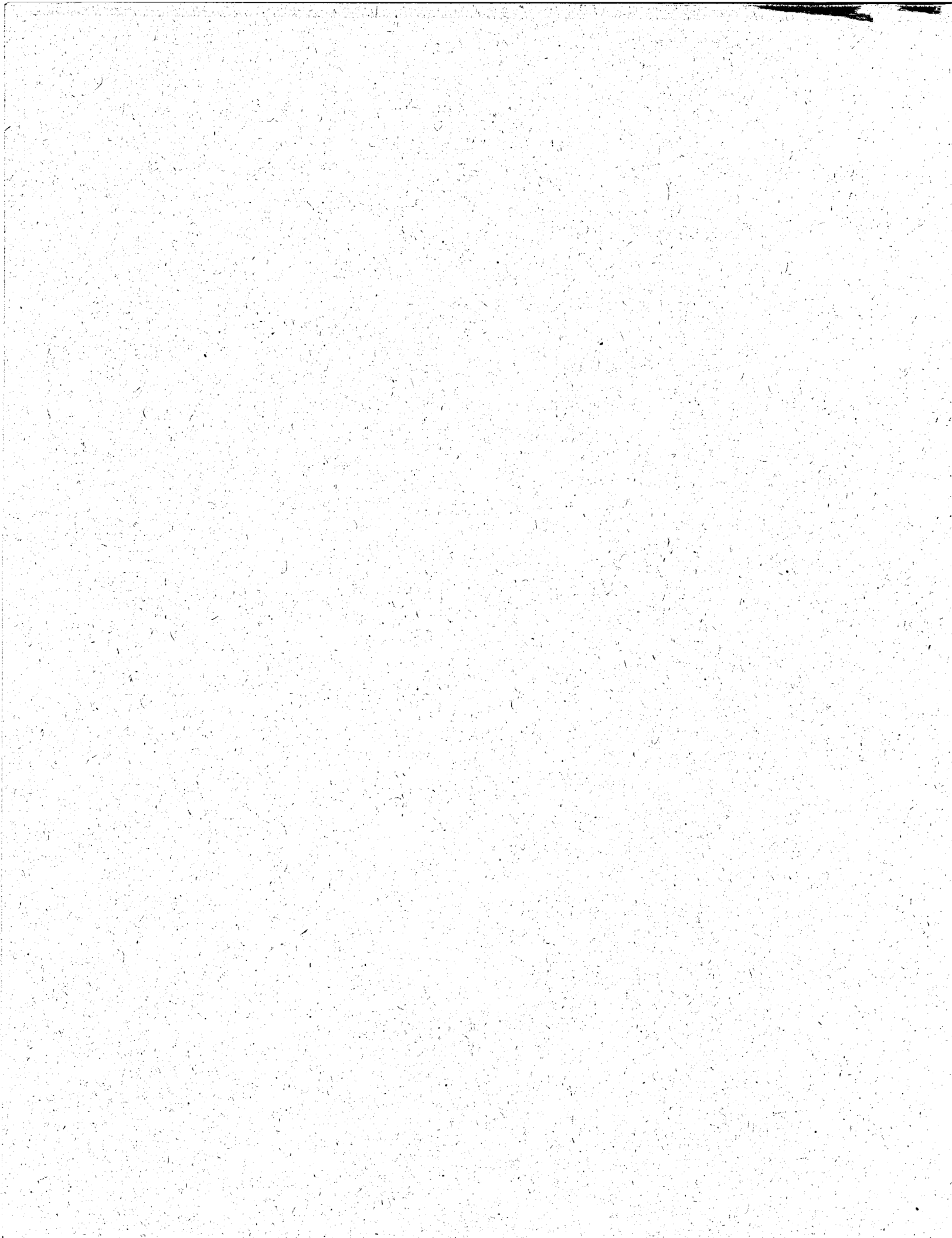
Table 1.2.2. Summary of Power Failures That Have Occurred During
Operation of Forced-Circulation Corrosion-Testing Loops

Date	Number of Loops Operating	Number of Loops Affected	Number of Loops in Which Salt Froze	Number of Loops That Failed as Result of Power Failure
December 17, 1957	5	5	5	1
April 6, 1958[a]	9	6	6	3
August 5, 1958	7	7	2[b]	None
November 7, 1958	14	14	None	None
January 15, 1959	15	15	None	None
March 15, 1959	15	12	None	None

[a]Automatic controls installed on most loops between April and August.

[b]These loops did not have automatic controls; only part of the salt froze.

to replenish the inventory and thus raise the fluid level to the normal height in loop 9377-5 after 27 samples had been taken. The molten salt was introduced into the pump bowl through the pump flange without interruption of the flow or operation of the loop. Analyses of the samples removed from these loops periodically are presented in Section 2.2.

In-Pile Loops

The in-pile loop which was operated in the MTR during the previous quarter was disassembled, and the cause of the partially plugged purge line, which resulted in the release of activity, was determined. Oil which leaked past the pump shaft seal and filled the oil trap on the purge outlet line was polymerized by radiation, and the polymerized oil plugged the outlet line. Chemical and metallographic analyses of the fuel and container materials have not been completed.

The second in-pile loop was completed and inserted during the MTR shutdown of April 27. Modifications were made to the internal

purge system to minimize the probability of purge line plugging. In addition, changes were made to the external purge system which should eliminate the possibility of a repetition of the activity release. These changes included the installation of a charcoal trap in the purge inlet line to prevent back-diffusion of fission gas into un-shielded lines. A prototype in-pile pump identical to that installed in the second loop has accumulated over 3600 hr of satisfactory operation.

1.3. ENGINEERING RESEARCH

Physical Property Measurements

Enthalpy and Heat Capacity

Determinations were made of the enthalpies, heat capacities, and heats of fusion of three additional beryllium-containing fluoride salt mixtures: salt 133 ($LiF-BeF_2-ThF_4$, 71-16-13 mole %), salt 134 ($LiF-BeF_2-ThF_4-UF_4$, 62-36.5-1-0.5 mole %), and salt 136 ($LiF-BeF_2-UF_4$, 70-10-20 mole %). The results of these measurements are presented in Table 1.3.1 as the constants a, b, and c appearing in the correlating equations,

$$H_T - H_{30^\circ C} = a + bT + cT^2$$

and

$$c_p = b + 2cT \quad ,$$

where H is the enthalpy (cal/g); c_p, the heat capacity (cal/g·$^\circ$C); and T, the temperature ($^\circ$C). The experimental enthalpy data for these three mixtures, along with earlier results[1] for related mixtures, are summarized in Fig. 1.3.1. It may be seen by comparing the results for salts 133 and 136 with the curve for mixture 130 ($LiF-BeF_2-UF_4$, 62-37-1 mole %) that altering the salt composition toward larger percentages of the high-molecular-weight fluorides (ThF_4 and UF_4) causes a substantial decrease in both the enthalpy and heat capacity (on a unit weight basis). Replacement of the LiF in salt 126 ($LiF-BeF_2-UF_4$, 53-46-1 mole %) with NaF (mixture 123; $NaF-BeF_2-UF_4$, 53-46-1 mole %) results in similar, though smaller, reductions in the enthalpy and heat capacity. This effect will be studied further in order to establish a general correlation for the prediction of enthalpies and heat capacities in the $LiF-BeF_2-UF_4-ThF_2$ system.

---

[1]W. D. Powers and R. H. Nimmo, MSR Quar. Prog. Rep. Oct. 31, 1958, ORNL-2626, p 44.

Table 1.3.1. Enthalpy Equation Coefficients and Heats of Fusion of
Several Fused Salt Mixtures

Salt Mixture	Phase	Temperature Range (°C)	Enthalpy Equation Coefficients[a]			Heat of Fusion (cal/g)	
			a	b	c	Temperature (°C)	$H_L - H_S$
					$\times 10^{-5}$		
LiF-BeF$_2$-ThF$_4$-UF$_4$	Solid	100-350	-4.9	+0.224	+34.65	450	64
(62-36.5-1-0.5 mole %)	Liquid	500-800	-2.1	+0.545	-4.03		
LiF-BeF$_2$-ThF$_4$	Solid	100-400	-7.7	+0.209	+4.58	500	74
(71-16-13 mole %)	Liquid	550-800	-47.4	+0.473	-11.90		
LiF-BeF$_2$-UF$_4$	Solid	100-400	-5.6	+0.153	+3.50	450	53
(70-10-20 mole %)	Liquid	550-800	-17.8	+0.289	-3.21		

[a]The enthalpy is given as $H_T - H_{30°C} = a + bT + cT^2$; the heat capacity is then evaluated as $c_p = b + 2cT$.

Viscosity

The viscosities of salt mixtures 133 and 136 have been obtained over the temperature range from 550 to 800°C with the "skirted" capillary efflux viscometer previously described.[2] The viscometer cups used for the measurements were those employed in the earlier studies with salts 130 and 134. Recalibration of these cups with the $NaNO_2$-$NaNO_3$-KNO_3 (40-7-53 wt %) mixture showed negligible changes in the kinematic viscosity—efflux time relation. The results, correlated in the form

$$\mu = Ae^{B/T} ,$$

where μ is the viscosity (centipoise), T is the temperature (°K), and A and B are experimentally determined constants, are as follows:

$$\text{Salt 133} \quad A = 0.0526; \; B = 4838$$
$$\text{Salt 136} \quad A = 0.0489; \; B = 4847$$

The data are plotted in Fig. 1.3.2 and compared with data from measurements of salts 123, 126, 130, and 134.[3] The "high" results with mixtures 123 and 126 will be rechecked with the new type of viscometer. In Fig. 1.3.3, the data for salt 136 are compared with Mound Laboratory results[4] for the same mixture that were obtained with a Margules design viscometer consisting of two concentric Inconel cylinders. The outer of the two cylinders contained the fused salt and was rotated at a fixed speed with reference to the inner stationary cylinder. The viscosity was determined from the torque exerted on the inner cylinder. The reason for the discrepancy between the two sets of data has not yet been established.

Surface Tension

The surface tension of molten-salt mixture 134 was experimentally determined using the maximum-bubble-pressure technique.[3] The results,

---

[2] MSR Quar. Prog. Rep. Jan. 31, 1959, ORNL-2684, p 65.

[3] W. D. Powers, MSR Quar. Prog. Rep. June 30, 1958, ORNL-2551, p 38.

[4] B. C. Blanke et al., Density and Viscosity of Fused Mixtures of Lithium, Beryllium, and Uranium Fluorides, MLM-1086 (March 23, 1959).
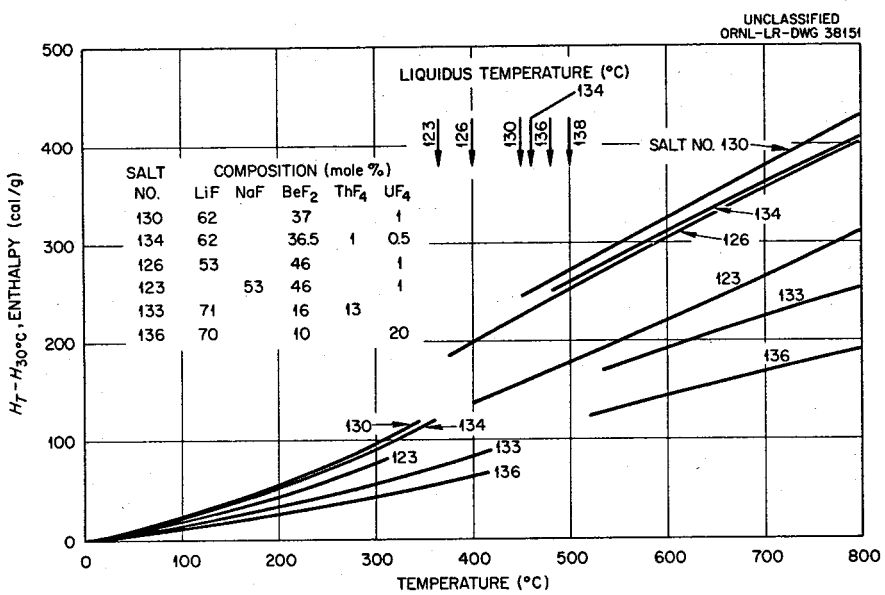
Fig. 1.3.1. Enthalpy-Temperature Relations for Several Beryllium-Containing Salt Mixtures.
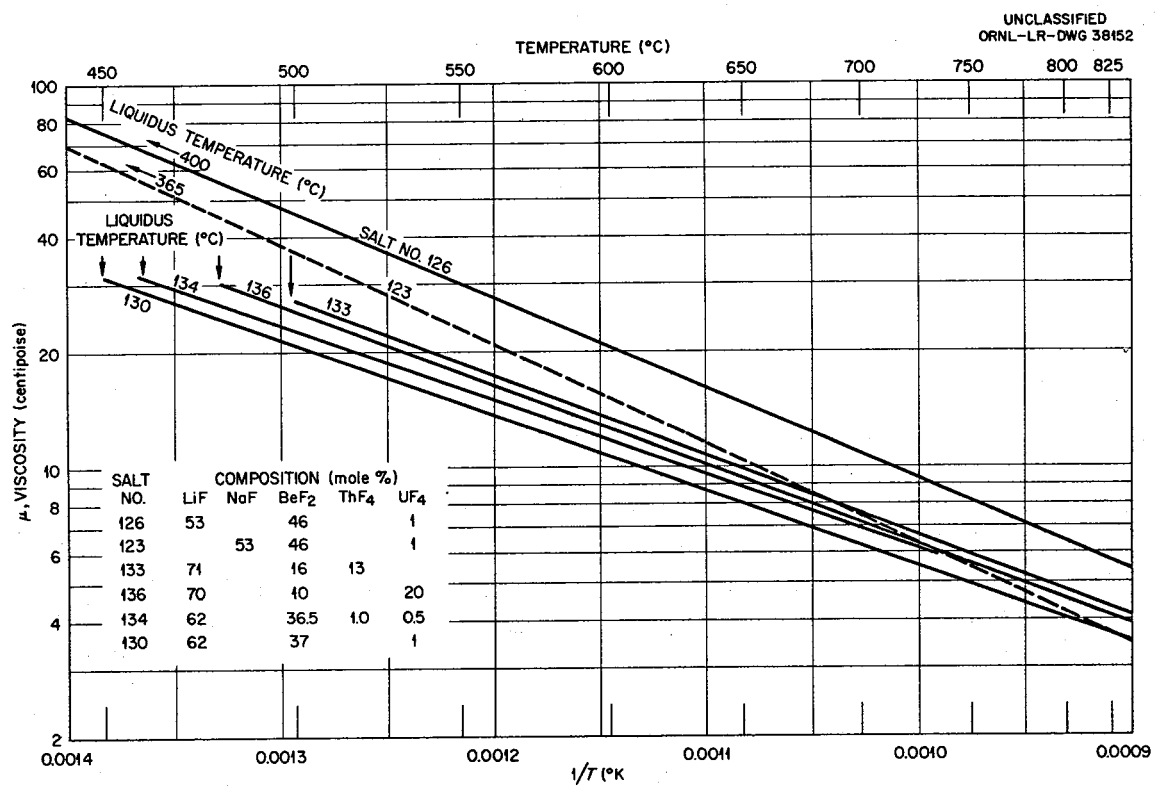
Fig. 1.3.2. Viscosity-Temperature Relations for Several Beryllium-Containing Salt Mixtures.

given in Fig. 1.3.4, can be represented by the equation,
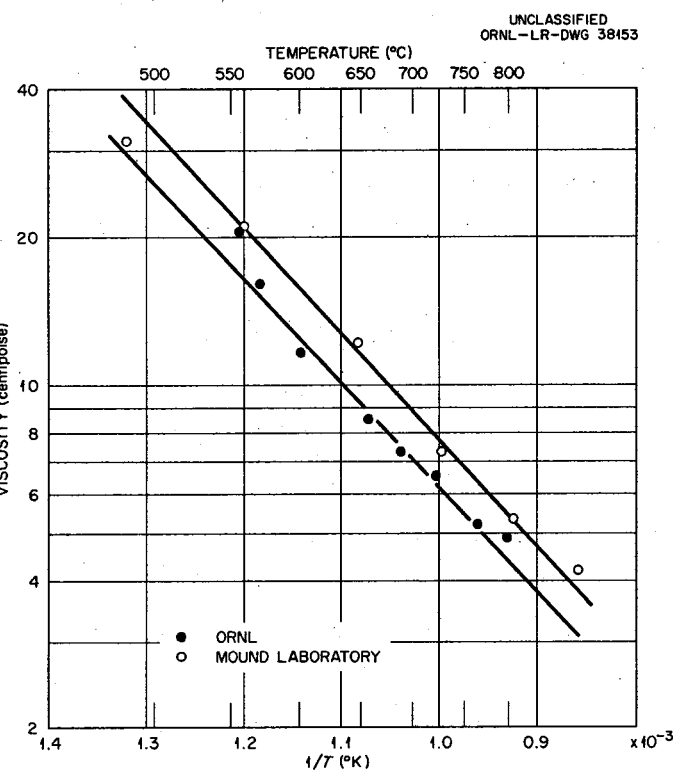
$$\sigma \, (\text{dynes/cm}) = 272.2 - 0.143 \, T \, (^\circ C),$$

to within $\pm 5\%$ over the temperature range from 500 to 800°C. The salt 134 data are essentially identical with the results obtained for salt 130, except for a slight difference in the temperature dependence.
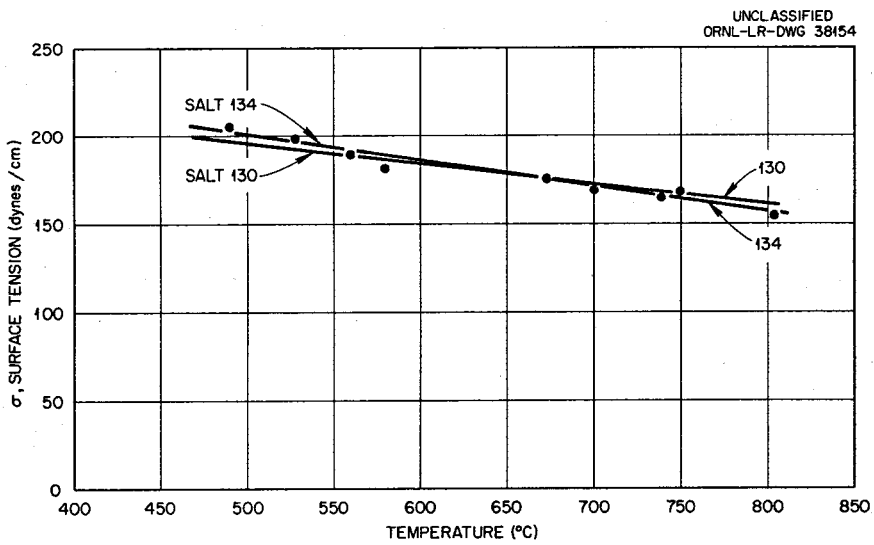
Heat-Transfer Studies

Flow calibration of the system designed for determining surface film formation in molten-salt systems by heat transfer coefficient measurements has been completed. A Tygon-coupled mockup was used, and water was the working fluid. The test unit is shown in Fig. 1.3.5, and the key components are indicated. The over-all system pressure drop was obtained with a 100-in. mercury manometer connected at the pump inlet and outlet lines. The data indicate a pressure difference of about 48 psig for a flow of 2.8 gpm. This corresponds to a test-section Reynolds modulus of 11,000 at 1200°F with a salt such as mixture 130 ($LiF\text{-}BeF_2\text{-}UF_4$; 62-37-1 mole %). Initial attempts to determine the flow rate vs pump speed characteristic by a weight method were unsuccessful, and a rotameter was used in the final calibration. A magnetic-pulse pickup coupled with a Hewlett-Packard counter yielded the pump speed to within ± 1 rpm over any 10-sec counting period. The characteristic curve obtained was very nearly linear between 2000 and 6000 rpm, ranging from 1 to 3 gpm, respectively.

Design work is continuing on the system support structure to ensure against buckling of the test sections due to thermal expansion and to prevent electrical short-circuiting of the test-section heating currents. Welding of system components is in progress.

Fig. 1.3.3. Comparison of Independent Measurements of the Viscosity of Salt Mixture 136 (LiF-BeF$_2$-UF$_4$, 70-10-20 mole %).

Fig. 1.3.4. Surface Tension of LiF-BeF$_2$-ThF$_4$-UF$_4$ (62-36.5-1-0.5 mole %).
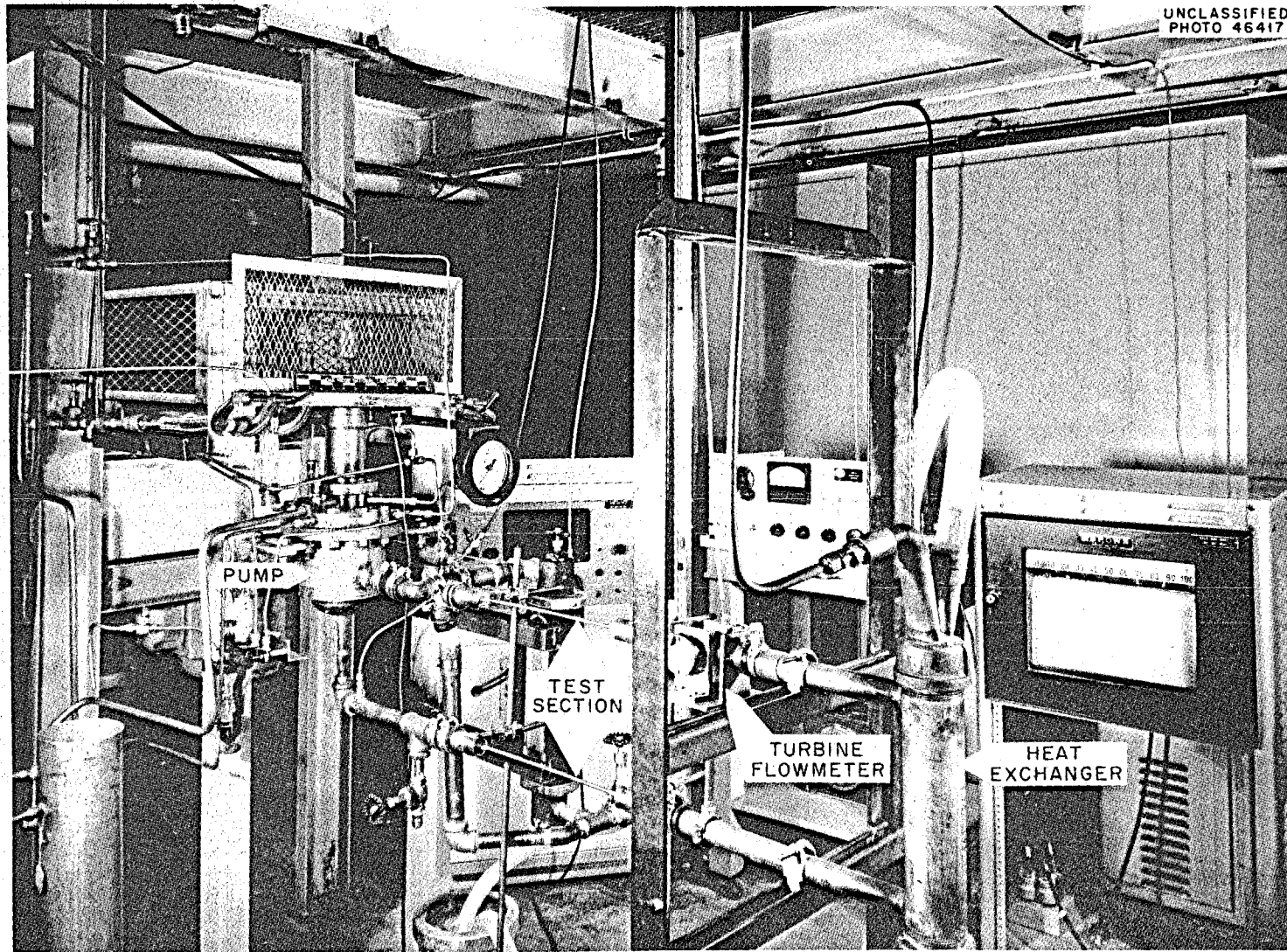
Fig. 1.3.5. Flow Calibration Mockup of Molten-Salt Heat Transfer System.

Hydrodynamic Studies

The pressure drop through the sintered-metal-filled annulus of a double-walled tube has been determined.[5] A tube of this construction has been proposed for use in steam-generation systems associated with molten-salt power reactors. It is hoped to provide good thermal contact between the low-pressure primary salt and the high-pressure steam and at the same time effectively isolate the two fluids in the event of a wall failure. The sintered medium would be filled with static helium, at an intermediate pressure, which would give an indication of a break in either wall.

The results of this study of the flow of helium through two specimens of double-walled Inconel tubing containing sintered Inconel of different porosities are given in Fig. 1.3.6. The correlating lines can be expressed by the equations:

$$G_g = 0.342 \left(\bar{\rho} \frac{\Delta P}{L} \right)^{0.979}$$

for specimen 1, with a porosity of approximately 59%, and

$$G_g = 0.0046 \left(\bar{\rho} \frac{\Delta P}{L} \right)^{0.960}$$

for specimen 2, with a porosity of approximately 25%. In these correlating expressions, G_g is the mass velocity based on the geometric cross-sectional area[6] (lb_m/ft^3), $\bar{\rho}$ is the mean helium density (lb_m/ft^3), ΔP is the pressure drop through the sintered material (lb_f/ft^2), and L is the length of the sintered section. The experimental precision was estimated to be $\pm 8\%$. The two curves in Fig. 1.3.6 are nearly parallel, with slopes only slightly less than unity, and are in accord with the statement of Darcy's law for the flow of gases in porous media,

---

[5]J. L. Wantland, H. W. Hoffman, and R. L. Miller, Flow Through Sintered Inconel Annuli, ORNL CF 58-9-36 (Sept. 17, 1958).

[6]As opposed to an estimated pore void area at any cross section.
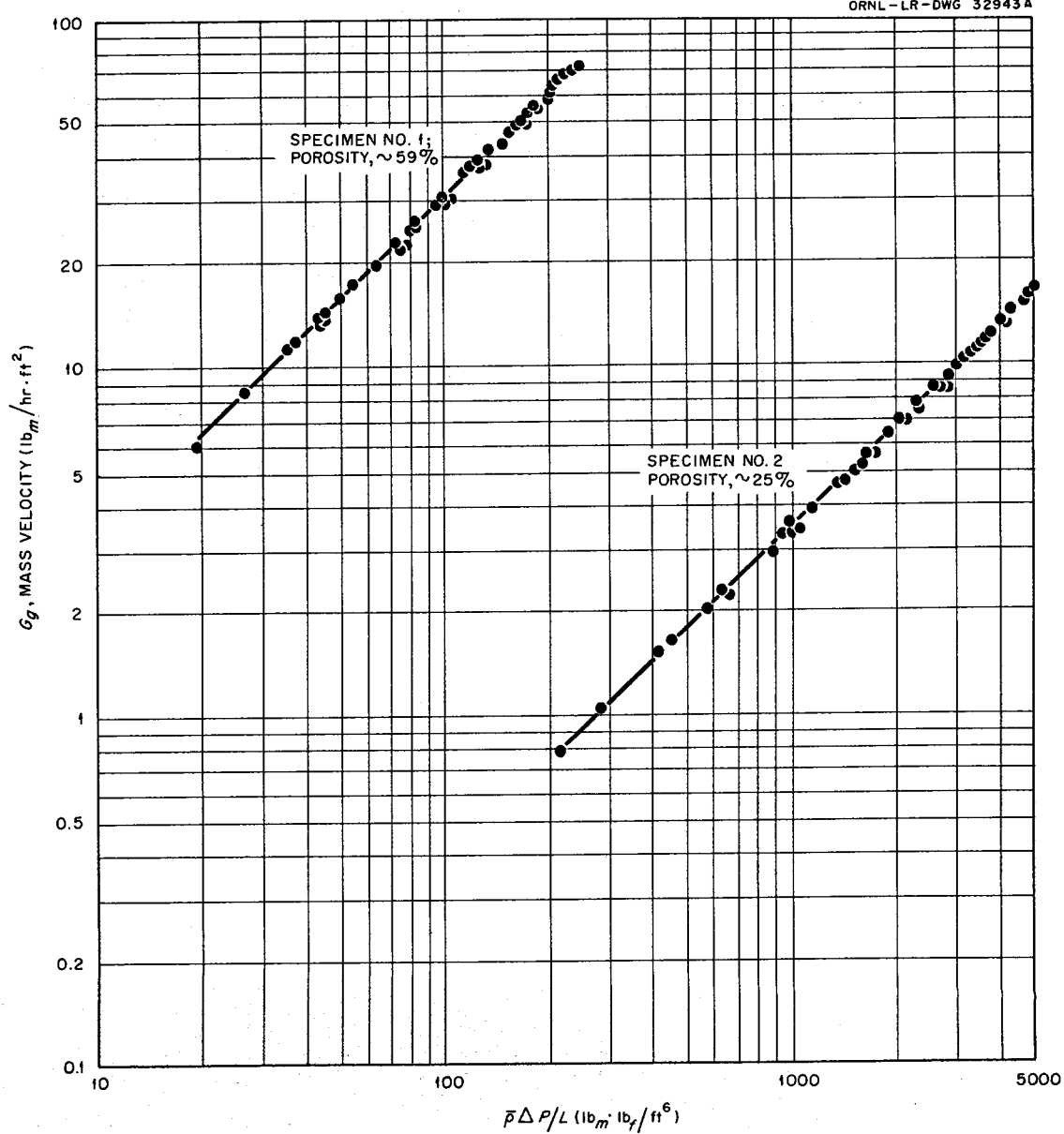
Fig. 1.3.6. Flow vs Pressure Drop Characteristics for Two Annuli Filled with Sintered Inconel.

$$G = g_c \frac{B_o}{\mu} \left(\overline{\rho} \frac{\Delta P}{L} \right) .$$

If it is assumed that the data follow Darcy's law exactly, the specific permeability coefficient, B_o, can be obtained for the two samples by using the given porosities and mid-range values of G_g and $\overline{\rho} \Delta P/L$. In this manner, B_o was calculated to be $\sim 62 \times 10^{-12}$ ft^2 for specimen 1 and $\sim 164 \times 10^{-14}$ ft^2 for specimen 2. These results can be compared with B_o values of 216×10^{-12} ft^2 for an unconsolidated sand of 37% porosity and 68×10^{-14} ft^2 for consolidated small alundum particles with a 24% porosity. In addition, the slope of approximately unity indicates that the flow is in the laminar regime.

1.4. INSTRUMENTS AND CONTROLS

Molten-Salt-Fuel Level Indicators

Visual and x-ray examination of a level probe used in the tests described previously[1] have been completed. The probe appears to be in excellent condition, both mechanically and electrically. Disassembly of the probe is in progress, and specimens have been sent to the metallurgy department for corrosion examination.

Two new Inconel "I"-tube-type level elements have been completed and installed in test vessels. Two identical level-measuring systems are now complete, and prefilling checkouts of the systems are in progress.

Fabrication of an INOR-8 level element and test vessel is approximately 80% complete.

INOR-8 High-Temperature Pressure Transmitters
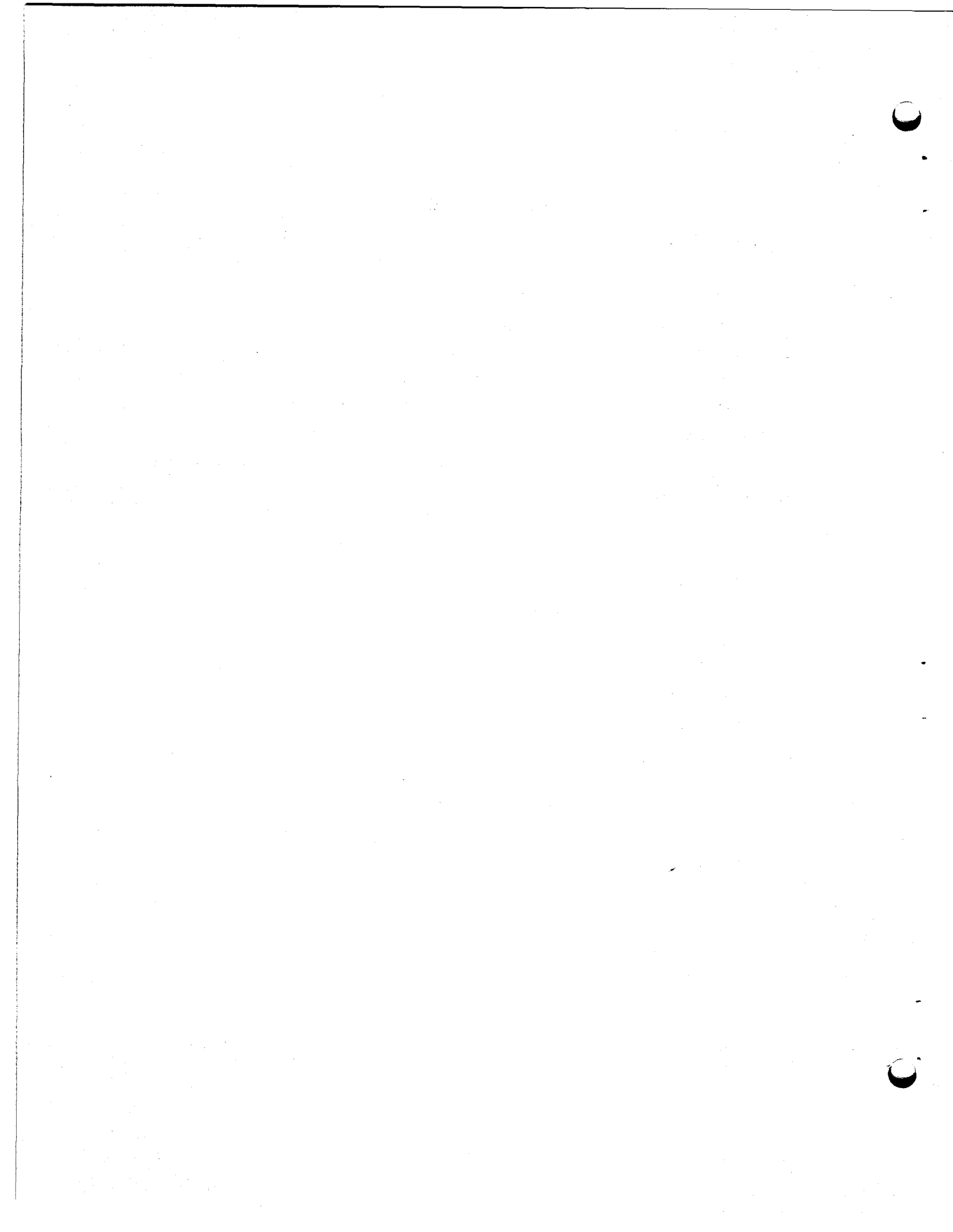
An order was placed with the Taylor Instrument Company for six INOR-8 pressure transmitters and indicating systems. The units are scheduled for delivery in early June.

The transmitter body will be fabricated from INOR-8 plate. The diaphragm material will be 0.005-in.-thick INOR-8 shim stock. The manufacturer believes on the basis of preliminary tests that satisfactory diaphragms can be made of this material. No unusual difficulties are expected in the fabrication of these units.
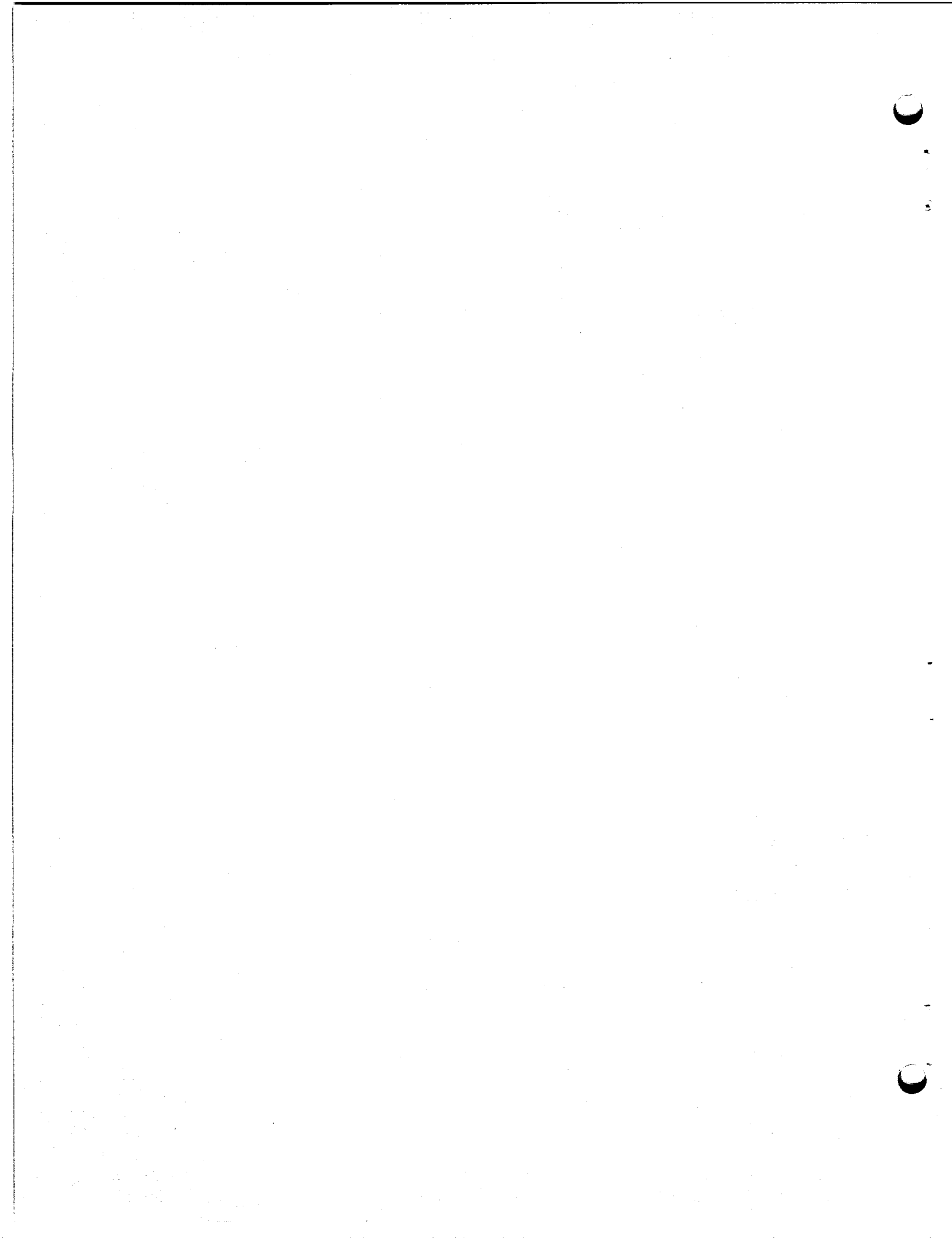
The six units will be composed of three having a range of 0 to 50 psig, and three with a range of 0 to 100 psig. All units are of the pneumatic-indicator type.

---

[1] R. F. Hyland, MSR Quar. Prog. Rep. Oct. 31, 1958, ORNL-2626, p 47.

PART 2.   MATERIALS STUDIES

2.1. METALLURGY

Dynamic Corrosion Studies

Corrosion studies were completed of four Inconel and four INOR-8 thermal-convection loops, and 12 thermal-convection-loop tests were initiated. The operating conditions for the new loops are given in Table 2.1.1. Two forced-circulation loops have completed the scheduled

Table 2.1.1. Operating Conditions for New Thermal
Convection-Loop Tests

Loop No.	Material	Composition Number of Salt Being Circulated[a]	Maximum Fluid-Metal Interface Temperature ($^\circ F$)	Scheduled Operating Period
1236	Inconel	134	1250	1 yr
1237	Inconel	134	1350	1 yr
1238	INOR-8	134	1350	1 yr
1239	Inconel	133	1350	1 yr
1240	INOR-8	133	1350	1 yr
1241	INOR-8	136	1250	1000 hr
1242	INOR-8	136	1350	1000 hr
1243	Inconel	135	1250	1000 hr
1244	INOR-8	135	1250	1 yr
1245	Inconel	135	1250	1 yr
1246	INOR-8	135	1350	1 yr
1247	Inconel	135	1350	1 yr

[a]Composition 134: $LiF\text{-}BeF_2\text{-}ThF_4\text{-}UF_4$ (62-36.5-1-0.5 mole %).
 Composition 133: $LiF\text{-}BeF_2\text{-}ThF_4$ (71-16-13 mole %).
 Composition 136: $LiF\text{-}BeF_2\text{-}UF_4$ (70-10-20 mole %).
 Composition 135: $NaF\text{-}BeF_2\text{-}ThF_4\text{-}UF_4$ (53-45.5-1-0.5 mole %).

test program but have not yet been examined, and one new forced-circulation loop test was started. The present status of all forced-circulation-loop tests now in progress is given in Chapter 1.2 of this report.

INOR-8 Thermal-Convection Loops

Metallographic examination of INOR-8 loop 1185, which circulated salt 126 ($LiF-BeF_2-UF_4$, 53-46-1 mole %) for one year at a hot-leg temperature of $1250°F$, revealed no observable attack in either the hot- or cold-leg sections. A photomicrograph of a typical hot-leg section from this loop is shown in Fig. 2.1.1. Further, no evidence of mass transfer was found in examinations of cold-leg sections or analyses of after-test salt samples. Results of salt analyses (presented in Table 2.1.2) indicate the level of metallic impurities

Table 2.1.2. Analysis of Salt Mixture 126 Before and After Circulation in Loop 1185 for One Year

Sample Taken	Major Constituents (wt %)		Minor Constituents (ppm)		
	U	Be	Ni	Cr	Fe
Before test	6.53	10.1	30	40	235
After test	6.40	10.6	35	140	250

in after-test salt samples to be effectively the same as in before-test samples.

Metallographic examination results for the INOR-8 loops 1227, 1228, and 1229 are summarized in Table 2.1.3. These three loops were each operated for 1000 hr, and the maximum fluid-metal interface temperature was $1250°F$. Metallographic examinations of the hot and cold legs of these loops showed no evidences of surface defects of the types normally associated with fluoride salt attack; however, well-developed intergranular cracks from 0.5 to 2 mils deep appeared

Table 2.1.3. Results of Metallographic Examinations of Inconel and INOR-8
Thermal Convection Loops

Loop No.	Material	Test Period	Maximum Fluid-Metal Interface Temperature (^{o}F)	Salt No.[a]	Metallographic Results	
					Hot-Leg Appearance	Cold-Leg Appearance
1182	Inconel	1 yr	1350	126	Heavy intergranular voids to a depth of 15 mils	Surface pitting 0.5 mil deep
1188	Inconel	1 yr	1250	84	Heavy intergranular voids to a depth of 9 mils	Grain-boundary penetrations to a depth of 1 mil
1189	Inconel	1 yr	1250	130	Heavy intergranular voids to a depth of 7 mils	Grain-boundary penetrations to a depth of 0.5 mil
1230	Inconel	1000 hr	1350	130	Moderate intergranular voids to a depth of 4 mils	Few penetrations < 1 mil deep
1227	INOR-8	1000 hr	1250	134	No attack	No attack
1228	INOR-8	1000 hr	1250	133	No attack; fabrication flaws found in both legs	No attack
1229	INOR-8	1000 hr	1250	135	Same as loop 1228	Same as loop 1228

[a]Composition 126: $LiF-BeF_2-UF_4$ (53-46-1 mole %).
 Composition 84: $LiF-NaF-BeF_2$ (35-27-38 mole %).
 Composition 130: $LiF-BeF_2-UF_4$ (62-37-1 mole %).
 Composition 134: $LiF-BeF_2-ThF_4-UF_4$ (62-36.5-1-0.5 mole %).
 Composition 133: $LiF-BeF_2-ThF_4$ (71-16-13 mole %).
 Composition 135: $NaF-BeF_2-ThF_4-UF_4$ (53-45.5-1-0.5 mole %).

at random intervals along the exposed surfaces of all three loops.
An examination of as-received specimens of tubing used for these loops
was subsequently made, and similar cracks were detected in these
specimens. A typical flaw is shown in Fig. 2.1.2. The flaws were
apparently not detected by x-ray inspection of the tubing before loop
fabrication. Therefore ultrasonic inspection of loop tubing is now
being utilized to supplement existing inspection practices.

Inconel Thermal-Convection Loops

Three of the four Inconel loops for which metallographic exami-
nation results have been recently obtained were operated for one year,
while the fourth was operated 1000 hr. The examination results are
summarized in Table 2.1.3. As indicated, the hot legs of all the
Inconel loops operated for one year showed heavy intergranular void
formation. Of particular interest is loop 1182, which circulated salt
126 for one year at 1350°F. Examination of this loop revealed heavy
intergranular void formation to a depth of 15 mils, as may be seen in
Fig. 2.1.3. Chemical analyses of the salt showed no significant
changes in the impurity content. However, examination of the trap
area, which was the coldest part of the loop, revealed a large quantity
of metallic particles. These particles are being analyzed.

General Corrosion Studies

Penetration of Graphite by Molten Fluoride Salts

The problems associated with the use of unclad graphite as a
moderator in a molten-salt reactor system are being studied. The
possibility exists that fuel salts would enter the pore spaces in the
graphite and create problems associated with (1) reactor fuel inventory,
(2) hot spots, (3) effects from fission-gas release associated with
fuel in the pores, and (4) effects of thermal expansion of the salt
as a result of thermal cycling of the reactor. The large volume change
which fluoride salts exhibit on melting could cause cracking or spalling
of the graphite if sufficient pressure were built up by salt entrapped

54
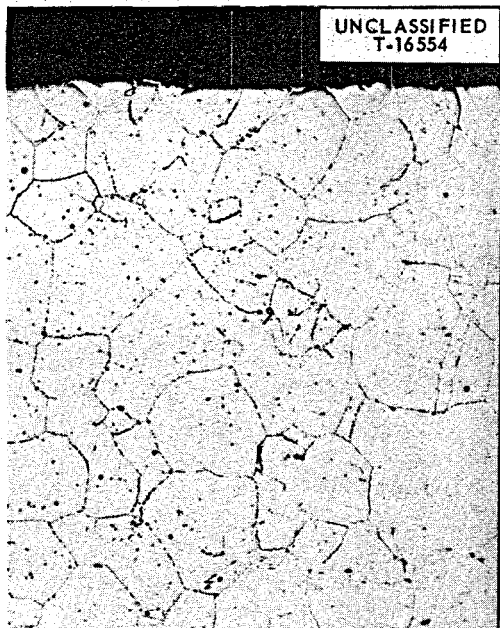
Fig. 2.1.1. Specimen Taken from Hot Leg of INOR-8 Thermal-Convection Loop 1185 at Point of Maximum Loop Temperature (1250°F). Loop was operated for 1 year with salt mixture LiF-BeF$_2$-UF$_4$ (53-46-1 mole %).
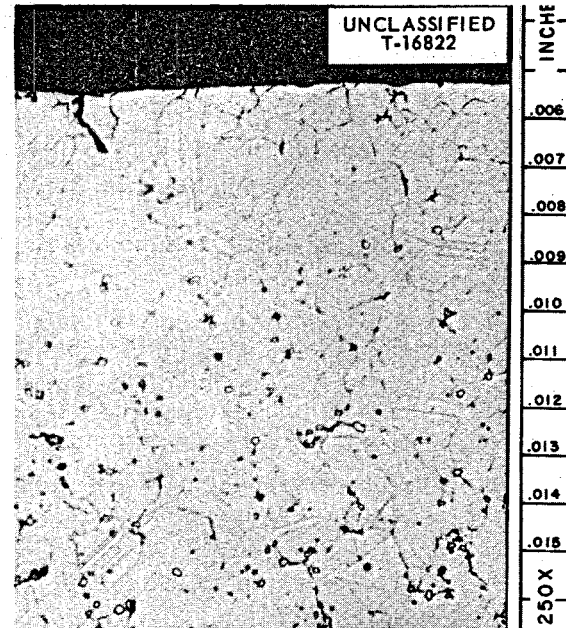
Fig. 2.1.2. Specimen of INOR-8 As-Received Tubing Used in Thermal-Convection Loops 1227, 1228, and 1229.
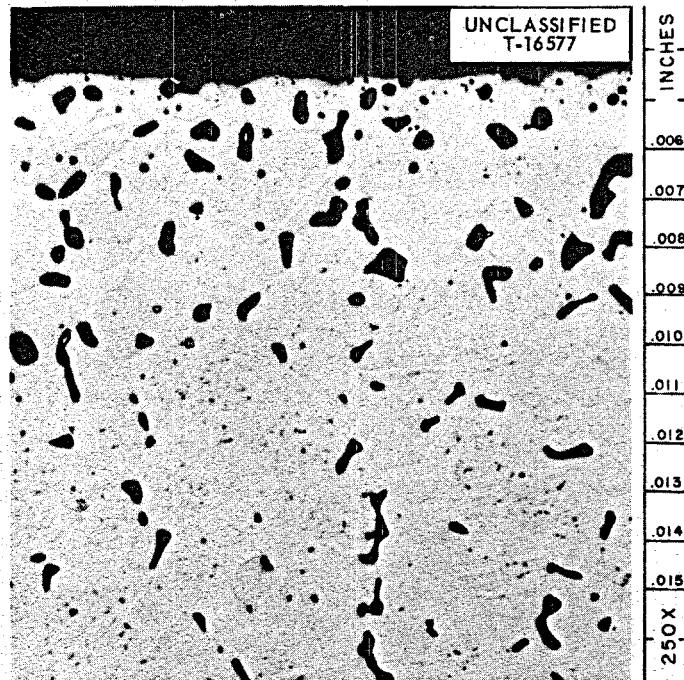
Fig. 2.1.3. Specimen Taken from Hot Leg of Inconel Thermal-Convection Loop 1182 at Point of Maximum Loop Temperature (1350°F). Loop was operated for 1 year with salt mixture LiF-BeF$_2$-UF$_4$ (53-46-1 mole %).

55

in pores.

An experimental investigation has been started to determine under what conditions salts will penetrate graphite and to ascertain the physical damage that might occur in the graphite as a result of thermal cycling. Both static-pressure and dynamic-pressure tests are being conducted.

Static-pressure penetration tests have been made with graphite-molten salt systems at 150 psia and $1300^{\circ}F$. In preparation for these tests, graphite specimens were partially degassed by heating at $2372^{\circ}F$ for 5 hr in a vacuum of $<4\ \mu$ and then cooled to room temperature in a pure argon atmosphere. When assembling the apparatus, the graphite was exposed to room atmosphere for approximately 5 hr. The apparatus was then evacuated to $<12\ \mu$ and held at $572^{\circ}F$ for 15 hr to remove lightly adsorbed contaminants.

In test, the graphite specimens were completely submerged in molten salts at $1300^{\circ}F$, and a 150-psi pressure was applied for 100 hr by using an argon blanket gas. After the tests the specimens were examined for penetrations of salt into the graphite by using radiographic, metallographic, and/or chemical analysis techniques. The specimens were also weighed to detect weight changes.

Both TSF and CCN graphite were tested individually in $LiF\text{-}BeF_2\text{-}UF_4$ (62-37-1 mole %, fuel 130). Macroscopic examination of radiographs of these graphite specimens did not reveal any penetration by fuel 130. There was essentially no weight gain (<0.01%) of the TSF graphite specimen, but there was a weight gain of approximately 1% for the CCN graphite specimen. Metallographic examinations and chemical analyses are being made to determine the location of the fuel 130 and/or reaction products in the CCN graphite. The TSF grade will be examined in like manner.

A static-pressure penetration test at $1300^{\circ}F$ was also made with fuel mixture 30 ($NaF\text{-}ZrF_4\text{-}UF_4$, 50-46-4 mole %) and CCN-grade graphite to assist in evaluating testing techniques. Radiographic examination of the graphite specimen used in this test indicated that the fuel had

penetrated it throughout. The weight gain of the specimen indicated that 29% of the calculated pore volume of the graphite had been filled. Additional static-pressure penetration tests are planned using fuel mixture 130 with TSF, AGOT, and ATJ grades of graphite to evaluate the effects of pressure and temperature on penetration.

A dynamic-pressure penetration test apparatus has been devised which allows the movement of fuel around the graphite specimen to wash away reaction products that might form at the graphite surface and thus plug pore spaces. This test equipment, which is further discussed later in this chapter under "Welding and Brazing Studies," is designed to apply pressures up to 350 psia on the fuel side of the graphite while the opposite side is being evacuated.

The CCN-graphite specimen that was penetrated by fuel 30, as mentioned above, was thermally cycled to determine whether thermal expansion of the fuel 30 in the graphite pore spaces would cause cracking or spalling of the graphite. During the thermal cycle, thermocouples indicated temperature changes from room temperature to $1436^{\circ}F$ near the outer surface and room temperature to $779^{\circ}F$ at the central axis of the specimen within a 3-min period. In the first two minutes of the cooling part of the cycle, the $1436^{\circ}F$ outer surface temperature was lowered to $842^{\circ}F$ and the $779^{\circ}F$ central temperature was lowered to $752^{\circ}F$. Radiographic and macroscopic examinations of the graphite specimen at room temperature did not reveal any damage to it.

Since the volume expansions of fuels 30 and 130 from room temperature to their melting temperatures are 17% and 11%, respectively, the lack of damage to the graphite suggests that some penetration of molten fluoride salts into the graphite pore spaces might be tolerated. The specimen will be subjected to additional thermal cycles, and other penetration and thermal-cycling tests of various types of graphite and fluoride salts will be made.

Uranium Precipitation from Molten Fluoride Salts in Contact with Graphite

The fuel mixture LiF-BeF$_2$-UF$_4$ (62-37-1 mole %) was reported previously[1] to have precipitated UO$_2$ in tests in which the fuel mixture was contained in graphite crucibles at 1300°F. The graphite-salt systems were tested in evacuated Inconel containers, and the precipitate was observed by using radiographic techniques. In control tests under similar conditions with two different batches of fuel mixtures in Inconel containers without graphite crucibles, no UO$_2$ precipitate was detected by radiographic examination.

To assist in determining the role of graphite in causing uranium precipitation from graphite-fuel systems, a set of five tests was run with different quantities of graphite and different salt-to-graphite contact areas. The tests were made concurrently at 1300°F, and the fuel mixture used in each test was from the same batch. Graphite, grade CCN, was used that had been machined and cleaned by sonic means in ethyl alcohol.

The test setups used are illustrated in Fig. 2.1.4, and the tests are described below. In test A, the fuel was tested in the absence of graphite in order to test both the quality of the fuel and the assembly methods used in fabricating all the test equipment. In test B, the fuel was in contact with a large area of a large quantity of graphite in order to establish a reference for uranium precipitation from the fuel; the dimensions and configuration of the test duplicated those of the standard graphite-fuel compatibility tests. In test C, the fuel was tested in the presence of, but not in direct contact with, a large quantity of graphite to determine whether the uranium precipitation was caused by degassing of the graphite. In test D, the fuel was tested in contact with a small area of a large quantity of graphite to determine, in conjunction with the results of test B, whether the contact surface-to-volume ratio for the graphite and fuel affected the quantity of uranium precipitation from the fuel. In test E, the fuel was tested

---

[1]MSR Quar. Prog. Rep. Jan. 31, 1959, ORNL-2684, p 80.

58
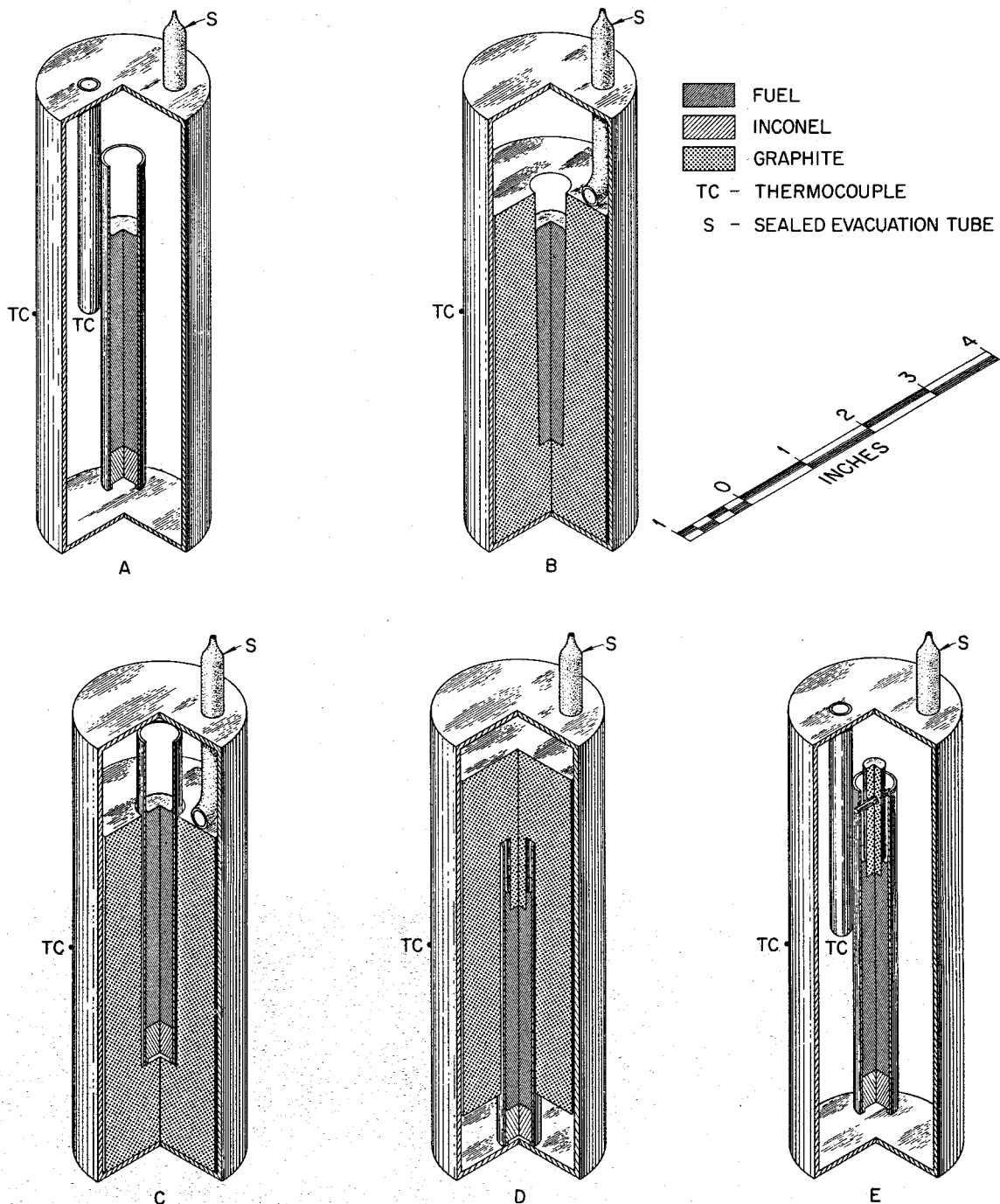
Fig. 2.1.4. Test Setups Used to Study the Precipitation of UO_2 from Fuel 130 in Graphite Crucibles.

in contact with a small area of a small quantity of graphite to determine, in conjunction with the results of test D, whether the quantity of graphite affected the quantity of uranium precipitation from the fuel.

Radiographic examinations of each of the test setups at total accumulated test times of 5, 10, and 100 hr were made. No uranium precipitation was observed for the control, test A (Fig. 2.1.4). A small amount of uranium precipitation occurred in test E. A moderate and approximately equal amount of uranium precipitation was found in each of the other three tests. These results support the conclusion arrived at previously[2] that the uranium precipitation observed in fuel 130 was the result of the fuel reacting with oxygen supplied by degassing of the graphite.

Tests are in progress to determine whether a suitable flush can degas the graphite to such a degree that it will contain fuel 130 without causing uranium to precipitate from the fuel.

Thermal-Convection-Loop Tests of Brazing Alloys in Fuel 130

A scheduled 1000-hr test of Inconel and INOR-8 lap joints brazed with various alloys and exposed to fuel 130 in the hot leg of a thermal-convection loop has been completed. Similar tests scheduled for 5,000- and 10,000-hr periods are continuing. The configuration of these thermal-convection loops and the manner in which the brazing alloys are incorporated in them was described previously.[3] The brazing alloys tested were:

Alloy	Composition
Coast Metals No. 52	89% Ni–5% Si–4% B–2% Fe
Coast Metals No. 53	81% Ni–8% Cr–4% Si–4% B–3% Fe
General Electric No. 81	70% Ni–20% Cr–10% Si
Gold–Nickel Alloy	82% Au–18% Ni
Copper	100% Cu

---

[2]W. H. Cook, MSR Quar. Prog. Rep. Oct. 31, 1958, ORNL-2626, p 62.

[3]E. E. Hoffman and D. H. Jansen, MSR Quar. Prog. Rep. June 30, 1958, ORNL-2551, p 62.

The temperature of the circulating salt in the region of the test specimens was $1300^\circ F$.

Metallographic examination showed that all the brazing alloys had good flowability on both Inconel and INOR-8 base metals. There was a tendency for the formation of diffusion voids in the fillets of the joints brazed with the gold-nickel alloy. The General Electric No. 81 alloy was heavily attacked on Inconel base material. Coast Metals Nos. 52 and 53 were depleted at the fillet surface to a depth of 1 to 2 mils. Some slight cracking of the alloys occurred at the brazing alloy-base metal interface. Pure copper showed good corrosion resistance and no cracking.

Thermal-Convection-Loop Tests of the Compatibility of INOR-8, Graphite, and Fuel 130

Fuel mixture 130 $(LiF-BeF_2-UF_4$, 62-37-1 mole %) was circulated in an INOR-8 thermal-convection loop containing a 10-in. tube of TSF graphite in the hot leg in order to ascertain whether the graphite would cause carburization of the INOR-8. The loop operated for 4000 hr with a hot-leg temperature of $1300^\circ F$.

Metallographic examination of a loop section adjacent to the graphite insert revealed that the carbide precipitates in the grain boundaries were slightly larger near the salt-metal surface than throughout the rest of the specimen (Fig. 2.1.5); however, similar precipitates have been observed in INOR-8 tubing from corrosion loop tests with no graphite present.

Microhardness measurements of the area 2 mils from the salt-metal surface were of the same magnitude as those observed in the rest of the specimen. These values ranged randomly from 160 to 180 DPH.

A carbon content of 0.037% was found by chemical analyses of two successive 5-mil layers taken at the inner surface of the INOR-8 tubing. An additional series of layers to a depth of 35 mils was analyzed and found to contain a range of carbon values from 0.014 to 0.026%. Consequently, these different values are not considered to be significant, especially in view of the large quantities of inclusions
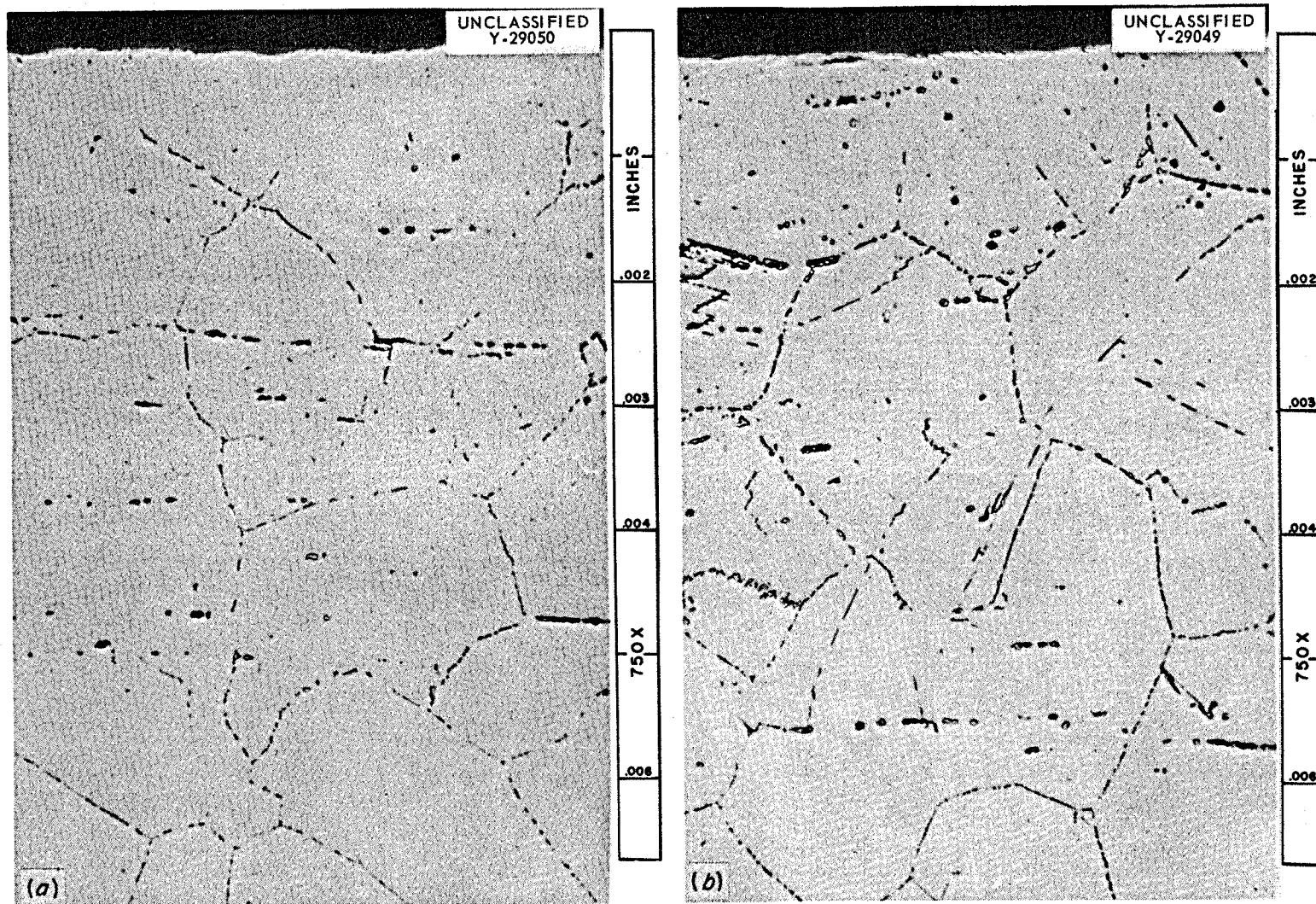
Fig. 2.1.5. The (a) Outer and (b) Inner Surfaces of an INOR-8 Specimen Taken from a Thermal-Convection Loop that Circulated LiF-BeF$_2$-UF$_4$ (62-37-1 mole %, fuel 130) for 4000 hr at a Hot-Zone Temperature of 1300°F. The specimen is from a section adjacent to a graphite capsule incorporated in the hot leg. Etchant: aqua regia.

in this heat of material, as shown in Fig. 2.1.6.

Mechanical Properties of INOR-8

Creep Tests

Most of the creep tests presently being conducted in fused salts are low-stress, long-time tests. The results of these tests will provide accurate data in terms of stress, total strain, and creep rates for INOR-8 at times in excess of 10,000 hr. None of the test specimens failed during the past quarter and therefore no data are available to report. These experiments are being run at 1100 and $1200^{\circ}F$.

Fatigue Studies

The fatigue properties of INOR-8 at 1100 and $1500^{\circ}F$ are being studied at Battelle Memorial Institute under a subcontract from the Metallurgy Division. A rotating-beam-type of test is used at frequencies of 100 and 3000 rpm. The initial results reported were for the 100 rpm and $1500^{\circ}F$ conditions. The data are summarized below:

Stress (psi)	Cycles to Failure
45×10^3	8×10^3
40	34×10^3
35	160×10^3
30	730×10^3
30	930×10^3
27	72×10^6 (discontinued)

Thus, the stress to produce fatigue failure in 1×10^6 cycles is slightly over 29,500 psi. Under similar test conditions, the stress to produce fatigue failure of Inconel in 1×10^6 cycles is about 18,000 psi.

Shrinkage Characteristics of INOR-8

A certain peculiarity in the behavior of INOR-8 has been noted almost since the start of the current testing program. In creep tests,
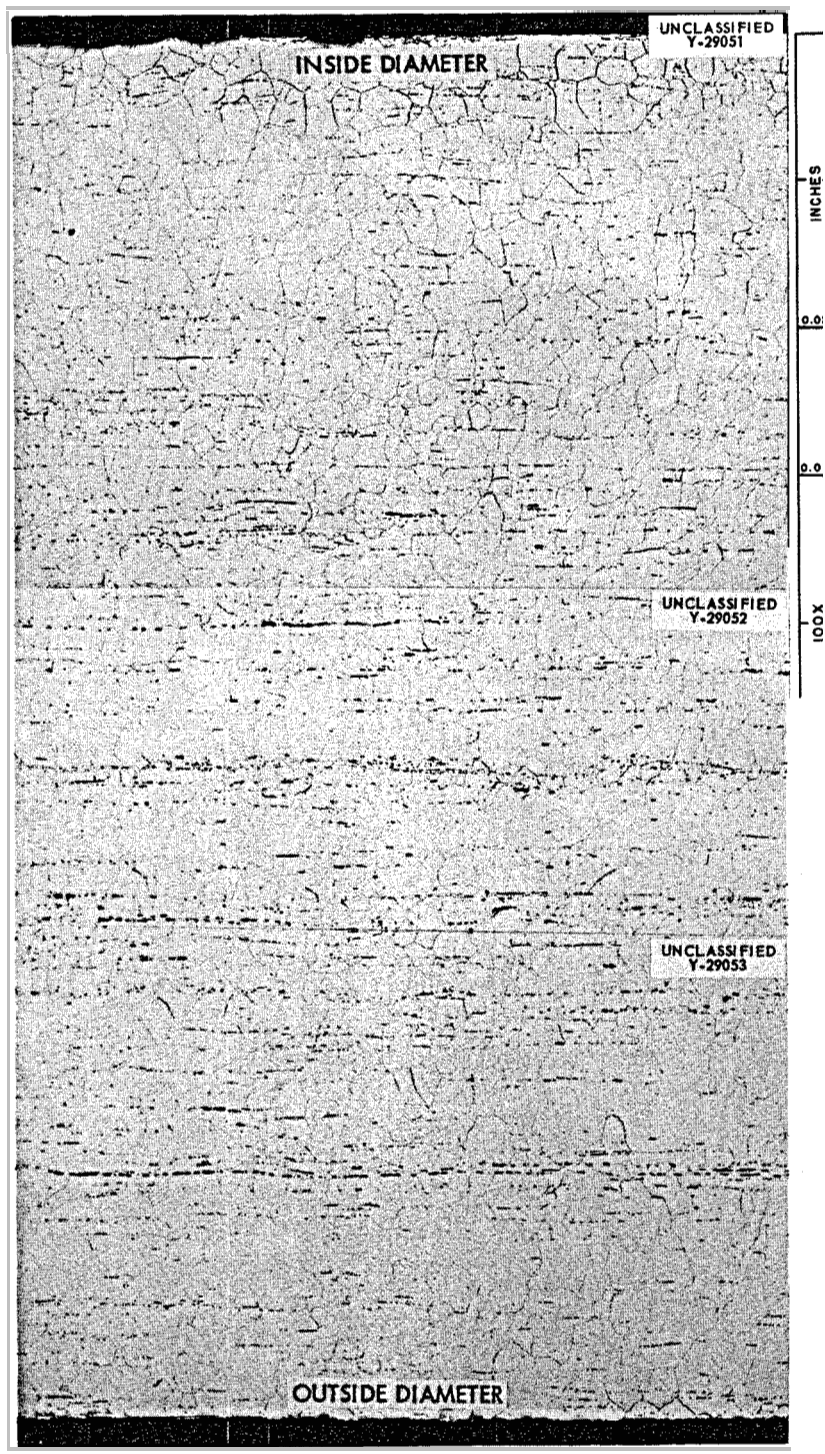
Fig. 2.1.6. Cross Section of INOR-8 Tube that was Adjacent to Graphite Insert in 4000-hr Thermal-Convection Loop Test.

there is an initial period during which virtually no creep occurs. This is followed by normal creep. In relaxation tests, the load must be increased during the early stages in order to maintain a constant strain. These observations are important, since at low stresses the effects are manifest over a thousand or more hours and the results in terms of creep rate and total strain vs time measurements are attenuated.

The behavior pattern suggested that the metal might be contracting as a result of metallurgical instabilities. Isothermal dilatometry measurements indicate that there is contraction in certain heats of INOR-8 but not in others, notably SP-16 and SP-19. Metallographic examinations showed that those specimens which contracted contained many large areas of second phase material. The stable heats had equi-axed grain structures with fine precipitates concentrated mainly in the grain boundaries. There appear to be no significant differences in either the major or minor alloying constituents in the heats examined, except for the carbon content. However, stable heats have been found that range from a special low-carbon melt up to heats containing carbon in excess of 0.1%. The specimens which contracted had carbon contents which fell within this range. Currently the contraction phenomenon is being studied by means of resistivity measurements to determine temper-ature-dependence and reaction rates. This study will be continued, since all heats have shown a plateau in the creep and relaxation values.

Materials Fabrication Studies

Effect on INOR-8 of Aging at High Temperatures

The experiments which were being run to determine whether INOR-8 exhibits a tendency to embrittle in the temperature range between 1000 and 1400°F have been completed. Specimens which had been aged for 10,000 hr have been tensile tested, and no significant differences from annealed specimens have been found. The data from these tests are presented in Table 2.1.4.

Table 2.1.4. Effect of Aging Upon the Tensile Properties of INOR-8 Specimens
from Heat SP-19 (0.06% C)

Test Temperature (°F)	Specimen Annealed 1 hr at 2100°F			Specimen Annealed and Aged 10,000 hr at Test Temperature			
	Tensile Strength (psi)	Yield Strength (psi)	Elongation (%)	Aging Temperature (°F)	Tensile Strength (psi)	Yield Strength (psi)	Elongation (%)
Room	114,400	44,700	50	1000	117,700	45,100	50
				1100	120,000	47,500	49
				1200	116,000	46,800	46
				1300	115,500	45,800	43
				1400	115,000	43,600	40
1000	93,000	28,300	46	1000	97,700		46
1100	93,000	28,900	50	1100	90,500		40
1200	82,400	27,500	37	1200	81,900		32
1300	69,900	28,000	24	1300	76,100		24
1400	61,800	26,200	21	1400	65,100		20

It is concluded from this group of tests and from the previous tests[4,5] of specimens aged for 500, 1000, 2000, and 5000 hr that INOR-8 does not exhibit any embrittling tendencies that can be attributed to high-temperature instability.

Triplex Heat Exchanger Tubing

Work is continuing on the development of techniques for fabricating a heat exchanger tube made up of two concentric tubes with a porous annulus between to permit the passage of a gas for leak detection. The materials of construction presently being investigated are a porous nickel core clad on the outer and inner surfaces with Inconel or INOR-8. Two methods of incorporating the porous core into the annular space of the concentric tubes are being considered: first, tamping loose nickel powder into the annulus and developing a porous core bonded to the outer and inner tubes by suitable drawing and sintering operations; and, second, bonding a prefabricated porous core to the outer and inner tubes by suitable drawing and sintering operations. Results obtained by the first method were described previously.[6] Because of difficulties encountered with an oxide layer being formed at the core-to-cladding interface and causing poor bonding, this method of fabrication has been discontinued in favor of the second method.

Porous nickel sheet is available from Micro Metallic Corp. in four common grades, which differ in mean pore opening, as follows:

Grade	Mean Pore Opening (in.)
E	0.0015
F	0.0008
G	0.0004
H	0.0002

---

[4]H. Inouye, MSR Quar. Prog. Rep. June 30, 1958, ORNL-2551, p 67.

[5]H. Inouye, MSR Quar. Prog. Rep. Oct. 31, 1958, ORNL-2626, p 67.

[6]MSR Quar. Prog. Rep. Jan. 31, 1959, ORNL-2684, p 85.

The sheet material has a density of approximately 50 to 60% of theoretical, and 1/16-in.-thick stock can be rolled into a 3/4-in.-OD tube. Twenty-five feet of both grades E and G rolled into tubular shape have been ordered for cladding studies.

An attempt is presently being made to clad with Inconel a small, sample, porous nickel strip received from Micro Metallic. The as-received strip was annealed for 1 hr at 1800°F and then bent around the outside of a 0.625-in.-OD Inconel tube. The porous nature of the resulting ring can be seen in Fig. 2.1.7, which shows an enlarged view of the surface. Channeled spacers were tack-welded to the Inconel tube adjacent to the porous ring to prevent slippage of the ring during drawing and to provide a means of filling the annular space. The assembly is shown in Fig. 2.1.8. An Inconel tube was placed over the assembly and the resulting triplex assembly was cold drawn from 1.000 in. OD x 0.500 in. ID to 0.855 in. OD x 0.468 in. ID. The triplex assembly is now being prepared for sintering to promote bonding of the porous ring to the Inconel cladding. A vacuum will be maintained in the annulus of the triplex assembly during sintering. An evaluation of the porosity and bond between ring and cladding will subsequently be made.

Similar cladding experiments are to be performed by Superior Tube Co. on Subcontract No. 1112. It is anticipated that these results will help determine the feasibility of fabrication of a triplex tube by a commercial vendor.

Welding and Brazing Studies

Procedures for Welding INOR-8

The fabrication of INOR-8 components for the wide variety of MSR applications requires that suitable welding procedures be developed for material ranging in size from thin-walled tubing to heavy plate. An inert-arc welding specification, RMWS-12 (ref 7) is available for

---

[7]R. M. Evans (comp. and ed.), Reactor Material Specifications, TID-7017, p 195 (Oct. 29, 1958).
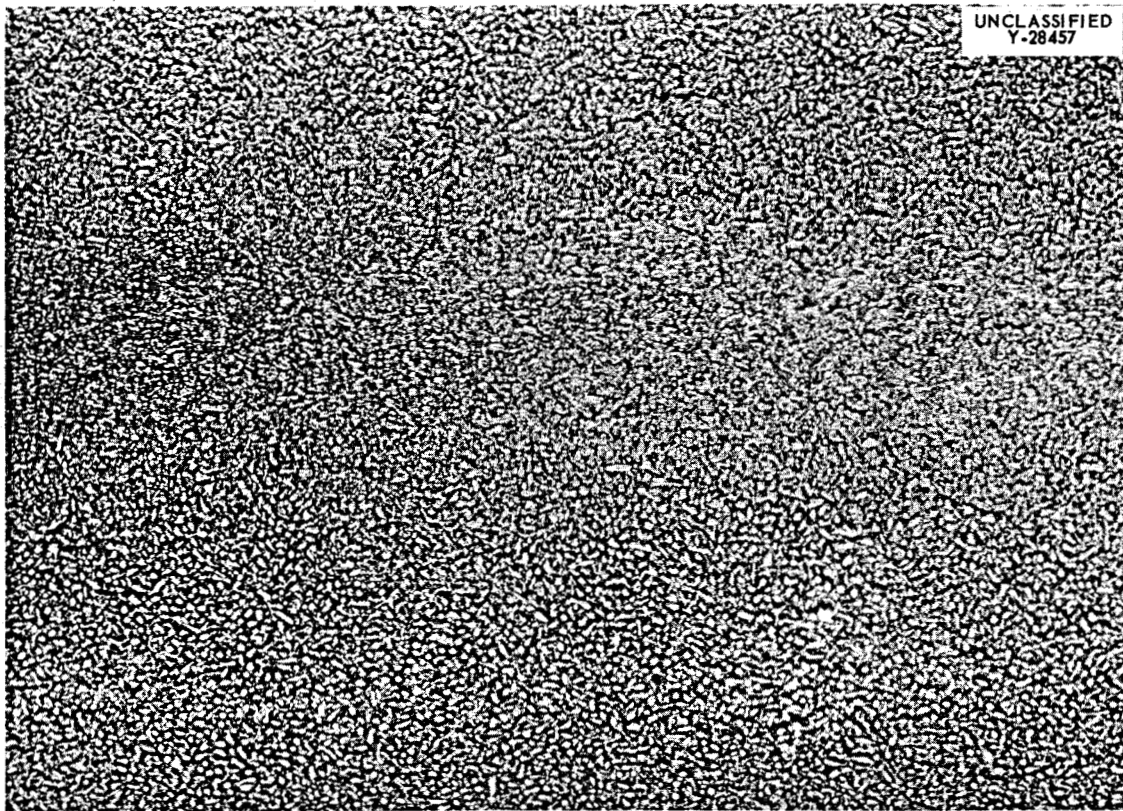
Fig. 2.1.7. Surface of Prefabricated Porous Nickel Strip Received from Micro Metallic Corp. After Bending Around a 0.625-in.-OD Inconel Tube. $7\frac{1}{2}$X.

INCHES

0   1   2
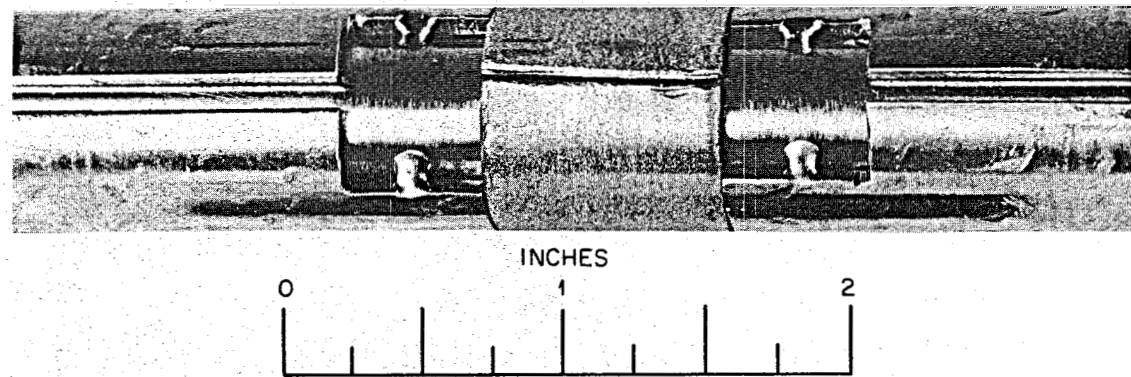
Fig. 2.1.8. Assembly for Cladding Porous Nickel Ring with Inconel. Channeled spacers provided for restraining ring, facilitating evacuation of assembly, and filling annular space.

INOR-8 material up to 0.100 in. thick, and additional procedures are being qualified for thicker sections in accordance with the methods prescribed by the ASME Boiler Code.[8]

Several lengths of 5-in. sched-40 pipe have been fabricated from 1/4-in.-thick plate, and a welding procedure will be developed which will be applicable over the thickness range 1/8 to 1/2 in. A welding procedure for 1/2-in. plate will also be developed, which will be applicable for thicknesses up to 1 in. The tests to be conducted include reduced-section tension, side-bend, face-bend, and root-bend tests, as well as radiographic and metallographic examinations.

It is expected that these welding procedures will be extremely useful in fabricating containment vessels and test components from INOR-8. These procedures will serve also as an essential supplement to the mechanical property data which are being accumulated for the presentation of INOR-8 as a case before the ASME Boiler and Pressure Vessel Code Committee.

Mechanical Properties of INOR-8 Welds

Studies are continuing in an effort to improve the high-temperature ductility of INOR-8 weld metal. These include the investigation of techniques to deoxidize and purify weld filler metal during the casting of original ingots. One promising method involves the use of a vacuum-melted basic charge with additions of small quantities of aluminum, titanium, manganese, silicon, boron, and magnesium. Several different heats of weld metal containing these and other additions have been cast and fabricated into weld wire. Analyses of these heats are presented in Table 2.1.5, and analyses of commercial materials are included for comparison. The mechanical property values obtained to date for these materials are summarized in Table 2.1.6, and properties of other materials are included for comparison. The results of the mechanical property tests on these filler metals will permit an evaluation of the relative merits of the various deoxidation and purification practices.

---

[8] ASME Boiler and Pressure Vessel Code, Section IX (1956).

70

Table 2.1.5. Analyses of INOR-8 Weld Metal Heats
Containing Alloying Additions

Basic melt charge: 72% Ni—16% Mo—4% Fe—8% Cr

Heat Number	Carbon Content (wt %)	Analysis Source	Additive (wt %)					
			Mn	Si	Al	Ti	B	Mg
Hastelloy W (25% Mo—7% Fe—5% Cr—2.5% Co—bal Ni)	0.03	ORNL	0.58	0.07	0.15	0.08		0.02
Westinghouse M-5	0.08	Vendor	0.79	0.19		0.02		
Haynes SP-19	0.06	Vendor	0.48	0.04				
ORNL MP-3	0.06	Intended	0.50	0.10	0.20	0.20	0.005	0.03
		ORNL	0.36	0.25	0.25	0.20	0.004	0.02
ORNL MP-4	0.06	Intended	0.50	0.10	0.20	0.20		0.03
		ORNL	0.34	0.05	0.20	0.24		0.002

Table 2.1.6. Mechanical Property Studies on INOR-8 Weld Metal
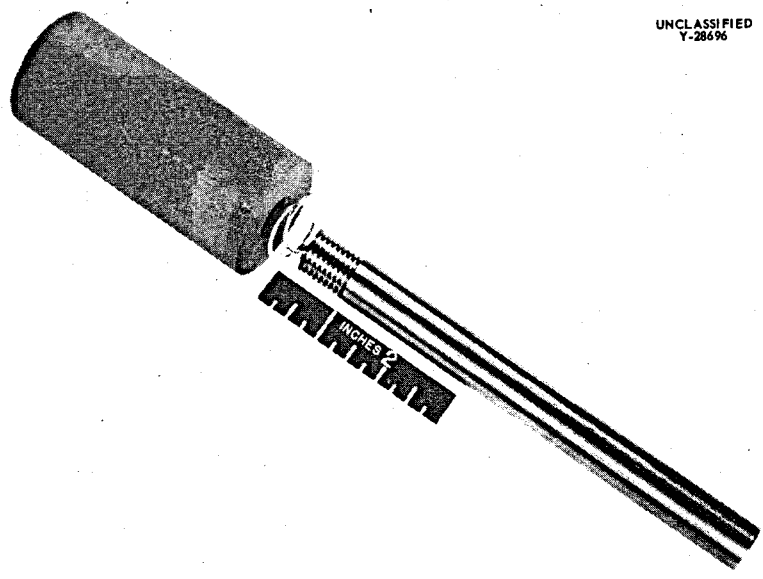
Heat Number	Tensile Strength (psi)			Elongation (% in 1 in.)		
	At Room Temperature	At 1200°F	At 1500°F	At Room Temperature	At 1200°F	At 1500°F
Hastelloy W	127,000	94,800	70,400	37	33	25
Westinghouse M-5	118,900	74,000	55,800	36	18	5
Haynes SP-19	115,900	70,400	53,000	38	18	10
ORNL MP-3	108,000	67,800	49,200	46	25	13
ORNL MP-4	107,600	68,000	50,100	45	22	9

Fabrication of Apparatus for Testing the Compatibility of Molten Salts and Graphite

Equipment was fabricated which will be used by the General Corrosion Group to study molten salt penetration of graphite in a dynamic, high-pressure system. Before this apparatus could be fabricated, it was necessary to develop a method of attaching an Inconel tube to a hollow cylindrical graphite specimen and thereby forming a leaktight connection. This was accomplished by brazing with a commercially available braze alloy composed of silver, titanium, and copper that was found to wet vacuum-degassed graphite.
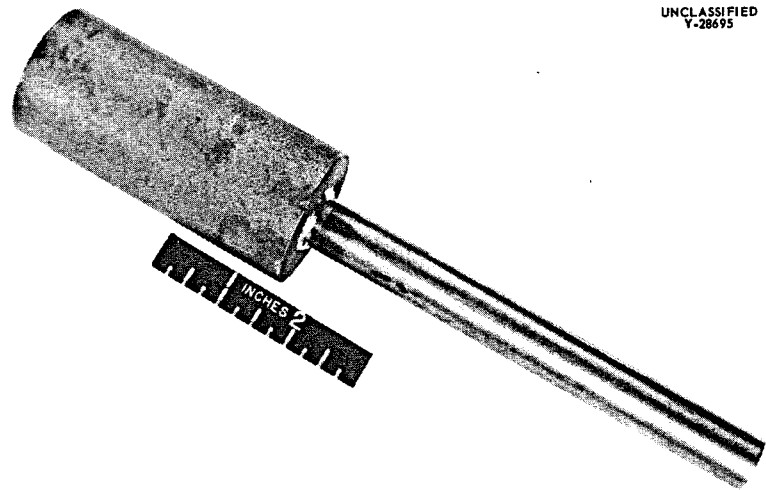
The large difference in thermal expansion of the graphite and the brazing alloy caused some shear cracking in the graphite. However, metallographic sectioning of sample joints indicated that the cracks were rather limited in length, and pressure testing of the completed joint with air indicated no leakage other than that associated with the inherent porosity of the base graphite.

The graphite-to-Inconel assembly prior to brazing is shown in Fig. 2.1.9, and the completed specimen is shown in Fig. 2.1.10. The completed Inconel test rig with associated entry, drain, and purge lines is shown in Fig. 2.1.11.

**Fig. 2.1.9. Graphite-to-Inconel Assembly Before Brazing.**

Fig. 2.1.11. Completed Inconel Test Rig.

Fig. 2.1.10. Graphite-to-Inconel Assembly After Brazing.

Phase Equilibrium Studies

The System $LiF-BeF_2-ThF_4$

A revised phase diagram for the system $LiF-BeF_2-ThF_4$ is presented in Fig. 2.2.1 that includes data obtained by increasing the equilibration period in thermal-gradient quenching experiments to three weeks. Quenched samples from such experiments revealed that the area of single-phase ternary solid solutions involving $3LiF \cdot ThF_4$ is greater than previously reported;[1,2] it occupies approximately the triangle indicated by cross hatching in Fig. 2.2.1. Invariant equilibria in the system $LiF-BeF_2-ThF_4$ are listed in Table 2.2.1. The limits of the area of the single-phase

Table 2.2.1. Invariant Equilibria in the System $LiF-BeF_2-ThF_4$

Composition (mole %)			Invariant Temperature (°C)	Type of Equilibrium	Solids Present at Invariant Point
LiF	BeF_2	ThF_4			
17	81	2	497	Peritectic	ThF_4, $LiF \cdot 4ThF_4$, and BeF_2
33.5	64	2.5	451	Peritectic	$LiF \cdot 4ThF_4$, $LiF \cdot 2ThF_4$, and BeF_2
47	51.5	1.5	355	Eutectic	$2LiF \cdot BeF_2$, $LiF \cdot 2ThF_4$, and BeF_2
60.5	36.5	3	431	Peritectic	$LiF \cdot 2ThF_4$, $3LiF \cdot ThF_4$ (ss), and $2LiF \cdot BeF_2$
66	29.5	4.5	448	Peritectic	LiF, $2LiF \cdot BeF_2$, and $3LiF \cdot ThF_4$ (ss)
63	29	8	452	Peritectic	$3LiF \cdot ThF_4$ (ss), $7LiF \cdot 6ThF_4$, and $LiF \cdot 2ThF_4$

[1] R. E. Thoma et al., MSR Quar. Prog. Rep. June 30, 1958, ORNL-2551, p 83.

[2] R. E. Thoma et al., MSR Quar. Prog. Rep. Oct. 31, 1958, ORNL-2626, p 79.
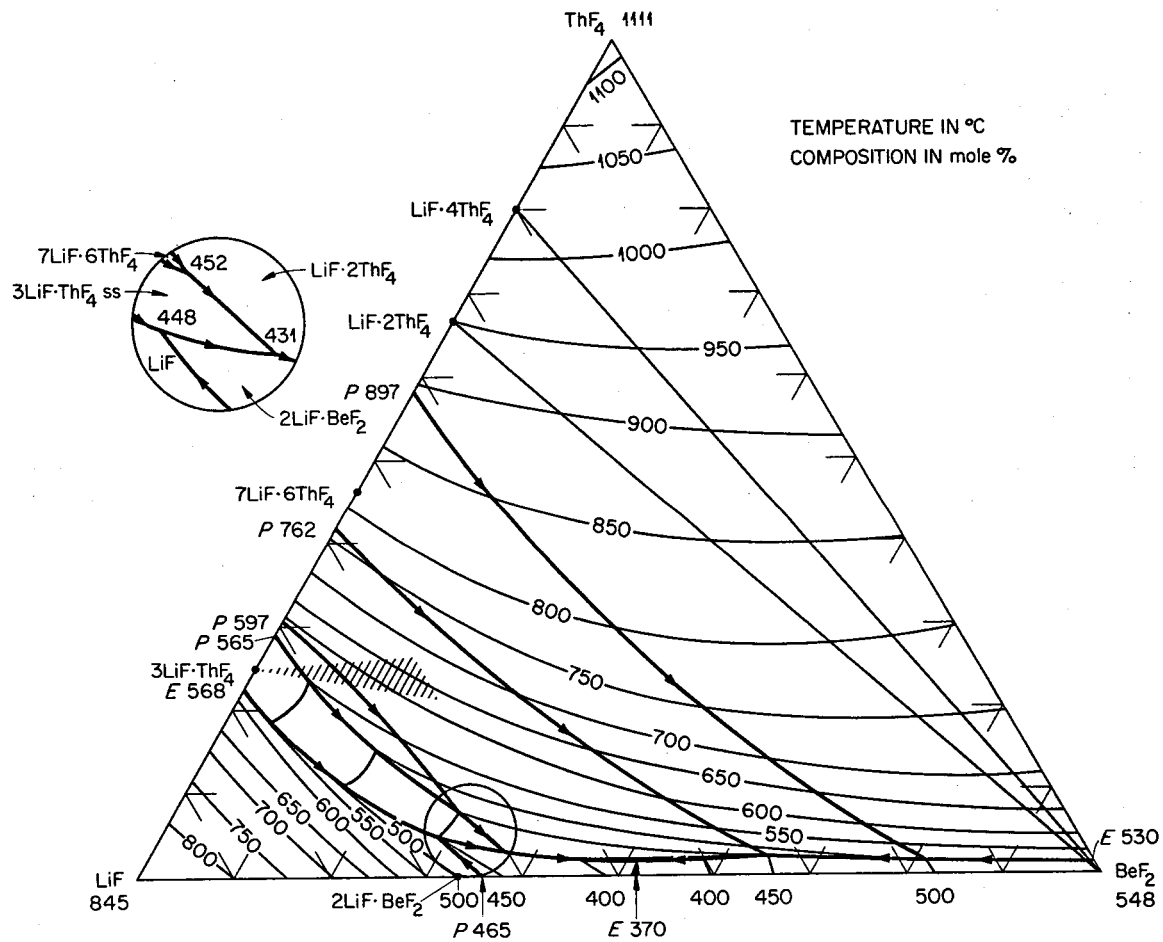
Fig. 2.2.1. The System LiF-BeF$_2$-ThF$_4$.

$3\text{LiF}\cdot\text{ThF}_4$ solid solution are:

Composition (mole %)		
LiF	BeF_2	ThF_4
75	0	25
58	16	26
58	21	21

The revised diagram shows that the composition $\text{LiF-BeF}_2\text{-ThF}_4$ (67.5-17.5-15 mole %; liquidus temperature, 500°C) has a higher ThF_4 concentration than breeding mixtures of current interest, such as $\text{LiF-BeF}_2\text{-ThF}_4$ (71-16-13 mole %); also the liquidus temperature is slightly lower. The occurrence of the unusual ternary solid solution in this system provides these breeding mixtures with an advantage; on cooling, the first solids and last liquid to freeze are much closer in composition that would be the case if no solid solution occurred. A description of the crystallization process for the composition $\text{LiF-BeF}_2\text{-ThF}_4$ (67.5-17.5-15 mole %) demonstrates this point. On cooling to 500°C, the two solid phases $3\text{LiF}\cdot\text{ThF}_4$ (composition located in triangular solid solution area) and $7\text{LiF}\cdot6\text{ThF}_4$ coprecipitate on a boundary curve. As these two solids continue to freeze upon further cooling, the equilibrium liquid decreases in thorium concentration and leaves the boundary curve before reaching the peritectic point at $\text{LiF-BeF}_2\text{-ThF}_4$ (63-29.5-7.5 mole %, 452°C). The liquid then changes composition toward another peritectic at $\text{LiF-BeF}_2\text{-ThF}_4$ (60.5-36.5-3 mole %) and freezes completely in the vicinity of the latter composition. Since the quantity of liquid remaining in the region of the peritectic is much less than if no solid solution existed, most of the solids formed on cooling $\text{LiF-BeF}_2\text{-ThF}_4$ (67.5-17.5-15 mole %) will be formed between 500 and 450°C, and tendencies toward segregation will be reduced.

The System $\text{NaF-BeF}_2\text{-ThF}_4$

Evidence has continued to accumulate on the extensive substitution of UF_4 for ThF_4 to give solid solutions in systems containing BeF_2 and alkali metal fluorides. The resulting solid solutions are compounds of

alkali metal fuorides with UF_4 and ThF_4; they melt at considerably lower temperatures than the corresponding thorium compounds. Accordingly, the phase diagrams of ternary systems of an alkali fluoride with BeF_2 and ThF_4 are useful as guides to selections of converter-reactor fuel mixtures from the otherwise extremely complex quaternary systems containing UF_4.

Progress toward completion of the phase diagram for the system NaF-BeF_2-ThF_4 is shown in Fig. 2.2.2. The composition of the single ternary compound occurring in the system and the location of the boundary curve separating the primary phase fields of ThF_4 and this ternary compound have not been determined. The compositions that show the maximum solubility of ThF_4 at $550^{\circ}C$ are NaF-BeF_2-ThF_4 (76-10-14 mole %) and NaF-BeF_2-ThF_4 (50-38.5-11.5 mole %).

The System NaF-ThF_4-UF_4

The identity and approximate locations of the primary phases in the system NaF-ThF_4-UF_4 have been determined. Because of the solubility of UF_4 in compounds such as $4NaF \cdot ThF_4$, $2NaF \cdot ThF_4$, $3NaF \cdot 2ThF_4$, and $7NaF \cdot 6ThF_4$, there are no phase fields for pure binary thorium compounds in the ternary diagram.

The System SnF_2-NH_4HF_2

The SnF_2-NH_4HF_2 system was investigated because of its potentialities as a strongly oxidizing, low-melting solvent for reprocessing fuels. Liquidus temperatures were noted by visually observing precipitation upon cooling. At temperatures higher than $150^{\circ}C$, the solution bubbled and formed a scum which not only interfered with observations but also changed the composition of the melt. Therefore reliable data were obtained only in the range 0 to 40% SnF_2. The compound NH_4HF_2 melts at $125^{\circ}C$, and a 15 mole % addition of SnF_2 lowers the melting point to about $100^{\circ}C$. Further additions of SnF_2 increase the liquidus temperature to $150^{\circ}C$ for the mixture containing 40 mole % SnF_2.

Heating a mixture of 35 mole % NH_4HF_2 and 65 mole % SnF_2 resulted in considerable evolution of gas and gave a melt with a liquidus temperature of $240^{\circ}C$, which is well above the melting point of SnF_2 ($218^{\circ}C$).
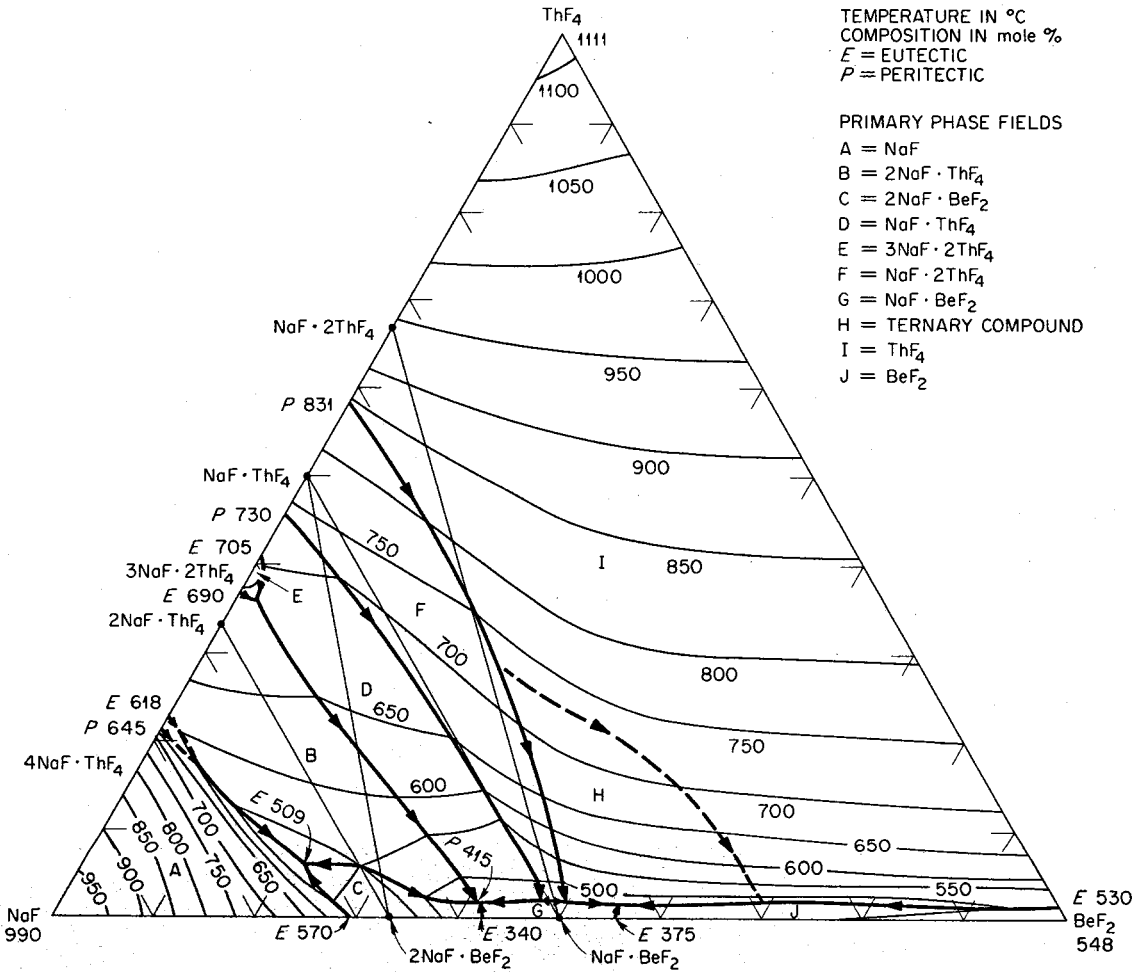
Fig. 2.2.2. The System NaF-BeF₂-ThF₄.

79

The solidified product gave a simple but unidentified x-ray diffraction pattern. Thus it appears that the sample was predominantly a new compound. Petrographic results confirmed the presence of a new compound and showed that still another unidentified phase was present to the extent of about 10%.

Solubility of PuF_3 in Converter Fuels

Interest in the possibility of converting U^{238} to the fissionable Pu^{239} in molten-fluoride-salt fuels led to measurements of the solubility of PuF_3 in the mixture $LiF-BeF_2-UF_4$ (70-10-20 mole %). The apparatus and techniques were described previously.[3] For the first solubility determination, weighed amounts of LiF, BeF_2, UF_4, and PuF_3 were melted directly in the filtration apparatus and heated to a maximum temperature of $716°C$ in a mixed atmosphere of argon and HF. The mixture was then cooled and equilibrated at 562 to $567°C$ for 105 min before filtering at $567°C$. Three other filtrates were obtained from a melt that was pretreated by heating LiF, BeF_2, and UF_4 in a platinum dish, with $NH_4F \cdot HF$ added to prevent hydrolysis, at a maximum temperature of $725°C$ for 30 min and cooling in an argon atmosphere. A plot of the data in Table 2.2.2 as the log of molar concentration of PuF_3 versus the reciprocal of the absolute temperature indicated that the solubility value obtained at $567°C$ was about 0.15 mole % too high to fit the straight line through the points for pretreated melts. The reason for this slight discrepancy is not known. All the PuF_3 solubilities obtained in $LiF-BeF_2-UF_4$ (70-10-20 mole %) are higher than those obtained with $LiF-BeF_2$ mixtures having about the same LiF concentration but no UF_4.

Separation of Li^7F from Li^7F-BeF_2

According to the $LiF-BeF_2-NaF$ ternary diagram[4] the addition of

[3]C. J. Barton, W. R. Grimes, and R. A. Strehlow, Solubility and Stability of PuF_3 in Fused Alkali Fluoride-Beryllium Fluoride Mixtures, ORNL-2530 (June 11, 1958).

[4]R. E. Thoma, Phase Diagrams of Nuclear Reactor Materials, ORNL-2548 (to be published).

Table 2.2.2. Solubility of PuF_3 in $LiF-BeF_2-UF_4$
(70-10-20 mole %)

Filtration Temperature (°C)	Plutonium in Filtrate	
	Pu (wt %)	PuF_3 (mole %)
558	3.43	1.27
567	4.07	1.52
597	4.57	1.70
658	6.50	2.48

NaF to $LiF-BeF_2$ (63-37 mole %) places the resulting composition in the primary phase field of LiF, where a decrease in temperature causes precipitation of LiF; under favorable conditions about 70% of the LiF should separate as solid. An initial experiment has been performed in which NaF was added to an $LiF-BeF_2$ mixture at 700°C and cooled to 490°C. Analytical results on filtrates at 600°C and 490°C showed that only 23% of the contained LiF remained in the solution at the lower temperature.

Fission-Product Behavior
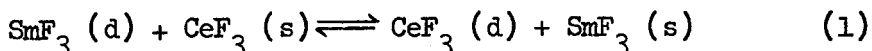
Precipitation of SmF_3 with CeF_3

Previously reported studies[5,6] of the solubility of rare earth fluorides in molten salts have shown that undesirable fission products, such as SmF_3, can be precipitated as solid solutions by CeF_3 additions and proper temperature adjustment. The removal is effected by the exchange[7] between the melt (d) and the solid solution (s):

---
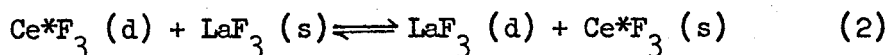
[5] W. T. Ward, MSR Quar. Prog. Rep. Oct. 31, 1958, ORNL-2626, p 88.

[6] MSR Quar. Prog. Rep. Jan. 31, 1959, ORNL-2684, p 100.

[7] The equilibrium constant for this exchange is independent of temperature; however, the total rare earth solubility shows an exponential variance with 1/T.

$$SmF_3 \ (d) + CeF_3 \ (s) \rightleftharpoons CeF_3 \ (d) + SmF_3 \ (s) \qquad (1)$$

Experiments have shown that the exchange

$$Ce^*F_3 \ (d) + LaF_3 \ (s) \rightleftharpoons LaF_3 \ (d) + Ce^*F_3 \ (s) \qquad (2)$$

is an analogue of exchange (1). Thus Ce^*F_3 (labeled), which has desirable tracer characteristics, can be used in exchange (2) to approximate the behavior of SmF_3 in exchange (1).

A proposed method of salt purification utilizing exchange (1) would be to pass the salt through an isothermal bed of solid CeF_3 to lower the SmF_3 content and then to lower the temperature of the effluent salt to decrease the total rare earth content. To determine the feasibility of the method, information is required on the rate of exchange. The first exploratory rate test was conducted at $500^\circ C$ with an agitated CeF_3-LiF-BeF_2 melt (1500 ppm CeF_3, 62 mole % LiF, 38 mole % BeF_2) to which an excess of LaF_3 was added. Within 1 min, the CeF_3 content was decreased to 400 ppm; within 5 min the system was at equilibrium (300 ppm CeF_3) with respect to exchange (2). The second test employed a 14-in. horizontal column of 3/4-in. tubing packed with 100 g of +18 mesh LaF_3. The packed column was charged at $300^\circ C$ with LiF-BeF_2 (62-38 mole %) containing 1000 ppm CeF_3, and 12 g of melt, not counting the holdup volume, was transferred through the LaF_3 at 18 gpm with a pressure drop of 3 psi. The CeF_3 content of the effluent ranged from 80 to 30 ppm. Attempts to continue the experiment at a later time with the same packing gave evidence that the liquid was bypassing the LaF_3 (s) and that future tests with vertical columns should give better performance.

Chemical Reactions of Oxides with Fluorides in Molten-Fluoride-Salt Solvents

The chemical reactions of oxides with UF_4 in molten fluoride solvents have indicated that uranium can be separated from fission products by fractional oxide precipitation. As mentioned previously,[8]

---

[8] J. H. Shaffer, MSR Quar. Prog. Rep. Oct. 31, 1958, ORNL-2626, p 92.

BeO and water vapor appear to be desirable precipitating agents because they do not introduce extraneous constituents into BeF_2 mixtures. Investigations have continued on the removal of uranium from solution by reaction of UF_4 with BeO in a column-extraction process and on the fractional precipitation of uranium with water vapor.

Extraction of Uranium with BeO. The reaction of UF_4 with BeO to produce UO_2 has been studied in several experiments.[8,9] Observations of the reaction in a packed column show several interesting characteristics. A eutectic mixture of LiF-KF (50-50 mole %) containing 1 mole % UF_4 was twice passed unidirectionally through a small column packed with extruded BeO (1/16 in. in diameter and 1/8 in. long) at 600°C. The column contained approximately three times the amount of BeO required for converting the UF_4 to UO_2. During the first pass, 34.6% of the uranium was removed from 2 kg of liquid mixture at an average flow rate of 700 gpm under a pressure drop of 5 psi. A second pass removed an additional 30% of the initial uranium from solution. However, the average flow rate during the second extraction was considerably slower (30 gpm), since a pressure drop of approximately 15 psi developed. A third extraction was not attempted.

Calculations based on the experimental data show that 16% of the beryllium oxide in the column reacted with UF_4. It is interesting to note, however, that only 18% of the reacted beryllium was present in the column effluent at the completion of the experiment. A similar retention of BeF_2, probably on the surface of the BeO pellets, was previously noted in the conversion of ZrF_4 to ZrO_2.

In future experiments, the effectiveness of BeO beds for removing lower concentrations of uranium from molten fluoride mixtures will be investigated.

Precipitation with Water Vapor. The effective removal of uranium as UO_2 from an LiF-BeF_2 (63-37 mole %) solvent by the reaction at 600°C

[9] J. H. Shaffer, MSR Quar. Prog. Rep. June 30, 1958, ORNL-2551, p 90.

of water vapor with UF_4 has been demonstrated.[8] In reprocessing
molten fluoride reactor fuels, however, the separation of uranium
from the fission-product rare earths would be a primary requisite.
An experiment has shown that the reaction of water vapor with CeF_3
in $LiF-BeF_2$ (63-37 mole %) is too slow for detection by a fairly
sensitive radiochemical tracer technique (precision, $< \pm 0.2\%$). In
two subsequent experiments, water vapor was allowed to react at $600^\circ C$
with UF_4 (1 mole %) in $LiF-BeF_2$ (63-37 mole %) containing 1.25 wt %
CeF_3. In each case, UO_2 was formed without any detectable precipitation
of Ce_2O_3 or BeO. The uranium concentration in solution at the stoichi-
ometric point of the reaction was on the order of 100 ppm in each
experiment.

The sharpness of this separation is very favorable from the
standpoint of reprocessing schemes, and it points to a method for
removing uranium without using fluorine. It also leads to a method
for removing uranium and thorium simultaneously that would permit the
rare earths to be selectively precipitated in another step that could
be followed by redissolution of the uranium and the thorium in
reclaimed barren solvent.

An experiment for studying the reaction of water vapor with UF_4
dissolved in LiF-KF (50-50 mole %) indicated a much lower rate of
reaction as a result of strong complexing of both $O^=$ and U^{4+} ions
in the melt. A negligible quantity of HF was evolved, and x-ray
diffraction examinations of filtrate samples taken from the reaction
mixture showed the presence of $KF \cdot 2H_2O$. Treatment with 8500 meq of
water resulted in the precipitation of 64 meq of uranium from solution
and the evolution of 30 meq of HF. A comparison with the reaction of
water vapor with UF_4 dissolved in LiF-NaF (60-40 mole %) is planned
as a further study.

84

Gas Solubilities in Molten Fluoride Salts

Solubility of Neon in LiF-BeF$_2$

The investigation of the solubility of neon in a mixture of LiF-BeF$_2$ (64-36 mole %) has been completed at 500, 600, 700, and 800°C covering the pressure range of 0 to 2 atm. As in all previous studies of the solubility of noble gases in molten fluoride salts, Henry's law is obeyed, and the solubility increases with temperature. The solubility decreases with increasing atomic weight of gas, and the enthalpy of solution increases.

Henry's law constants for this system are $(3.09 \pm 0.09) \times 10^{-8}$, $(4.63 \pm 0.01) \times 10^{-8}$, $(6.80 \pm 0.09) \times 10^{-8}$, and $(9.01 \pm 0.15) \times 10^{-8}$ moles of He per cm^3 of melt per atm at 500, 600, 700, and 800°C, respectively. A heat of solution of 5880 cal/mole was calculated from the temperature dependence of these constants.

Solubility of CO$_2$ in NaF-BeF$_2$

The solubility of CO$_2$ in molten NaF-BeF$_2$ (57-43 mole %) has been examined at 500, 600, 700, and 800°C at pressures from 0 to 2 atm. The experimental data illustrate the linear dependence of solubility with saturating pressures. Henry's law constants, K, at these temperatures are $(7.93 \pm 0.36) \times 10^{-8}$, $(7.05 \pm 0.14) \times 10^{-8}$, $(8.32 \pm 0.08) \times 10^{-8}$ moles of CO$_2$ per cm^3 of melt per atm. Of all the gas solubility data for molten salt systems obtained to date, these are the first to show a nonlinear log K versus 1/T plot. A minimum is observed on this plot in the vicinity of 600°C.

Preliminary measurements of CO$_2$ solubility in the eutectic mixture LiF-NaF-KF (46.5-11.5-42 mole %) were questionable. It appears that the presence of dissolved oxygen-containing species increases the solubility of CO$_2$. This will be checked by measurements in a meticulously purified solvent before and after adding known quantities of a soluble oxide.

Chemistry of the Corrosion Process

Samples from Operating Loops

Periodic sampling of the melts in forced-circulation corrosion-test loops, as described in the previous report,[10] has continued. One loop is fabricated from INOR-8 and the other from Inconel. Both loops were charged with the salt composition $LiF-BeF_2-ThF_4-UF_4$ (62-36.5-1-0.5 mole %) containing about 400 ppm of chromium, and the maximum wall temperature is $1300°F$.

The chromium concentration in the INOR-8 loop (MSRP No. 12) reached a plateau at about 550 ppm after about 1200 hr of operation and has maintained this level for the last 1000 hr. In the Inconel loop (9377-5) the chromium concentration in the salt rose gradually during the first 400 hr of operation to a value of 550 ppm. The increase was more rapid than in the INOR-8 loop but was uniform. However, after the first 400 hr, the chromium concentration began increasing very rapidly, as indicated below:

| Time (hr)	Chromium Concentration (ppm)
500	800
650	950
800	1100
1700	2000

Since sample removals decreased the quantity of salt in the loop, more salt was added after 2250 hr to permit further monitoring. Samples taken before and after the addition of 0.6 kg of fresh salt showed 2100 and 1900 ppm of chromium, respectively. The loop was allowed to circulate for three days (72 hr) and again sampled, and 2050 ppm of chromium was found; after 2600 hr, 2350 ppm of chromium was present. The latter value may represent an approach to a steady-state level, but the chromium

---
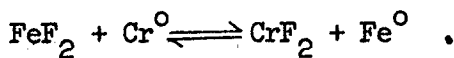
[10]MSR Quar. Prog. Rep. Jan. 31, 1959, ORNL-2684, p 106.

concentration is considerably higher than was expected in the absence
of oxidizing impurities.

Radioactive Tracer Analyses for Iron in Molten Fluoride Salts

Most investigations of corrosion behavior depend on accurate
analyses at low dilution of Fe^{++} and other structural metal ions. For
example, the validity of chromium diffusion experiments in systems
consisting of a molten salt and a chromium alloy depends on the purity
of the salt with respect to NiF_2 and FeF_2. Both compounds form CrF_2
from chromium; for example,

$$FeF_2 + Cr^o \rightleftharpoons CrF_2 + Fe^o \quad .$$

Experimental equilibrium constants show that the equilibrium concen-
tration of FeF_2 in the presence of chromium should be too low to detect.
However, analyses obtained in the diffusion experiments indicated that
FeF_2 was present at concentrations ranging from 100 to 200 ppm in
$NaF-ZrF_4$ (53-47 mole %) which had been in contact with Inconel ($[Cr^o]=$
0.16 wt fraction). This anomaly suggested that finely divided iron
might be passing through the sample stick filters under certain con-
ditions. To investigate this possibility, 800 ppm of labeled FeF_2 was
dissolved in a nickel container filled with $NaF-ZrF_4$ (53-47 mole %)
solvent and then completely removed from solution by reduction with
zirconium. Standard counting procedures verified that no labeled Fe^{++}
or iron was present in filtered portions of the melt after the zirconium
addition, although an average wet analysis of 205 ppm of iron was
reported for the same material. It seems definite that currently used
procedures result in misleading results from wet chemical analysis and
that the presence of iron in the melt as sampled is not the explanation.
The discrepancy is being investigated.

Activities in Metal Alloys

The measurements of thermodynamic activities for nickel in the
Ni—NiO system, as obtained from an electrode concentration cell with
a molten electrolyte, have been delayed by a series of experiments

designed to test the approach to equilibrium obtained by various annealing procedures for the electrodes. These experiments have not given definite results. Another series of experiments has established that the results are not being invalidated by thermoelectric potentials.

Vapor Pressures of Molten Salts

The lowering of the vapor pressure of CsF (vapor pressure, 83 mm Hg) at $1000^\circ C$ by 20 mole % additions of alkaline earth fluorides has been measured as part of a study of the effect of cation size and charge on the thermodynamic properties of fluoride melts. The smallest cation Mg^{++} (radius, $0.78\mathring{A}$) gives a lowering of 30 mm Hg; Ca^{++} (radius, $1.06\mathring{A}$), 26 mm Hg; and Ba^{++} (radius, $1.43\mathring{A}$), 18 mm Hg, following the expected order. Freezing-point depressions that reflect the same effects are also being measured.

Permeability of Graphite by Molten Fluoride Salts

Permeability tests on various types of reactor-grade graphite with molten fluoride salts have continued. In the routine procedure for impregnating graphite with a molten salt, the graphite samples were degassed under vacuum at 900 to $950^\circ C$ and then treated with a molten salt, such as $LiF-MgF_2$ (67.5-32.5 mole %), while still held under vacuum. After the graphite samples were completely covered with salt the vacuum was relieved and a pressure of 15 psig of helium was applied to the system for 48 hr. At the end of 48 hr, the pressure was relieved, and the molten salt was transferred away from the graphite.

In previous tests, graphite rods 3-in. long and 1/4, 1/2, and 1 in. in diameter had been used. For routine testing, 1-in.-dia rods have been adopted.

By using welded container vessels, shortening vacuum lines, and using extreme care in assembly, the efficiency of impregnation has been increased, as indicated by an average weight gain of 12.5% compared with 8.5% in earlier runs on reactor-grade TSF and AGOT graphite samples.

The objectives of the current exploratory tests are to determine (1) how effective salt impregnation of graphite is in preventing or decreasing penetration of possible molten-salt reactor fuels at the maximum reactor temperature, (2) the degree of penetration into untreated graphite of typical reactor fuels under forced impregnation (vacuum and pressure) conditions at the maximum reactor temperature (1250°F), (3) the degree of penetration of typical reactor fuels into untreated graphite under normal reactor operating conditions (in a 1000-hr test in a circulating-salt system), and (4) the distribution of the main fuel components (uranium, thorium, and beryllium) in the graphite when penetration occurs.

Samples of three special types of graphite were obtained from the National Carbon Company for testing. These were identified as follows: ATJ-82, ATL-82, and AGOT-82. The number 82 after each type refers to a special process used by National Carbon to make impervious graphite. Because of the geometry of the available samples, the rods were machined to 3/4 in. OD and 3 in. long. Attempts to impregnate these rods of special graphite with LiF-MgF$_2$ in the usual manner gave the following results. The ATJ-82 graphite showed a loss in weight of 0.9%. The ATL-82 graphite showed a loss in weight of about 0.1%. The AGOT-82 graphite showed a gain of 2.0%, and samples of TSF graphite, included for comparison, gained 5.5%.

The rods were then subjected to a 1000-hr soaking test at 1250°F under a static helium pressure of 1 psig in stirred LiF-BeF$_2$-UF$_4$ (62-37-1 mole %). The ATJ-82 gained 0.2% in weight, the ATL-82 gained 0.4%, the AGOT-82 gained 2.1%, and the TSF gained 2.8%. These gains are based on the weights of the rods before and after the 1000-hr test and do not include the forced-impregnation gains or losses.

To determine the penetration of uranium and beryllium into these rods, successive 1/32-in. layers were machined from the rods and submitted for chemical analysis. When the rods became too small to machine without breaking, the ends were cut off and the center section was submitted for analysis. Typical results are listed in Table 2.2.3.

Table 2.2.3. Analyses of Cuts Taken from Graphite Rods Impregnated with LiF-MgF$_2$ and Then Soaked in LiF-BeF$_2$-UF$_4$

Cut No.	Type of Graphite							
	TSF		AGOT		ATL-82		ATJ-82	
	U (ppm)	Be (ppm)	U (ppm)	Be (ppm)	U (ppm)	Be (ppm)	U (ppm)	Be (ppm)
1	3500	6400	2200	4300	1000	1800	600	1000
2	3300	6400	1500	3800	700	1200	150	270
4	3100	6300	1300	3300	550	900	25	85
8	3500	7000	940	2900	450	600	10	100
Center	3700	5200	1200	1400	1900	450	9200	350

The cut numbers were assigned so that cut No. 1 was the first cut taken on the rod, cut No. 10 was the last cut taken, and "center" indicates the remaining center section, which was also submitted for analysis.

It appears that the ATL-82 and ATJ-82 grapites are resistant to forced impregnation with LiF-MgF$_2$ salt and are considerably resistant to penetration by a typical reactor fuel. The most startling observation, however, is the unexpectedly high concentration of uranium in the center section of the ATL-82 and ATJ-82 rods. Subsequent long-term soaking tests of reactor-grade graphites TSF and AGOT in a fuel mixture of the same LiF-BeF$_2$-UF$_4$ composition also showed disproportionately high uranium concentrations in the center in every case. Efforts are being made to determine the mechanism of this phenomenon and to further verify it.

An experiment was carried out to determine whether untreated TSF graphite could be forcibly impregnated with the LiF-BeF$_2$-UF$_4$ (63-37-1 mole %) fuel mixture of current interest by using vacuum and pressure techniques at the maximum reactor temperature of 1250°F. Six TSF graphite rods were used in this experiment, and weight gains that ranged from 0.1% to 1.85% were obtained. To determine depth of penetration, these rods were machined, as previously described, and

the machine cuttings plus the center section were submitted for analysis. In all cases, the bulk of the salt penetration was in the first and second machine cuttings. However, it was noted again that, in general, the center sections contained several times (occasionally 200 times) more uranium than the last cutting taken at about 1/4 in. from the center.

Radiation Damage Studies

INOR-8 Thermal Convection Loop for Operation in the LITR

The in-pile thermal-convection loop for testing fused-salt fuel in INOR-8 tubing in the LITR was operated in preliminary tests outside the reactor, and satisfactory circulation of the salt ($LiF-BeF_2-UF_4$, 62-37-1 mole %) was obtained. Radiography of the fuel tube after these tests demonstrated that no opaque material had deposited at the bottom, as in a previous loop test.[11]

Thermocouples have been installed on the fuel tube of this loop, and the air annulus tube has been assembled around the loop. Detailed examinations of the thermocouples were made, and complete records of their condition, including individual photomicrographs of each thermocouple, are available. This examination record will be used to correlate thermocouple performance during operation in the reactor with the initial conditions of the thermocouples. The information obtained will be useful in the construction of future in-pile loops.

Modifications were made in the cooling-air control system at the reactor to provide for individual temperature control of various portions of the loop. After resistance-heating elements have been installed and the loop inserted in the outer can, the loop will be operated in the LITR.

In-Pile Static Corrosion Tests

Two fuel-filled INOR-8 capsules, which were described previously,[11] were installed in the MTR and are being irradiated at a temperature of

---

[11]MSR Quar. Prog. Rep. Jan. 31, 1959, ORNL-2684, p 112.

$1250°F$. The fuel is $LiF-BeF_2-UF_4$ (62-37-1 mole %), and the power density in the fuel is 1200 w/cm^3. Two additional capsules of the same type are being prepared for irradiation in the ORR.

Preparation of Purified Materials

Purification, Transfer, and Service Operations

The processing of small batches of various molten-fluoride-salt compositions for use in corrosion tests, physical property studies, and small-scale component testing decreased considerably during the first half of this quarter. However, demands have gradually increased during the past month, and a normal rate of operation is now being maintained. A total of 35 kg of mixtures not containing beryllium and 85 kg of beryllium-containing mixtures was processed during the quarter. Transfer and service operations to assist engineering groups in handling high-temperature fluids were continued at a slightly increased rate.

Fuel Replenishment Tests

A simple device for testing the proposed fuel sampling and enriching mechanism[12] was constructed and tested. The device employs two salt storage pots interconnected by a transfer line, with the enriching device on one pot and the sampling device on the other pot. The molten salt is moved alternately from one pot to the other with semiautomatic controls by using differential gas pressures.

Solid, cast, UF_4 fuel slugs weighing 40 g each were introduced to the dissolution pot in a copper basket and the salt, $LiF-BeF_2$ (50-50 mole %), was cycled between the two pots. The rate of dissolution was measured by withdrawing and weighing the amount of UF_4 remaining; samples of the solution were also taken for chemical analysis.

A 40-g slug of UF_4 dissolved in 20 cycles (1 1/2 hr), but it was not completely dissolved in 15 cycles (1 hr). This rate of solution

---

[12]MSR Quar. Prog. Rep. Jan. 31, 1959, ORNL-2684, p 9.

appears to be adequate for convenient enrichment procedures.

Pure Compounds Prepared with Molten Ammonium Bifluoride

Molten ammonium bifluoride (mp, 125°C) has served as a reactant for preparing both simple and complex fluorides.[13,14] Recent trials show that commercial chromic oxide is not noticeably attacked by molten ammonium bifluoride. Magnesium oxide is converted into NH_4MgF_3, which can be decomposed into pure magnesium fluoride. Beryllium oxide (calcined at 900°C) is also converted to an ammonium complex.

When commercial "Co_2O_3" powder is treated for 1 hr with molten ammonium bifluoride, a small amount of oxide is left unchanged. The reaction product has an x-ray diffraction pattern somewhat shifted from that of $KCoF_3$, so it is presumed to be NH_4CoF_3.

Nickel oxide was found to be more resistant to attack than "Co_2O_3." A 1-hr treatment left almost all the oxide unreacted.

The oxides GeO_2, UO_2, ThO_2, and CeO_2 seem to react completely with molten ammonium bifluoride, but the products have not yet been identified.

Vanadium pentoxide reacts with molten ammonium bifluoride to evolve yellow fumes. Presumably, vanadium pentafluoride is formed; it is reported to react with moist air to form yellow oxyfluorides.[15]

For all the reactions with oxides, at least a 100% excess of ammonium bifluoride was used in order to form a mixture which was sufficiently fluid to stir.

Electrolytic iron powder reacted with molten ammonium bifluoride to form ammonium hexafluoferrate (III). Chromium metal reacted to form ammonium hexafluochromate (III), but the reaction was slow. Granulated metal, finer than 100 mesh, was treated with the melt for 70 min, and the unreacted ammonium bifluoride was volatilized. Extraction of this

[13]B. J. Sturm and C. W. Sheridan, Preparation of Vanadium Trifluoride by the Thermal Decomposition of Ammonium Hexafluovanadate (III), ORNL CF 58-5-95 (May 28, 1958).

[14]B. J. Sturm, MSR Quar. Prog. Rep. Oct. 31, 1958, ORNL-2626, p 107.
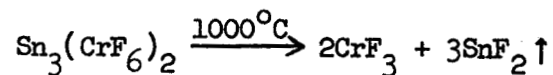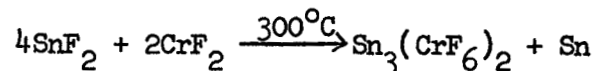
[15]O. Ruff and H. Lickfett, Ber. deut. chem. Ges. 44, 2539 (1911).

product with aqueous nitric acid to remove the ammonium hexafluochromate (III) showed that 60% of the chromium metal had not reacted with the ammonium bifluoride.

Reaction of Chromous Fluoride with Stannous Fluoride

The reaction of chromium metal with molten stannous fluoride provides a useful method of preparing pure chromous fluoride;[14] however, an excess of stannous fluoride can further oxidize the chromium. The predominant phase resulting from the reaction of equal molar portions of stannous fluoride and chromous fluoride is a compound thought to be $Cr_3(CrF_6)_2$.[16]

The product obtained by fusing 1 mole of chromous fluoride with 2 moles of stannous fluoride appears to be stable at the boiling point of stannous fluoride ($\sim$700°C). At 1000°C, all the stannous fluoride volatilizes and leaves a residue of chromic fluoride. The probable intermediate, $Sn_3(CrF_6)_2$, has not been definitely identified, but the reaction is presumably:

$$4SnF_2 + 2CrF_2 \xrightarrow{300°C} Sn_3(CrF_6)_2 + Sn$$

$$Sn_3(CrF_6)_2 \xrightarrow{1000°C} 2CrF_3 + 3SnF_2\uparrow$$

---

[16] MSR Quar. Prog. Rep. Jan. 31, 1959, ORNL-2684, p 113.

2.3. FUEL PROCESSING

Processing of molten-fluoride-salt reactor fuel by volatilization of the uranium as UF_6 appears to be feasible. The barren $LiF-BeF_2$ can be recovered for reuse by treatment with nearly anhydrous HF, in which it is appreciably soluble, and in which rare earth neutron poisons and most other polyvalent element fluorides are insoluble. Development work on the process has continued with a study of the behavior of neptunium, which is possibly the most important neutron poison other than the rare earths.[1]

Further measurements of the solubility of Np(IV) have indicated that its solubility (Table 2.3.1) in aqueous HF solutions saturated with $LiF-BeF_2-ThF_4-UF_4$ (61.5-37-1-0.5 mole %) will be considerably less than reported previously. Apparently the Np(IV) solubility is decreased by the presence of excess ThF_4 and UF_4. The addition of nickel and iron metals to solutions saturated with LiF, BeF_2, and NpF_4 also caused a significant reduction in the neptunium solubility, except in anhydrous HF. This is probably the result of reduction of Np(IV) to Np(III). In a reactor processing system the solution will contain much larger amounts of rare earths, plutonium, uranium, and thorium than of neptunium, and the container will be a metal, probably a nickel alloy. Therefore a neptunium solubility of the order of 0.0002 to 0.00005 mole % is expected in actual processing.

---

[1] MSR Quar. Prog. Rep. Jan. 31, 1959, ORNL-2684, p 115.

Table 2.3.1 Solubility of Np(IV) in Aqueous HF

HF Concentration (%)	Np(IV) Solubility[a] in HF Saturated with LiF-BeF$_2$		Np(IV) Solubility in HF Saturated with LiF-BeF$_2$-ThF$_4$-UF$_4$		Fe and Ni Added	
	mg/g of solution	mole % relative to salt	mg/g of solution	mole % relative to salt	mg/g of solution	mole % relative to salt
80	0.026	0.0031	0.0013	0.00012	0.0043	0.00052
90	0.011	0.0012	0.00046	0.00005	0.0014	0.00016
95	0.0086	0.00072	0.00054	0.00005	0.0029	0.00025
100	0.0029	0.00024	0.0047	0.00039	0.0029	0.00025

[a]Values previously reported in ref. 1 for LiF-BeF$_2$ salt in absence of UF$_4$ and ThF$_4$.

INTERNAL DISTRIBUTION

1.	R. G. Affel	46.	M. T. Kelley
2.	L. G. Alexander	47.	F. Kertesz
3.	E. S. Bettis	48.	B. W. Kinyon
4.	D. S. Billington	49.	M. E. Lackey
5.	F. F. Blankenship	50.	J. A. Lane
6.	E. P. Blizard	51.	R. S. Livingston
7.	A. L. Boch	52.	H. G. MacPherson
8.	C. J. Borkowski	53.	W. D. Manly
9.	W. F. Boudreau	54.	E. R. Mann
10.	G. E. Boyd	55.	L. A. Mann
11.	M. A. Bredig	56.	W. B. McDonald
12.	E. J. Breeding	57.	H. F. McDuffie
13.	R. B. Briggs	58.	J. R. McNally
14.	W. E. Browning	59.	H. J. Metz
15.	D. O. Campbell	60.	R. P. Milford
16.	W. H. Carr	61.	E. C. Miller
17.	G. I. Cathers	62.	J. W. Miller
18.	C. E. Center (K-25)	63.	K. Z. Morgan
19.	R. A. Charpie	64.	J. P. Murray (Y-12)
20.	J. H. Coobs	65.	M. L. Nelson
21.	F. L. Culler	66.	G. J. Nessle
22.	J. H. DeVan	67.	W. R. Osborn
23.	D. A. Douglas	68.	P. Patriarca
24.	L. B. Emlet (K-25)	69.	A. M. Perry
25.	W. K. Ergen	70.	D. Phillips
26.	J. Y. Estabrook	71.	P. M. Reyling
27.	D. E. Ferguson	72.	J. T. Roberts
28.	A. P. Fraas	73.	M. T. Robinson
29.	E. A. Franco-Ferreira	74.	H. W. Savage
30.	J. H. Frye, Jr.	75.	A. W. Savolainen
31.	W. R. Gall	76.	J. L. Scott
32.	A. T. Gresky	77.	H. E. Seagren
33.	J. L. Gregg	78.	E. D. Shipley
34-36.	W. R. Grimes	79.	M. J. Skinner
37.	E. Guth	80.	A. H. Snell
38.	C. S. Harrill	81.	E. Storto
39.	M. R. Hill	82.	C. D. Susano
40.	H. W. Hoffman	83.	J. A. Swartout
41.	A. Hollaender	84.	A. Taboada
42.	A. S. Householder	85.	E. H. Taylor
43.	W. H. Jordan	86.	R. E. Thoma
44.	G. W. Keilholtz	87.	D. B. Trauger
45.	C. P. Keim	88.	F. C. VonderLage

89. G. M. Watson
90. A. M. Weinberg
91. M. E. Whatley
92. J. C. White
93. G. D. Whitman
94. G. C. Williams
95. C. E. Winters
96. J. Zasler
97-100. ORNL - Y-12 Technical Library, Document Reference Section
101-140. Laboratory Records Department
141. Laboratory Records, ORNL R.C.
142-144. Central Research Library

EXTERNAL DISTRIBUTION

145. D. H. Groelsema, AEC, Washington
146. Division of Research and Development, AEC, ORO
147-734. Given distribution as shown in TID-4500 (14th ed.) under
Reactors-Power category (75 copies - OTS)

Reports previously issued in this series are as follows:

ORNL-2378	Period Ending September 1, 1957
ORNL-2431	Period Ending October 31, 1957
ORNL-2474	Period Ending January 31, 1958
ORNL-2551	Period Ending June 30, 1958
ORNL-2626	Period Ending October 31, 1958
ORNL-2684	Period Ending January 31, 1959